THE ASSEMBLY, ASSESSMENT AND DEVELOPMENT OF SOME ATOMISING SYSTEMS FOR ATOMIC SPECTROSCOPY

BY

MARY HARGREAVES, B.Sc., A.R.C.S.

A Thesis submitted for the Degree of
Doctor of Philosophy of the University of London.

August 1972.

Department of Chemistry,
Imperial College of Science and Technology,
London, SW7 2AY.

ABSTRACT

This thesis concerns the application of atomic spectroscopy to analytical chemistry. Work has included the assembly and assessment of flame spectroscopic, laser microprobe and carbon filament atom reservoir atomising systems and their application to atomic emission, absorption and fluorescence spectroscopic measurements. An especial aim has been the detection of some non-metallic elements whose most sensitive spectral lines are at less than 200.0 nm, which are generally awkward to determine by flame spectroscopy and other analytical methods.

ACKNOWLEDGEMENTS

This thesis describes work carried out in the Chemistry Department of the Imperial College of Science and Technology between October 1969 and August 1972.

Thanks are due to the Ministry of Defence and the Science Research Council for financial support and provision of equipment for the projects, also to many members of the analytical section and departmental workshops for practical advice and use of general facilities.

Particularly, I thank my supervisor, Professor T.S. West, for the opportunity of this research training and experience, and for his continued encouragement.

C O N T E N T S

TITLE PAGE 1

ABSTRACT 2

ACKNOWLEDGEMENTS 3

CONTENTS 4

INTRODUCTION 6

CHAPTER 1 FLAME SPECTROSCOPY

1.1 Introduction to flame spectroscopy and this project 9

1.2 Description and assembly of the spectrometer .. 11

1.3 Assessment of the subcomponents of the system .. 14
Nebuliser — Monochromator
Flame — Photomultiplier
Light sources — Recorder

1.4 Experimental 20
Spectra — Atomic emission
Atomic absorption — Atomic fluorescence

1.5 Conclusion 35

CHAPTER 2 LASER MICROPROBE EMISSION SPECTROSCOPY

2.1 Introduction to the technique and this project 36

2.2 Review: The development of the laser microprobe and its application to chemical analysis 37
Introduction
Instrumentation
The ruby laser microprobe
The neodymium-glass laser microprobe
Applications to chemical analysis

2.3 Instrumentation assembly 46

2.4 Choice of working conditions 49
Technique and normal parameters
Laser — Signal optics
Microscope — Monochromator
Sample — EHT
Electrodes — Oscilloscope

CHAPTER 2 (continued)

2.5 Analysis 58
Aims
Approach
Metals
Non-metals
Termination

2.6 Evaluation and future prospects 72

CHAPTER 3 THE CARBON FILAMENT ATOM RESERVOIR (CFAR)

3.1 Introduction to the CFAR and its application in this project 75

3.2 Description of the CFAR and the assembly of the analytical system 76
Description
Assembly
Conversions
CFAR
Electrical connections
Gas and water supplies
Optical system
Sampling

3.3 Preliminary Analysis 80
Aims and approach
Zinc
Thallium
Assessment of CFAR modifications

3.4 Choice of conditions for the AA detection of sulphur 86
Problem
Approach
Development
Interim conclusions

3.5 Alternative vacuum uv analyses 102
Approach
Modifications to the analytical system
Cadmium
Choice of elements for vacuum uv analyses
Exploratory tests: mercury, arsenic, selenium, phosphorus, iodine and sulphur
Comment on results

3.6 Non-dispersive atomic fluorescence 121
Technique
Components
Assembly
Applications
Suggestions for development

BIBLIOGRAPHY 139

INTRODUCTION

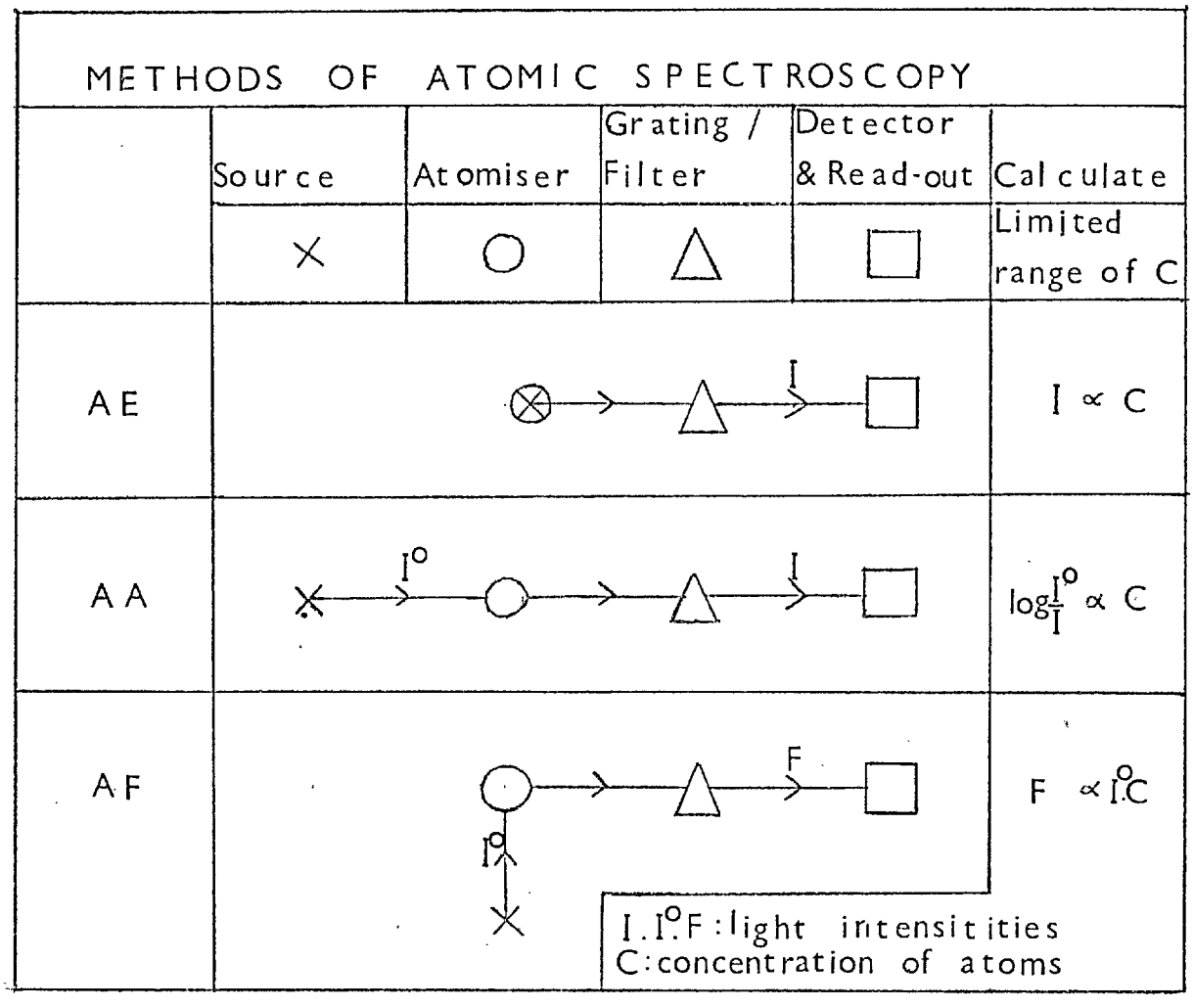
In atomic spectroscopy, atoms are excited from the electronic ground state to higher energy levels which are characteristic of the elemental composition of the component materials, and will absorb and emit radiation at specific wavelengths corresponding to these levels.

The phenomenon is widely applied for chemical analysis, and several sample forms, means of excitement, and methods for detection and measurement of radiation, are available (1).

Associated instrumentation comprises four basic items: the radiant source, an excitation method, radiation filter or diffraction grating to resolve component wavelengths, and a detector and read-out system for quantitative measurements. These may be variously arranged, the form adopted for a particular determination depending on the nature of the element and the equipment available.

The three alternative approaches to atomic spectroscopic analysis are emission, absorption and fluorescence. In atomic emission (AE), the radiant source is the thermally excited sample itself, and an elemental emission at a specific wavelength is measured after atomisation. This is related to sample concentration by comparison to a calibration curve prepared with a series of standards. In atomic absorption (AA), the alteration in intensity of an atomic line source which passes through the atomised species is related to the sample concentration. In atomic fluorescence (AF), a fluorescence signal is measured at right angles to the incident atomic line beam through the atomised

sample, the wavelength and magnitude again being dependent on the nature and concentration of atomised sample.



Each component of the arrangements can be developed for optimum sensitivity and selectivity of the analytical method. In this project, a particular concern was to investigate three different atomising systems: just one aspect of the many variable parameters.

The aim of the atomising process is to produce a maximum amount of element in its (free) atomic form. This requires the evaporation of solvent, if present, to yield undissociated compound. There follows volatilisation and dissociation to atomic species.

This is generally achieved by the application of thermal energy; the use of flames as atomising systems is well established and was further tested here. Flameless methods now provide some promising alternatives, and the laser microprobe, which comprises a laser and auxiliary spark discharge, and the carbon filament atom reservoir (CFAR), a hot rod in an argon atmosphere, were also examined.

CHAPTER 1

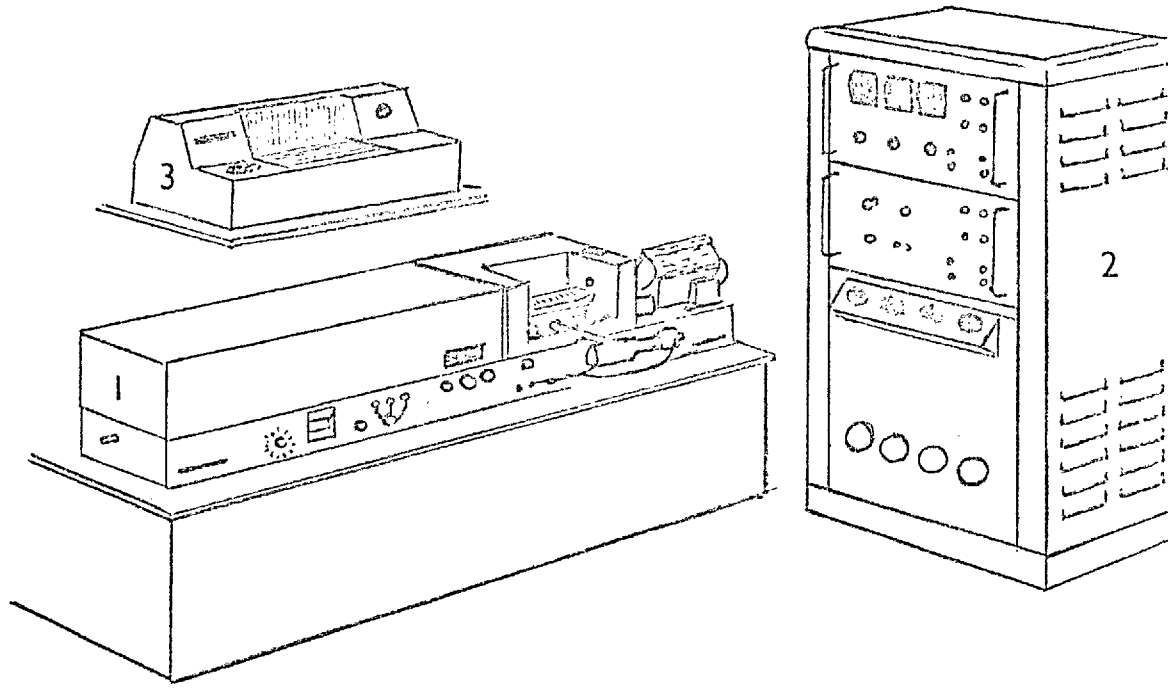
FLAME SPECTROSCOPY

1.1 Introduction to flame spectroscopy and this project.

Analytical techniques of flame spectroscopy, based on the emission, absorption or fluorescence of atomic line radiation, have recently been used very widely. In all of these methods an analyte solution is nebulised into a flame and the constituent species are converted to free atoms in the flame gases. In flame emission the free atoms are excited to emit their characteristic line radiation and its intensity is measured after dispersal by a prism or grating. In atomic absorption, the absorption of resonance line radiation from a hollow-cathode lamp by the ground-state atoms in the flame is measured. In atomic fluorescence a stronger line source, such as a continuous source, is used, and radiation absorbed by the analyte atoms in the flame causes them to emit fluorescence. This is usually measured in a direction at right angles to the incident radiation to minimise contamination of the fluorescence signal by radiation from the source.

Here, an assessment of the 'delta Modèle Kuhlmann' Jobin Yvon atomic absorption flame spectrometer provided useful experience and some practical understanding of the three atomic spectroscopic techniques. It established a good basis for subsequent use of the laser microprobe and CFAR atomisation methods. A knowledge of the conventional techniques also aided a comparative assessment and application of the latter.

Fig 1.1 THE JOBIN YVON SPECTROMETER (2)



key

1 spectrometer

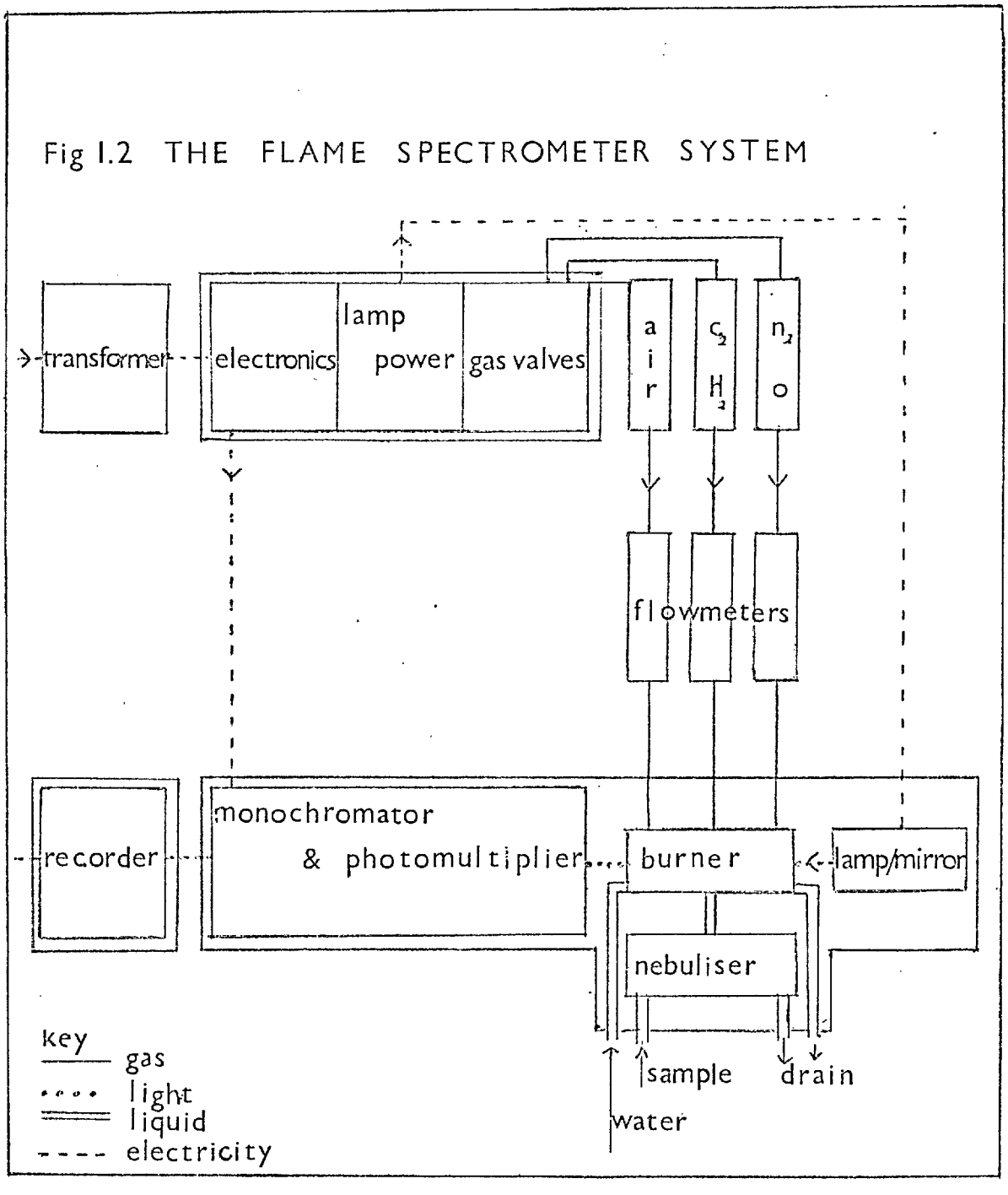
2 control unit

3 recorder

1.2 Description and assembly of the spectrometer.

The Jobin Yvon (France) spectrometer comprises three basic components: a unit containing gas regulator valves, lamp power supplies, and controlling electronic circuitry; another containing the long burner, and light sources; and a separate pen chart recorder.

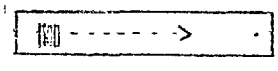
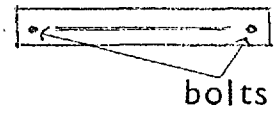
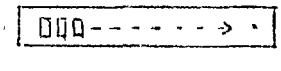
Fig 1.2 THE FLAME SPECTROMETER SYSTEM



After translation of the manufacturer's handbooks, the components were assembled with appropriate gas, electrical and water connections as illustrated (Fig.1.2).

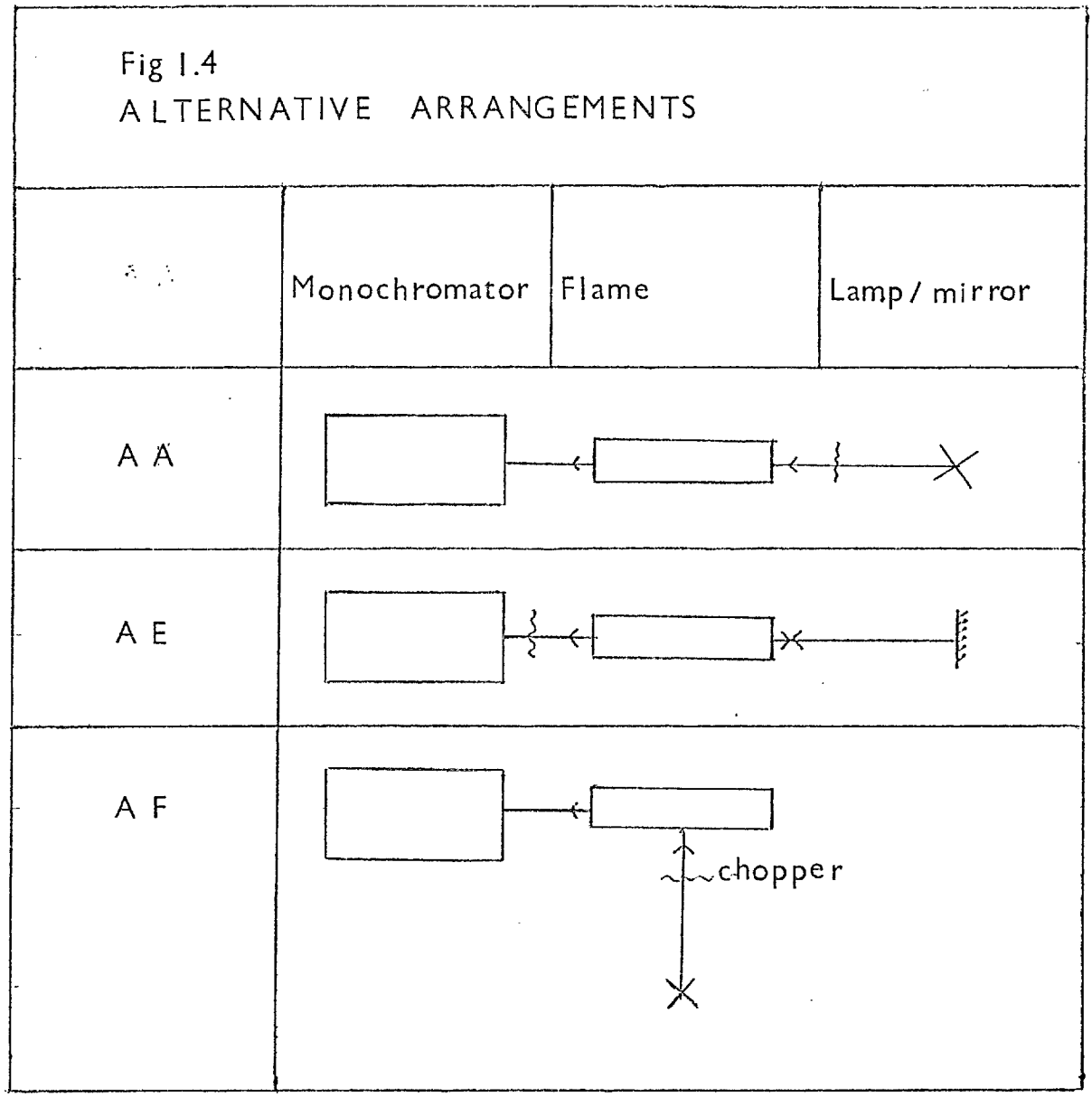
Air-acetylene, nitrous oxide-acetylene and air-butane flames could be run on the different stainless steel, long-path, laminar-flow burners supplied for each (Fig.1.3).

Fig 1.3 ALTERNATIVE BURNERS

Flame	Scale illustration of burner 1 in ≡ 10 cm	Number & size of slots	Used
air—C_2H_2		37 (0.8 x 0.5)mm	yes
N_2O—C_2H_2		1 (0.5 x 54) mm	yes
air—C_4H_{10}		19 (0.8 x 1.5)mm	no

The equipment was designed for use in atomic absorption or emission. Three hollow-cathode lamps: copper/zinc, iron and lead were provided. For emission measurements a reflector mirror could be used in place of a lamp to aid the collection of signals. Two rotating sectors (choppers) appropriate to each type of measurement were available to convert the d.c. signals to a.c. radiation for the purpose of amplification. Only a slight re-arrangement was necessary to adapt the system for atomic fluorescence measurements (Fig.1.4).

Fig 1.4
ALTERNATIVE ARRANGEMENTS



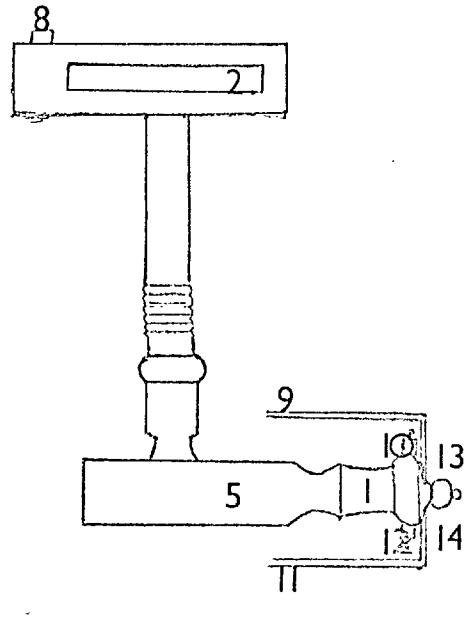
1.3 Assessment of the sub-components of the system.

The performance of the spectrometer was assessed, and practical experience gained, by the recording of spectra and preparation of some standard calibrations. Optimum operating conditions, effects of variation of the variable parameters and some shortcomings of the system were found. Aspects examined will be considered in turn as indicated below:

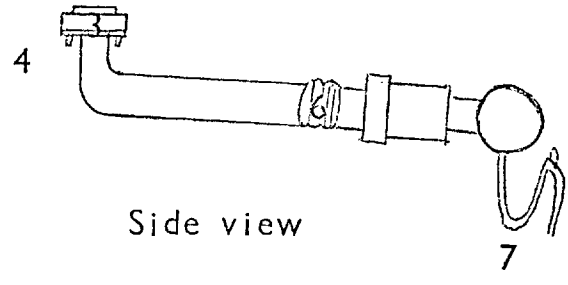
NEBULISER → FLAME → LIGHT-SOURCES → MONOCHROMATOR → PHOTOMULTIPLIER → RECORDER

Nebuliser

Fig 1.5



View from above



Side view

Key

1 atomiser
2 burner head
3 water cooling
4 water inlet and outlet
5 atomisation chamber
6 thermal insulation
7 drainage syphon
8 alarm bell
9 oxidant entry
10 screw to regulate oxidant flow
11 fuel entry
12 screw to regulate fuel flow
13 capillary adjustment
14 tube to sample

The sample solution was sprayed into the flame from a 5 ml beaker via the demountable metal capillary with a needle valve to control uptake rate. The entrance passage had the usual tendency of such systems to become blocked, but was cleared quite easily with the nylon filament provided. The soldered joint between tube and valve was very delicate, however, and on one occasion the end of the capillary was broken off flush with the open end of the valve.

Flame

The stability of the flame used affects reproducibility of results and the sensitivities attainable in experimental work.

Running on air-acetylene, which should provide a hot enough flame for most ordinary determinations, initial difficulties were related to the use of a compressor with a faulty silencer, and by the passage of condensation water through the burner line. The introduction of a water-trap is therefore recommended.

The possibility of the production of toxic gas fumes was recognised and the flame burnt originally under an exhaust hood, but it was necessary to use minimum draught lest noise on the flame be increased beyond usable limits.

Very important in flame spectroscopy is the choice of correct gas ratios, firstly to light the flame safely, then to burn at an optimum temperature and in a suitably oxidising or reducing environment for each determination. To achieve both of these aims, gas flow-rates must be easily regulated. Here, the gas valves on the control unit were insufficiently sensitive, so the gas cylinder head regulators controlled initial gas intake rate. Then flowmeter knobs and atomiser needle valves

were used for fine adjustment and to make adjustments during burning.

A safety device is incorporated: two plastic discs are dislodged to prevent the metal atomiser exploding, an especial hazard when lighting if the gas flow is low or the burning velocity is high. Unfortunately, it was necessary to dismantle the burner to replace the discs.

Sometimes the flame deteriorated during a run, due to the fluctuation and diminution of fuel gas pressure as a cylinder emptied. More serious was the restriction of time for a run when using the nitrous oxide-acetylene flame. Carbon produced as the gases burned accumulated increasingly around the edges of the burner and eventually affected the flame, making it noisy, unstable and unsafe to run. The carbon was removed between runs, with a razor blade. That it did not accumulate in the burner groove itself may be due to the water-cooling system or pressure of unburnt gas, but the deposition needs careful control.

Burner height was variable with respect to the monochromator slit so that the viewing position could be chosen to eliminate as much background as possible while recording the majority of emission at an analytical line.

Light Sources

To examine characteristic flame and hollow-cathode lamp spectra, the absorption chopper and automatic scanning facility of the spectrometer were used. Slit dimensions and current ratings were pre-set according to the manufacturer's recommendations and found suitable for the copper/zinc and iron lamps. The lead lamp was unstable at the recommended 5 mA,

but ran well at 4 mA. Absorption spectra are obtained when the instrument is used in this mode.

Some alkaline earth elements were examined by flame emission using the emission chopper and reflector mirror. The mirror increased signals but also background. Stray reflections did not contribute greatly to signal noise despite the large area of reflecting metal casing surrounding the burner.

Monochromator

This monochromator was fitted with a 1220 lines/mm 70 x 70 mm diffraction grating, with 1.2 nm/mm dispersion in the first order and band-pass 0.02 - 1.82 nm. A manual or variable speed automatic scan of the 190.0 - 800.0 nm wavelength range was possible and found useful for running spectra. The monochromator was well provided with variable controls including slit width and height variation to a maximum of 1.5 mm width x 15.0 mm height.

Usually the manufacturer's recommended slit dimensions were used initially, but a slit height of more than 10.0 mm was inconvenient in conjunction with the preferred burner height. In general, for a determination the minimum slit width which would provide an adequate signal at the concentration range studied was found, and then the slit height attenuated as far as possible.

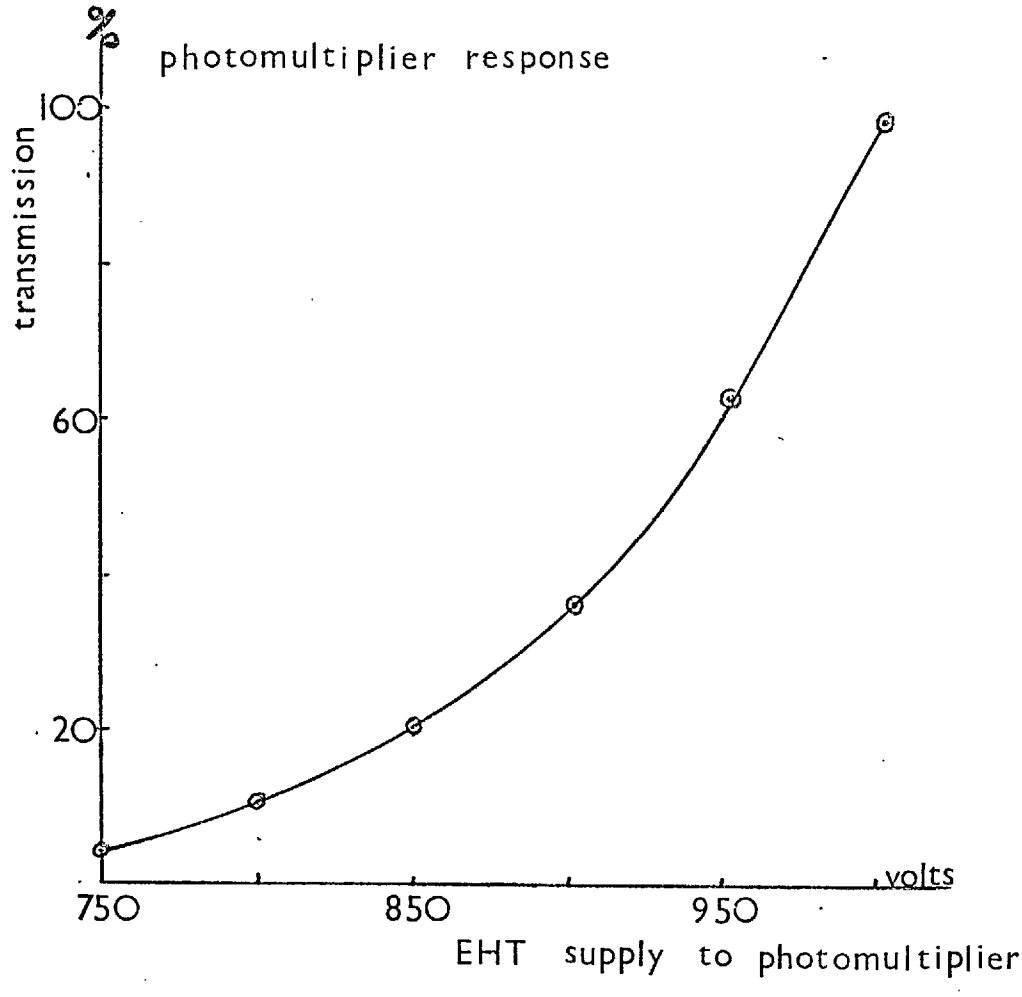
To set a wavelength line accurately, solution was sprayed and the grating turned to provide the maximum signal. This was generally found to be within 0.1 nm of the predicted value on the wavelength scale.

Photomultiplier

The Jobin Yvon electronic power supply unit included a nominally 1000 V EHT supply, but this was found to provide 750 V rather than 1000 V. Therefore, a Brandenburg Type PM 2500 R EHT power supply was connected between the mains and the output to the photomultiplier: EMI Type No. 6256 B, and the HT of the Jobin Yvon power supply, disconnected.

A graphical plot of transmission against applied EHT could be used to choose a steady working EHT of adequate magnitude within the capacity of the photomultiplier while minimising noise levels associated with the signal.

Fig 1.6 TRANSMISSION V EHT



Recorder

The recorder was poor compared to the rest of the unit. Two chart speeds were offered: 15 mm/MIN and 60 mm/MIN, but the paper tended to jam at the higher speed, and because also the recorder response was slow, the lower rate was generally used to make sure of registering peaks accurately.

The basic potentiometric range was 10 mV, with an output chart width of 220 mm. An attenuation facility was available and utilised in conjunction with the slit size variation.

Similar advantage was not achieved from the x 5 scale expansion facility. Noise was very high and the baseline drifted badly always. A faulty contact in the controlling circuitry was suspected but never located. Another practical disadvantage is that x 5 scale expansion can only be applied to transmission measurements so that absorbance values must be obtained indirectly.

To work with moderate signal damping was sometimes an advantage, despite delayed response times. The damping diminished noise levels so that a detection range could sometimes be extended. For example, some measurements were successful with no damping initially, high damping over signal peak, then no damping to return to the baseline.

1.4 Experimental.

The previous section has made a critical examination of some instrumental aspects of the spectrometer. This experimental section indicates the practical performance and results attainable with the system as a whole.

Calibration graphs were prepared for transmission or absorbance against ppm of elemental concentration with respect to a water baseline. Some spectral scans were made recording regions of linearity and optimum running conditions. Noise levels were minimised, and measurements made by running 0.5 - 1.0 of chart at low speeds for both signal and baselines.

Results for standard systems.

Spectra

Characteristic spectra from the hollow-cathode lamps, the air-acetylene and nitrous oxide-acetylene flames were recorded, and lines identified: Cu 324.7 nm and Zn 213.9 nm from the copper/zinc lamp on a scan of 200.0 - 400.0 nm, for example.

Spectra from hollow-cathode lamps: a comparison of the manufacturer's recommendations (R) and the preferred working conditions (P).

Lamp	Element	Atomic line nm	mA Lamp current	mm Slit width	mm Slit height	atten-uation	R/P
Cu/Zn	Copper	324.7	4.0	0.2	5.0	-	R
Cu/Zn	Copper	324.7	4.0	0.2	2.0	9	P
Cu/Zn	Zinc	213.9	4.0	0.5	10.0	-	R
Cu/Zn	Zinc	213.9	4.0	±0.2	±2.0	8	P
Pb	Lead	217.0	5.0	0.5	14.0	-	R
Pb	Lead	217.0	4.0	0.3	5.0	9	P
Fe	Iron	248.3	8.0	0.2	5.0	-	R
Fe	Iron	248.3	8.0	0.2	5.0	8	P

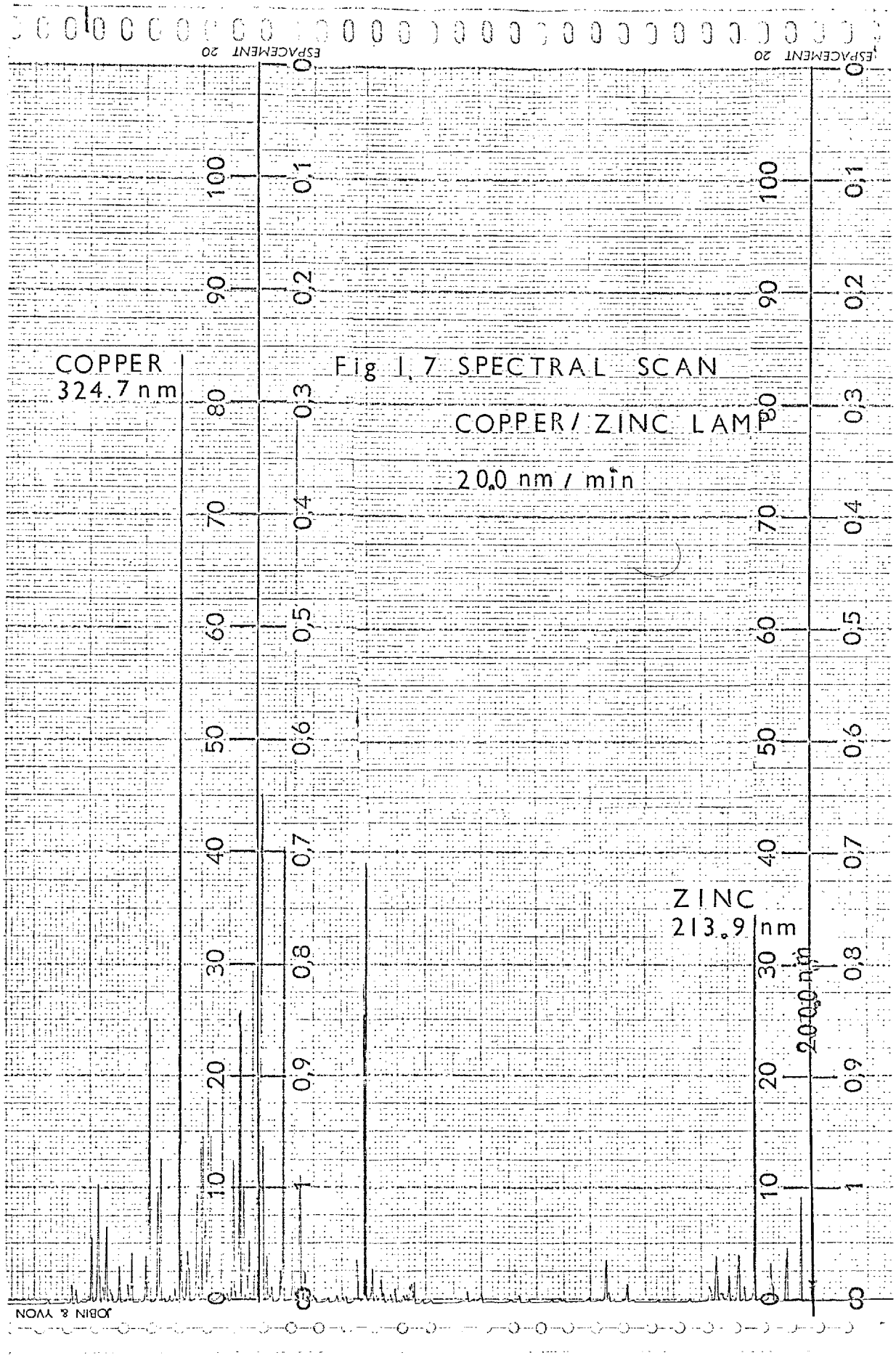


Fig I.7 SPECTRAL SCAN COPPER / ZINC LAMP

Atomic absorption.

All three hollow-cathode lamps were tested using oxidising air-acetylene flames and standard salt solutions. Detection limits were defined as that concentration of element which would produce a recorder deflection equivalent to twice the standard deviation of the baseline. They are indicative of the potential sensitivity of the determinations.

Optimum working conditions.

Element	Atomic line nm	Lamp	mA Lamp current	mm Slit width	mm Slit height	Salt
Copper	324.7	Cu/Zn	4.0	0.2	5.0	$CuSO_4.5H_2O$
Zinc	213.9	Cu/Zn	4.0	0.5	10.0	$ZnSO_4.7H_2O$
Lead	217.0	Pb	4.0	0.5	14.0	$Pb(NO_3)_2$
Iron	248.3	Fe	8.0	0.2	5.0	$(NH_4)_2SO_4.FeSO_4.6H_2O$

Standard calibrations.

Element & figure		x: Concentrations in ppm y: Equivalent absorbance ranges	Detection limit ppm
Cu(1.8)	x	0.5 - 1.0 - 2.0 - 4.0	0.15
	y	0.03 - 0.08 - 0.14 - 0.28	
Zn(1.8)	x	0.125 - 0.25 - 0.5 - 1.0	0.03
	y	0.04 - 0.09 - 0.18 - 0.40	
Pb	x	2.0 - 4.0 - 10.0 - 20.0	-
	y	0.05 - 0.10 - 0.26 - 0.52	
Pb(1.9)	x	0.4 - 0.8 - 1.2 - 1.6	0.25
	y	0.06 - 0.15 - 0.24 - 0.36	
Fe	x	2.0 - 4.0 - 10.0 - 20.0	-
	y	0.08 - 0.16 - 0.42 - 0.71	
Fe(1.10)	x	0.4 - 0.8 - 1.2 - 1.6	0.05
	y	0.03 - 0.06 - 0.10 - 0.16	

Fig 1.8 COPPER AND ZINC A A

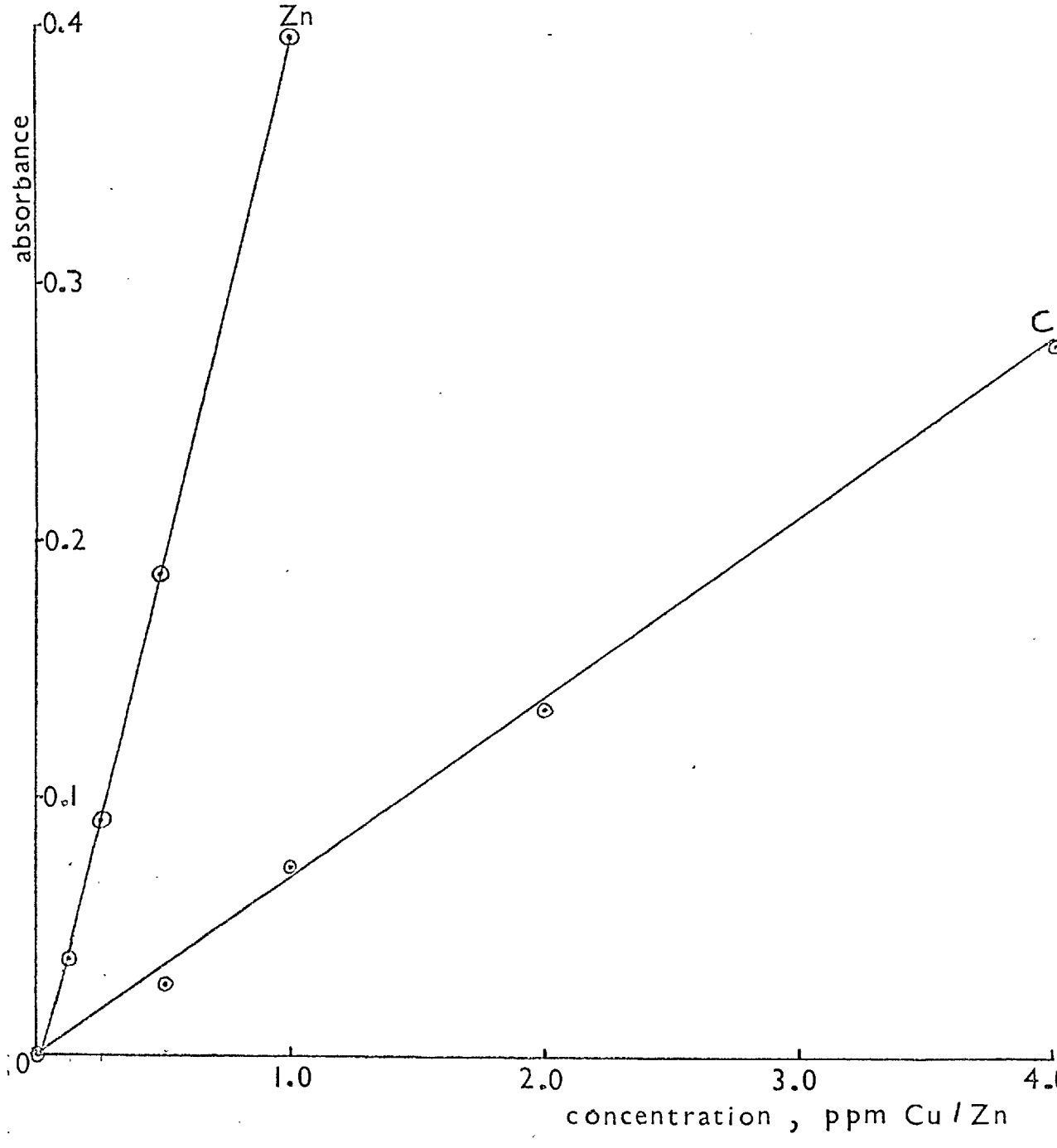


Fig 1.9 LEAD A A

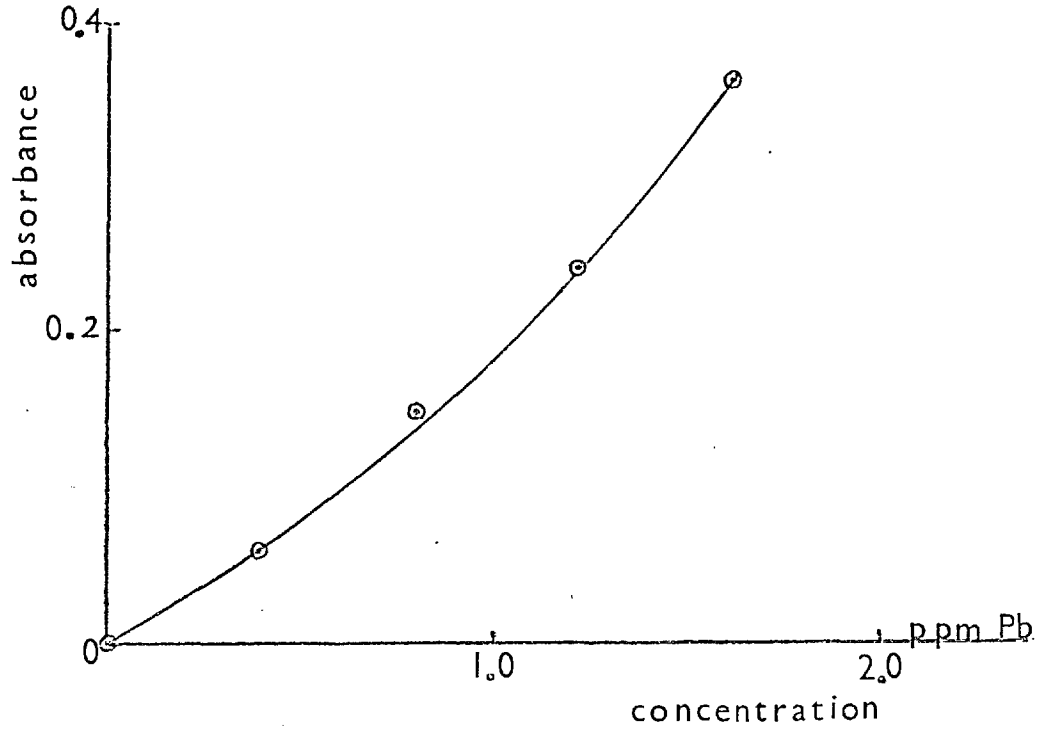
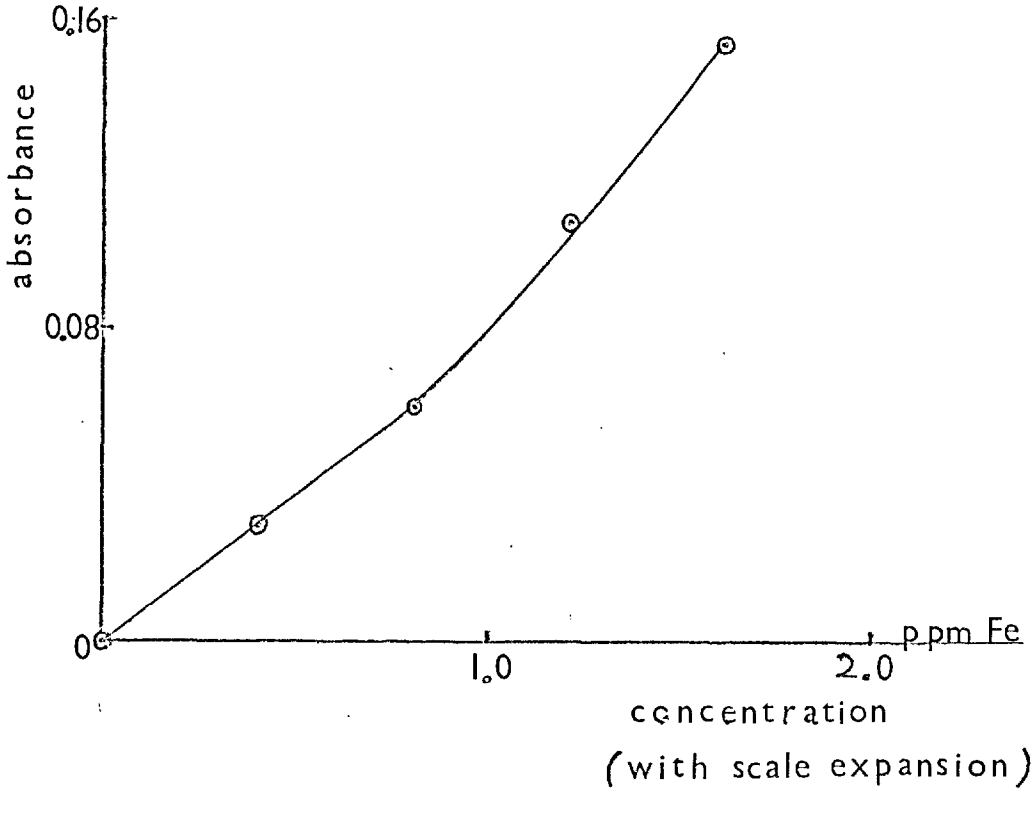


Fig 1.10 IRON A A



Atomic emission: air-acetylene flame.

Calcium, strontium and barium were determined first, using diluted solutions which contained salts of all three, and a reducing air-acetylene flame. Emission was measured at the most sensitive emission line for each element. The response was poorest for barium. The reflector mirror was used to enhance emission signals, but the scale expansion facility was unavailable.

Optimum working conditions.

Element	Atomic line nm	mm Slit width	mm Slit height	Salt
CALCIUM	422.7	0.1	2.5	$CaCo_3$
STRONTIUM	460.7	0.1	4.0	$SrCl_2.6H_2O$
BARIUM	493.5	0.4	8.0	$Ba(NO_3)_2$

Standard calibrations.

Element & figure		x: Concentrations in ppm y: Equivalent transmission %				Detection limit ppm
Ca(1.11)	x	2.0	- 4.0	- 10.0	- 20.0	
	y	10.5	- 22.5	- 54.0	- 82.0	-
Ca	x	1.0	- 2.0	- 4.0	- 10.0	0.1
	y	5.0	- 11.5	- 25.0	- 49.5	
Sr(1.11)	x	0.5	- 1.0	- 2.5	- 5.0	-
	y	5.5	- 12.0	- 37.5	- 75.0	
Sr(1.12)	x	0.25	- 0.5	- 1.25	- 2.5	-
	y	5.5	- 11.0	- 25.5	- 52.0	
Sr(1.12)	x	0.0125	- 0.025	- 0.05	- 0.1	0.007
	y	2.5	- 6.5	- 10.0	- 20.0	
Ba(1.11)	x	5.0	- 10.0	- 25.0	- 50.0	-
	y	3.0	- 5.0	- 20.0	- 48.5	
Ba	x	2.5	- 5.0	- 12.5	- 25.0	1.25
	y	12.5	- 20.0	- 47.5	- 90.5	

Fig 1.11 CALCIUM, STRONTIUM AND BARIUM A E

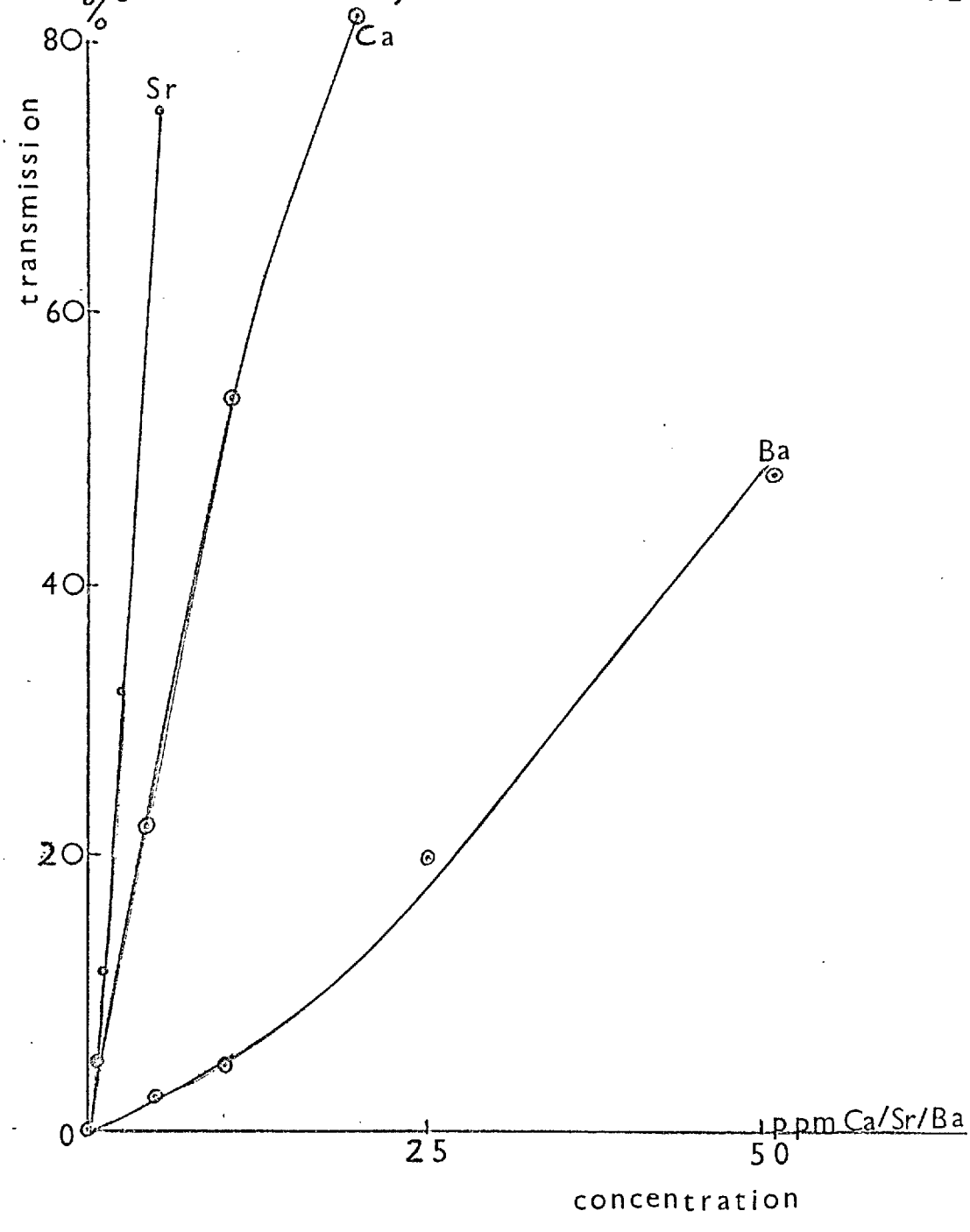
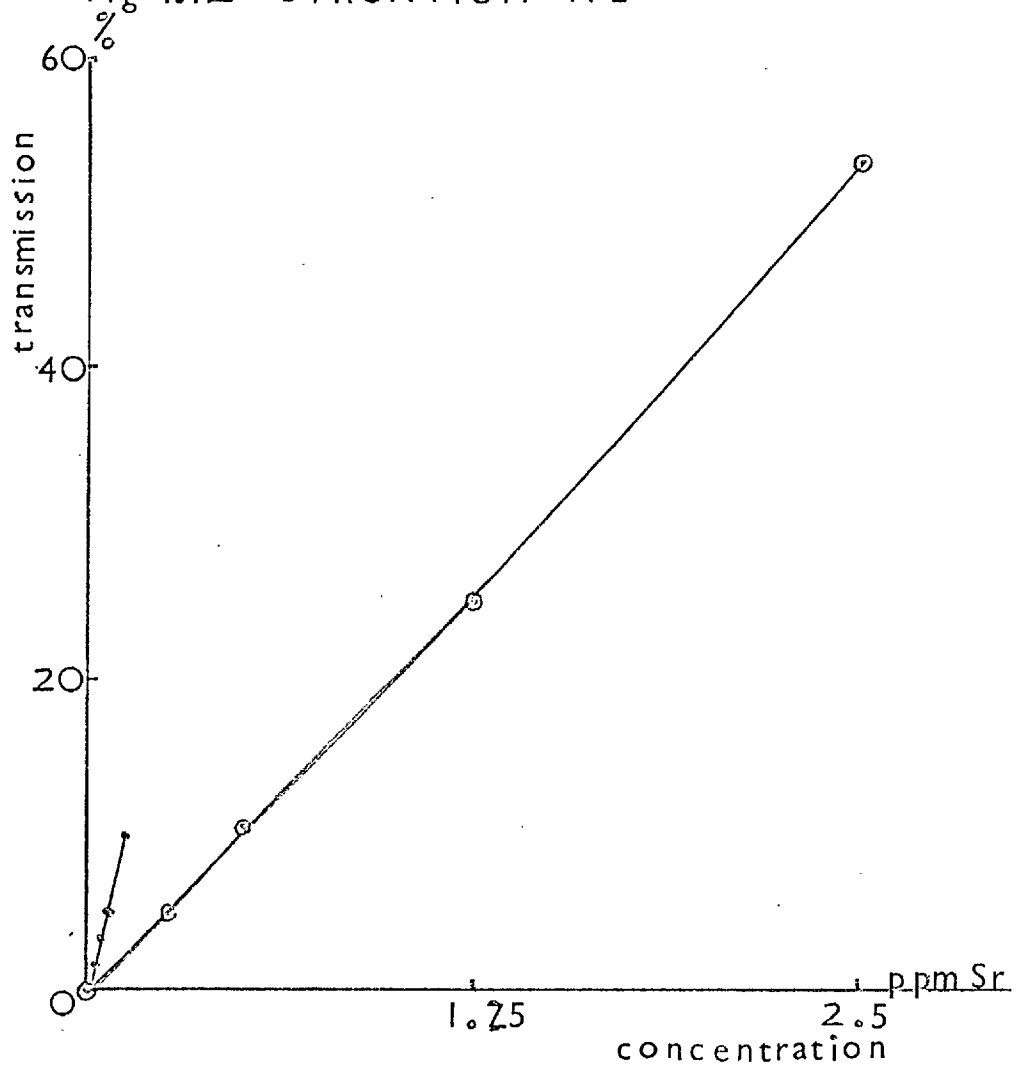
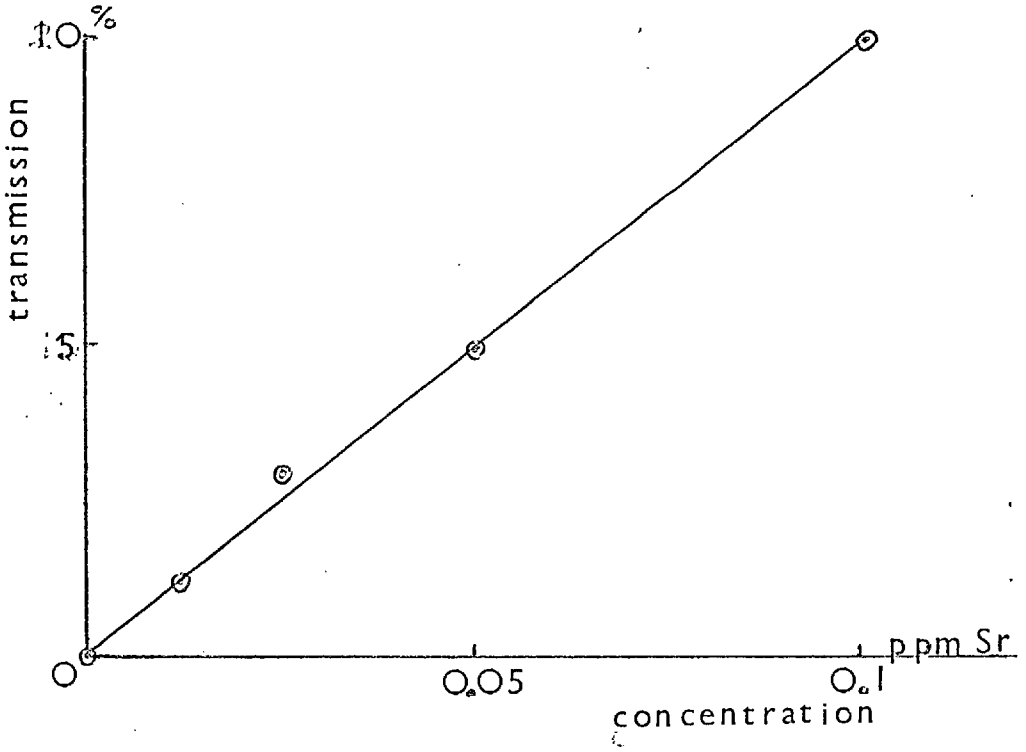


Fig 1.12 STRONTIUM A E





Atomic emission: nitrous oxide-acetylene flame.

Aluminium, which forms a refractory oxide, could be easily determined using the high temperature nitrous oxide-acetylene flame. Molybdenum emission from this flame was examined in greater detail but less successfully.

Optimum working conditions.

Element	Atomic line nm	mm Slit width	mm Slit height	Salt
ALUMINIUM	396.1	0.1	2.0	K_2SO_4. $Al_2(SO_4)_3 .24H_2O$

Standard calibrations.

Element & figure		x: Concentrations in ppm y: Equivalent transmission %	Detection limit ppm
Al	x	10.0 - 20.0 - 50.0 - 100.0	-
	y	8.0 - 17.0 - 40.5 - 70.5	
Al	x	0.5 - 1.0 - 2.0 - 5.0 - 10.0	-
	y	4.0 - 7.0 - 14.0 - 36.0 - 69.0	
Al(1.13)	x	0.1 - 0.2 - 0.5 - 1.0	0.04
	y	3.5 - 6.5 - 17.0 - 38.0	

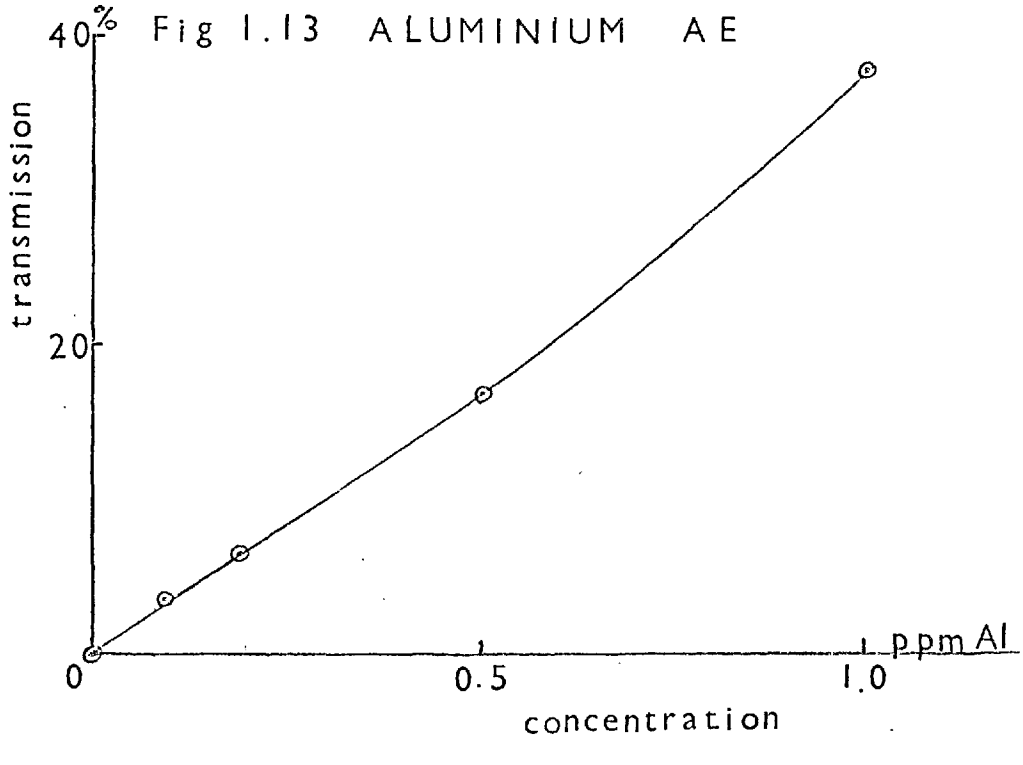


Fig 1.13 ALUMINIUM AE

Molybdenum has been determined by AE, but requires a high temperature flame to avoid interference effects due to the refractory nature of its oxide. It was, therefore, decided to test the equipment with this emission determination. Several analytical lines are available, although sometimes the sensitivity is low or flame background interferes. In these experiments the reflector mirror was usually used, and a fuel-rich flame. The acetylene pressure was adjusted so that the red feather flame was just without yellow lines due to C_2, thus minimising the formation of Mo-O species.

A spectrum of the nitrous oxide-acetylene flame was run from 300.0 nm to 700.0 nm. Then 100 ppm molybdenum solution and water were nebulised separately, and measured at the molybdenum atomic lines, to test initial responses. Molybdenum lines coincident with emissions by -CN, -OH, etc. species, were avoided, and results considered in conjunction with general recommendations before selecting lines to examine in detail.

Choice of atomic line for molybdenum AE.

Atomic line nm	Literature recommended use *		Selected here for tests
311.2			-
313.3	AA		1
315.8			4
317.0	AA		-
319.4			3
320.9			5
379.8	AA	AE	-
386.4		AE	-
390.3		AE	2

* Most references are to non-nitrous oxide flames, where cyanide bands, which interfere at 379.8 nm for example, are absent.

Calibrations produced smooth curves, linear up to approximately 20 ppm molybdenum, then bending down toward the concentration axis. Reproducibility was poor at low concentrations, and time for calibrations limited by the accumulation of carbon around the burner slit. All conditions except the lowest concentration ranges of 313.3, 315.8, 320.9 nm provided fair calibrations. The 390.3 and 319.4 nm lines were most sensitive, with good signals obtainable down to 0.1 ppm, linear calibrations and low background emission. This range could be extended by careful choice of slit-width, use of damping, and a working x 5 scale expansion facility.

Optimum working conditions.

Element	Atomic line nm	Slit mm width	Slit mm height	Salt
MOLYBDENUM	various	0.25	10.0	$(NH_4)_6 Mo_7 O_{24} .4H_2O$

Standard calibrations for molybdenum AE.

nm line & figure		x: Concentrations in ppm y: Equivalent transmission %	Detection limit ppm
313.3	x	10.0 - 20.0 - 40.0 - 60.0 - 80.0 - 100.0	-
	y	6.5 - 20.0 - 31.0 - 37.5 - 42.0 - 45.5	
313.3	x	2.0 - 5.0 - 10.0 - 20.0	-
	y	5.0 - 8.0 - 13.5 - 20.0	
313.3	x	1.0 - 2.0 - 5.0 - 10.0 - 20.0	0.7
	y	1.5 - 3.5 - 7.5 - 17.5 - 24.0	
313.3 (1.14)	x	20.0 - 40.0 - 60.0 - 80.0 - 100.0	-
	y	33.0 - 55.5 - 73.5 - 89.0 - 100.0	
313.3 (1.14)	x	20.0 - 40.0 - 60.0 - 80.0 - 100.0	(without mirror)
	y	27.5 - 42.0 - 52.0 - 61.0 - 67.5	
390.3	x	10.0 - 20.0 - 40.0 - 60.0 - 80.0 - 100.0	-
	y	12.0 - 23.0 - 44.0 - 62.0 - 78.0 - 92.0	
390.3	x	10.0 - 20.0 - 40.0 - 60.0 - 80.0 - 100.0	(without mirror)
	y	4.0 - 9.5 - 19.0 - 33.0 - 44.0 - 53.0	
390.3	x	4.0 - 6.0 - 10.0 - 20.0 - 30.0 - 40.0	-
	y	10.0 - 14.0 - 22.0 - 40.0 - 59.0 - 77.0	
390.3 (1.15)	x	0.5 - 1.0 - 2.0 - 3.0 - 4.0 - 5.0	-
	y	4.0 - 7.0 - 14.0 - 20.0 - 24.5 - 30.0	
390.3	x	0.1 - 0.2 - 0.3 - 0.4 - 0.5 - 1.0	0.08
	y	1.3 - 2.5 - 5.5 - 6.8 - 9.8 - 12.3	
319.4	x	5.0 - 10.0 - 20.0 - 40.0 - 60.0	-
	y	9.0 - 13.5 - 23.0 - 41.5 - 58.0	
319.4 (1.16)	x	0.5 - 1.0 - 2.0 - 5.0 - 10.0	-
	y	4.5 - 9.0 - 32.5 - 32.5 - 55.0	
319.4	x	0.1 - 0.2 - 0.3 - 0.4 - 0.5 - 1.0	0.05
	y	2.0 - 3.5 - 4.0 - 6.0 - 7.5 - 9.8	
315.8	x	5.0 - 10.0 - 20.0 - 40.0 - 60.0	-
	y	2.0 - 3.0 - 5.2 - 9.5 - 14.2	
315.8	x	0.5 - 1.0 - 2.0 - 5.0 - 10.0	0.5
	y	1.1 - 1.8 - 2.5 - 5.2 - 7.5	
320.9	x	5.0 - 10.0 - 20.0 - 40.0 - 60.0	-
	y	3.5 - 5.5 - 11.0 - 20.0 - 62.0	
320.9	x	0.5 - 1.0 - 2.0 - 5.0 - 10.0	0.8
	y	0.6 - 1.2 - 2.7 - 5.7 - 9.7	

Fig 1.14 MOLYBDENUM A E 313.3 nm

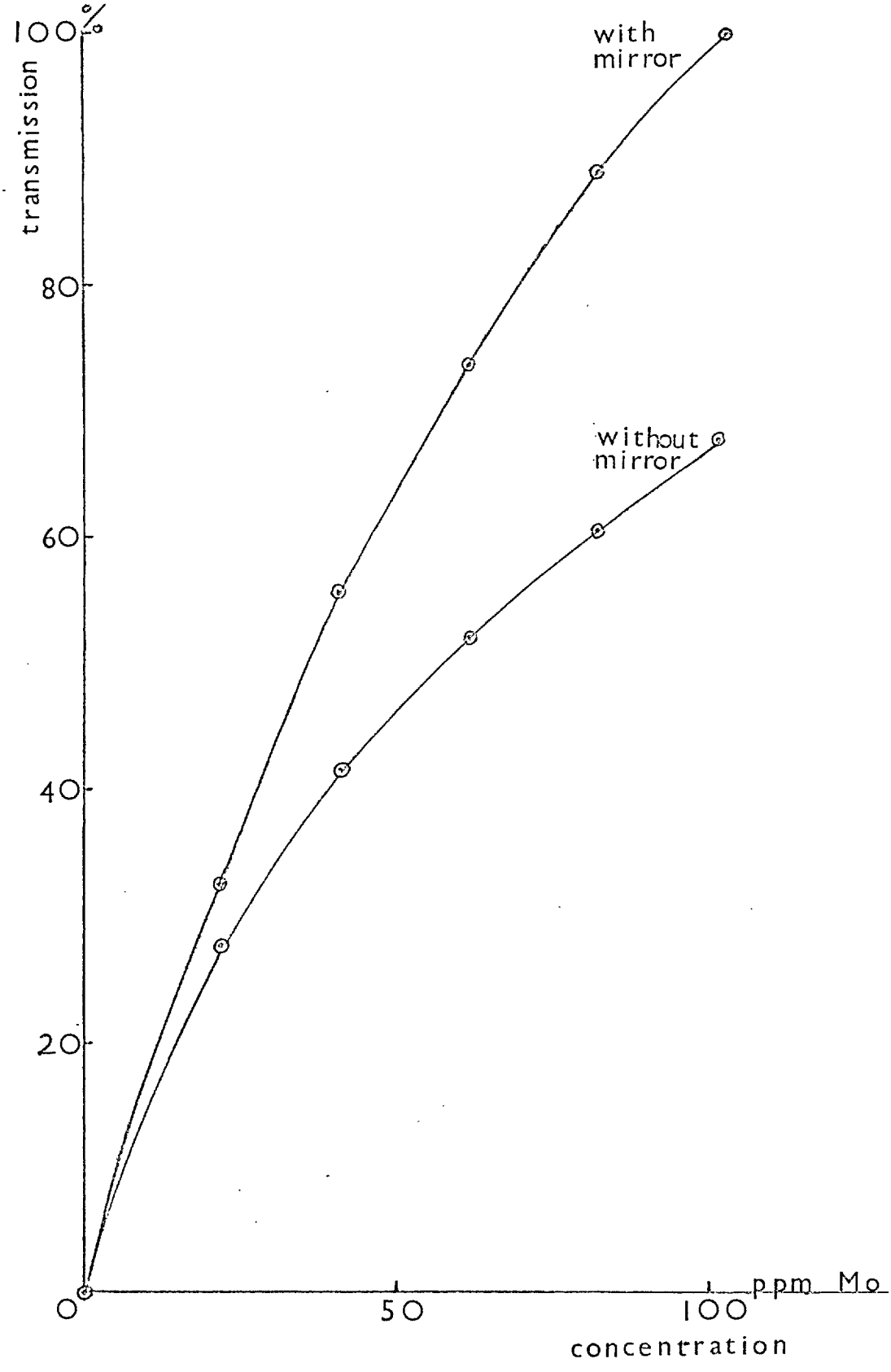


Fig 1.15 MOLYBDENUM A E 390.3 nm

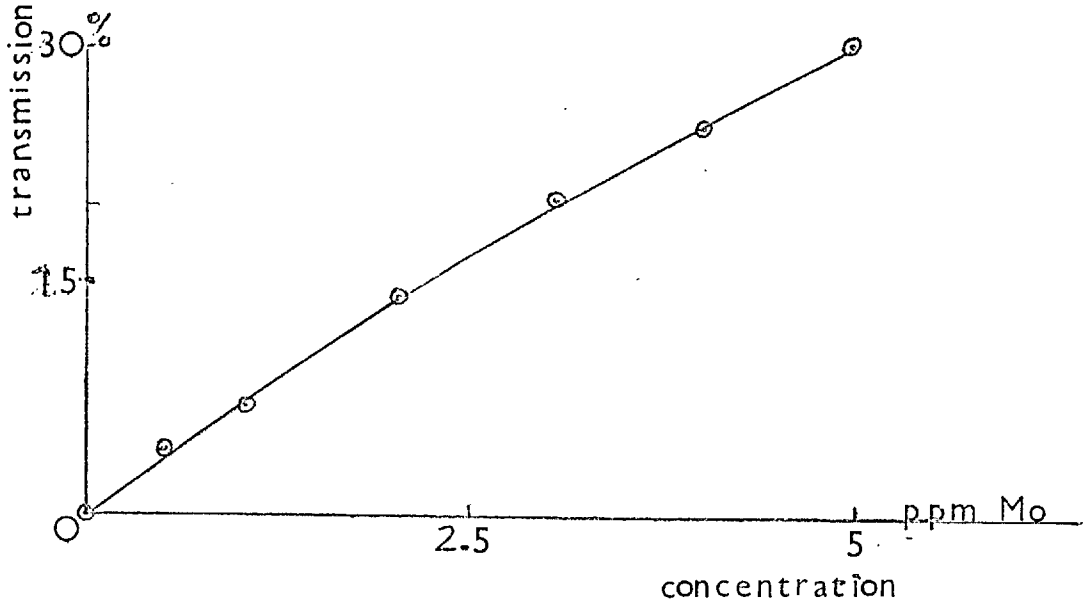
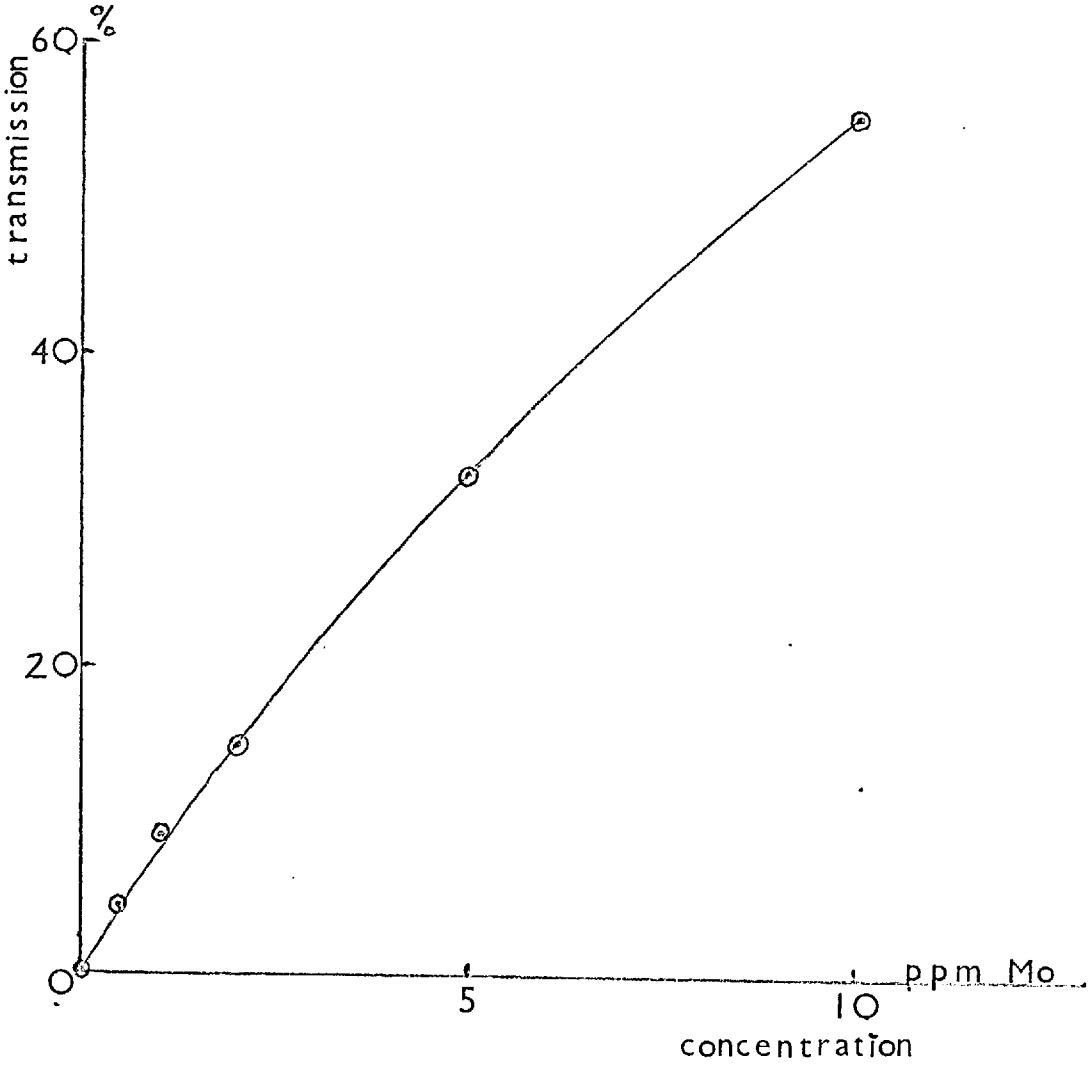


Fig 1.16 MOLYBDENUM A E 319.4 nm



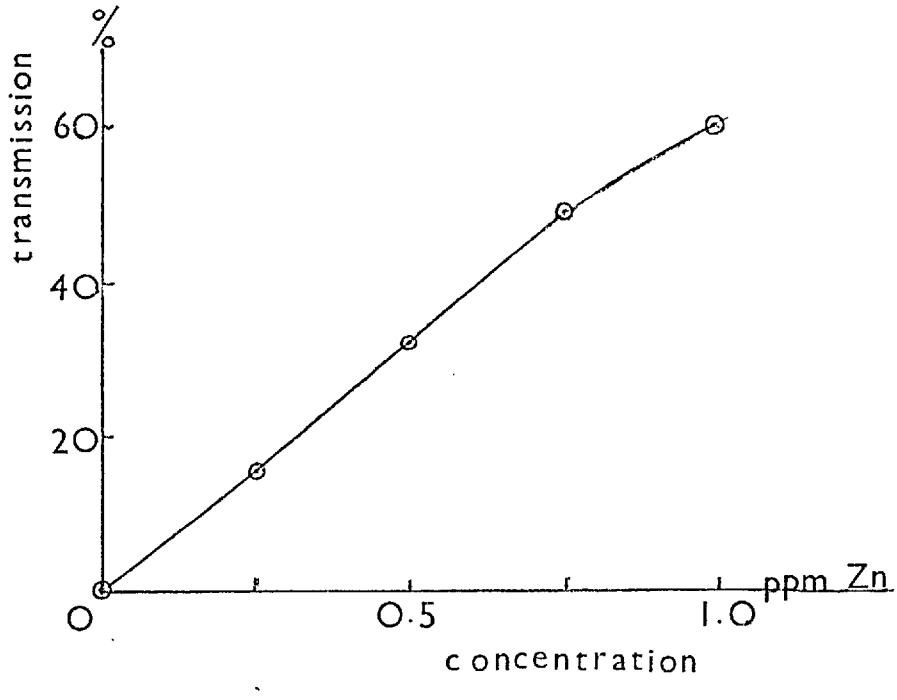
Atomic fluorescence.

Since the equipment was not intended for AF it was necessary to move the emission chopper round by 90° and provide an electrodeless discharge lamp (EDL) for the atomic line source. Neither is the long-path burner suited to fluorescence measurements. Therefore, only zinc AF was tested; a reasonable exploratory calibration curve was obtained.

Optimum working conditions.					
Element	Atomic line nm	Flame	nm Slit-width	Slit-height	Salt
ZINC	213.9	air-C_2H_2	0.1	10.0	$ZnSO_4.7H_2O$

Standard calibration.			
Element & figure	x: Concentrations in ppm y: Equivalent transmission %		Detection limit ppm
Zn(1.17)	x	0.25 - 0.5 - 0.75 - 1.0	0.02
	y	15.0 - 32.0 - 49.0 - 60.5	

Fig 1.17 ZINC AF



1.5 Conclusions.

The flame spectroscopy experiments ended when sufficient components of the laser microprobe system were available for its assembly to begin.

The foregoing experiments served to assess individual aspects of the equipment and demonstrate its suitability for the analysis of simple aqueous solutions, although interference studies were not included. Despite some criticism of the components the equipment promises to be versatile in practice. In conjunction with the informative handbook (2) and after preparation of calibration curves appropriate to the conditions, it should prove useful for a variety of analytical control tests.

During the work, experience of equipment assessment and the theory and practice of atomic spectroscopic techniques was gained, which was of value in subsequent studies.

CHAPTER 2

LASER MICROPROBE EMISSION SPECTROSCOPY

2.1 Introduction to the technique and this project.

The availability of a Jarrell-Ash Mark II Laser Microprobe provided an opportunity to assess and develop an uncommon atomisation source for atomic spectroscopy. In this technique, a laser beam is used to vaporise small areas of solid surfaces, and the resultant sample is analysed *in situ* by atomic spectroscopic methods.

The original aim of this project was to examine the suitability of the laser microprobe for the determination of trace amounts of sulphur, nitrogen, oxygen, carbon or hydrogen in nickel base and niobium base alloys. However, due to unforeseen circumstances and instrumental breakdown, much of the work concerned only the assembly of the microprobe and auxiliary equipment. Optimum operating conditions for atomic emission spectroscopy were found by examining simple metallic samples before attempting to extend the range to more complex systems.

2.2 Review: The development of the laser microprobe and its application to chemical analysis.

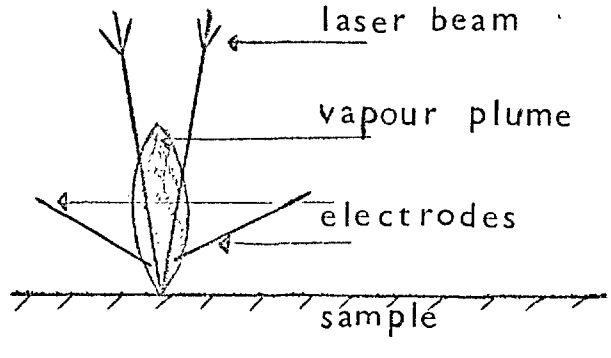
Introduction.

In the attempt to obtain complete sample atomisation for atomic spectroscopy, many methods have been tried.

Among the so-called flameless techniques, methods of vaporising material from the solid state include sampling by a laser pulse. An intense, monochromatic and coherent, laser light beam is focussed on the sample.

The costly and destructive concentrated output of a giga-watt pulsed laser has been tried (3). Now a moderated pulse of medium power is used to vaporise microportions of material for analysis, and so provide a vapour plume spectroscopic source. Efficient excitation of the vapour to spectral emissive levels is achieved by cross-excitation: discharge between two graphite electrodes positioned symmetrically over the sample, as illustrated (Fig.2.1), (4). Radiation is detected either by direct emission spectrography or indirectly by incorporation into an AA system.

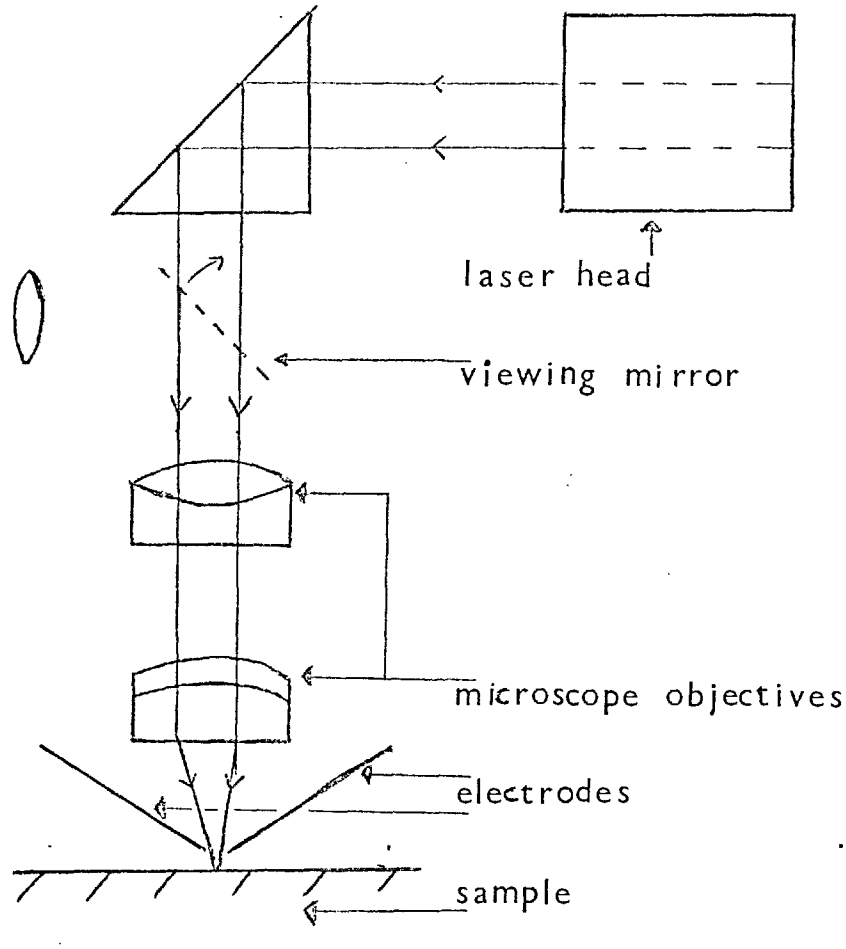
Fig2.1 LASER SAMPLING WITH CROSS-EXCITATION



Instrumentation.

In 1962, the Jarrell-Ash Mark I Laser Microprobe was introduced: the first commercially available equipment to use a laser beam for sampling and primary excitation in emission spectrographic analysis (5). Most workers have used this system, and alternatives introduced to overcome shortcomings of the original have usually followed the same basic form (Fig.2.2).

Fig 2.2 THE LASER MICROPROBE OPTICAL SYSTEM



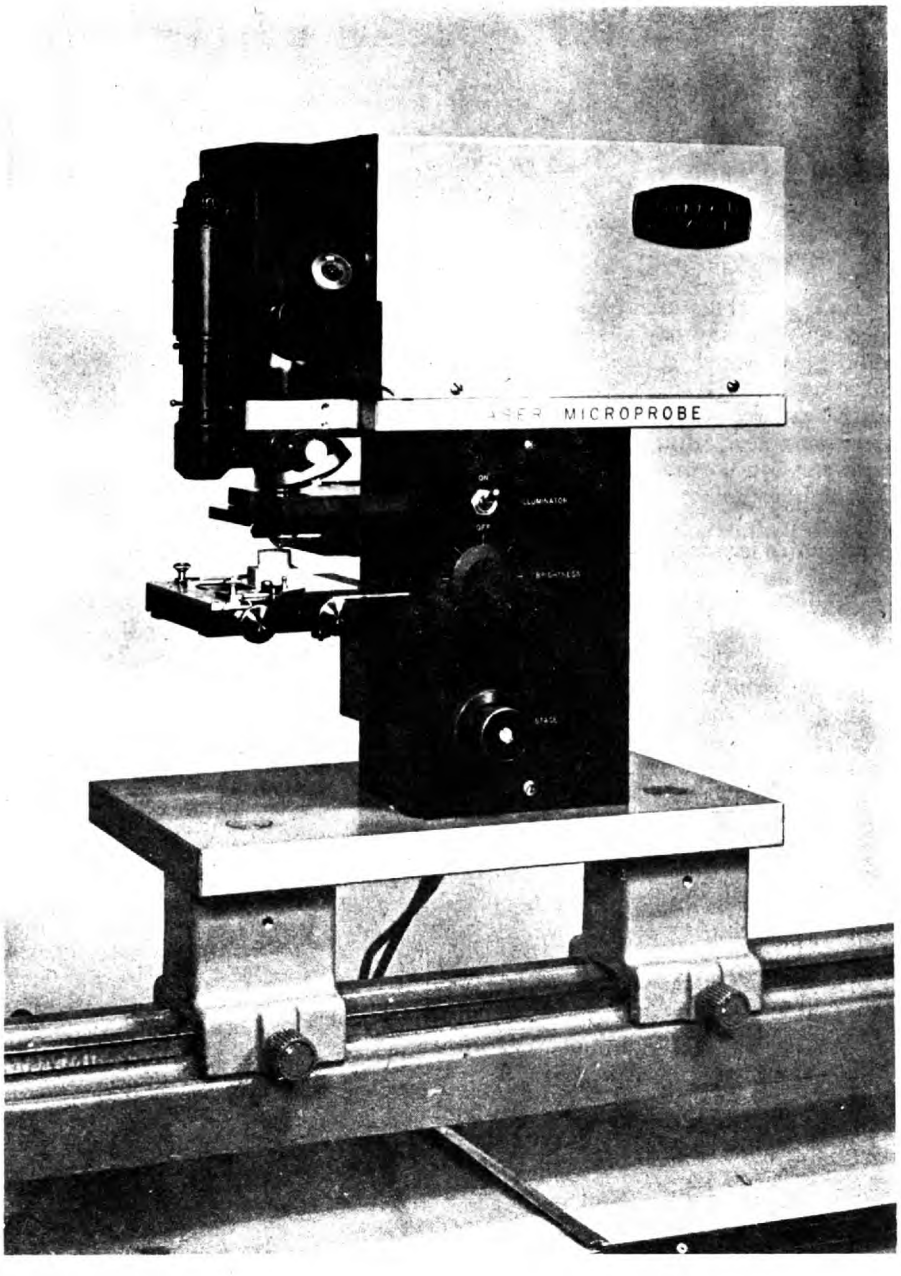


Fig 2.3 THE JARRELL–ASH MARK I LASER MICROPROBE

The ruby laser microprobe.

Operation and probable numerical parameters.

A 30 nanosecond pulse from a Q-switched ruby laser is focussed by a metallurgical microscope onto a pre-selected area of sample. Sufficient energy is absorbed to vaporise 0.5-20 μg of material from a hemispherical portion of radius 25-100 microns. The actual amount ejected and the crater shape are related to the type of substance examined. In the process of atomisation some of the atoms are excited, but additional excitation is achieved by causing the vapour plume to short-circuit an electrical gap of 1-2 mm between graphite electrodes. A capacitive standing voltage of 1-2 Kv is applied between these. Firing takes 1-2 milliseconds and may be repeated at one-minute intervals.

The microscope unit normally operates aligned to a spectrograph and a separate unit contains power supplies, energy storage banks and the laser triggering system.

Several workers have given detailed descriptions of this instrumentation (7, 8). Two others include a photograph of a microscope unit, and of these the former includes a full account of the laser and microscope optics (9, 10).

Experimental limitations.

Practical applications demonstrate some disadvantages of the ruby laser microprobe. It is a qualitative rather than quantitative tool. Therefore, several modifications to improve performance have been suggested (4).

The basic system requires samples and standards of similar geometry, and must be operated in an air-conditioned laboratory to obviate temperature-dependent laser output.

The intense laser beam damages the lens system through which it travels so the introduction of a filter at the exit of the laser-head to transmit only 40% of the light pulse is recommended. The front lens of the objective can also be protected from sample deposition by covering it with transparent plastic film. The exchange of this lens for one of different power increases selectivity of the area and depth of the crater formed when the laser is fired.

Operation in argon suppresses oxidation of the sample surface and decreases cyanogen emission bands. Also, due to the consequent constant humidity, this provides a more reproducible spark discharge.

There remain serious problems of reproducibility of laser output, crater volumes and spectra. Coefficients of variation of up to 30% are reported for 'quantitative' measurements and are generally $\pm$ 10% (4, 11).

The neodymium-glass laser microprobe.

Subsequent laser microprobes have included many of the recommended modifications, examples being the Jarrell-Ash Mark II (11, 12), the Carl Zeiss Jenoptic LMA I (26, 33) and Loma MSL-2 (25).

Typically the laser-head is adapted to contain a neodymium-glass laser which is less temperature sensitive than a ruby crystal, of longer life and of more reproducible

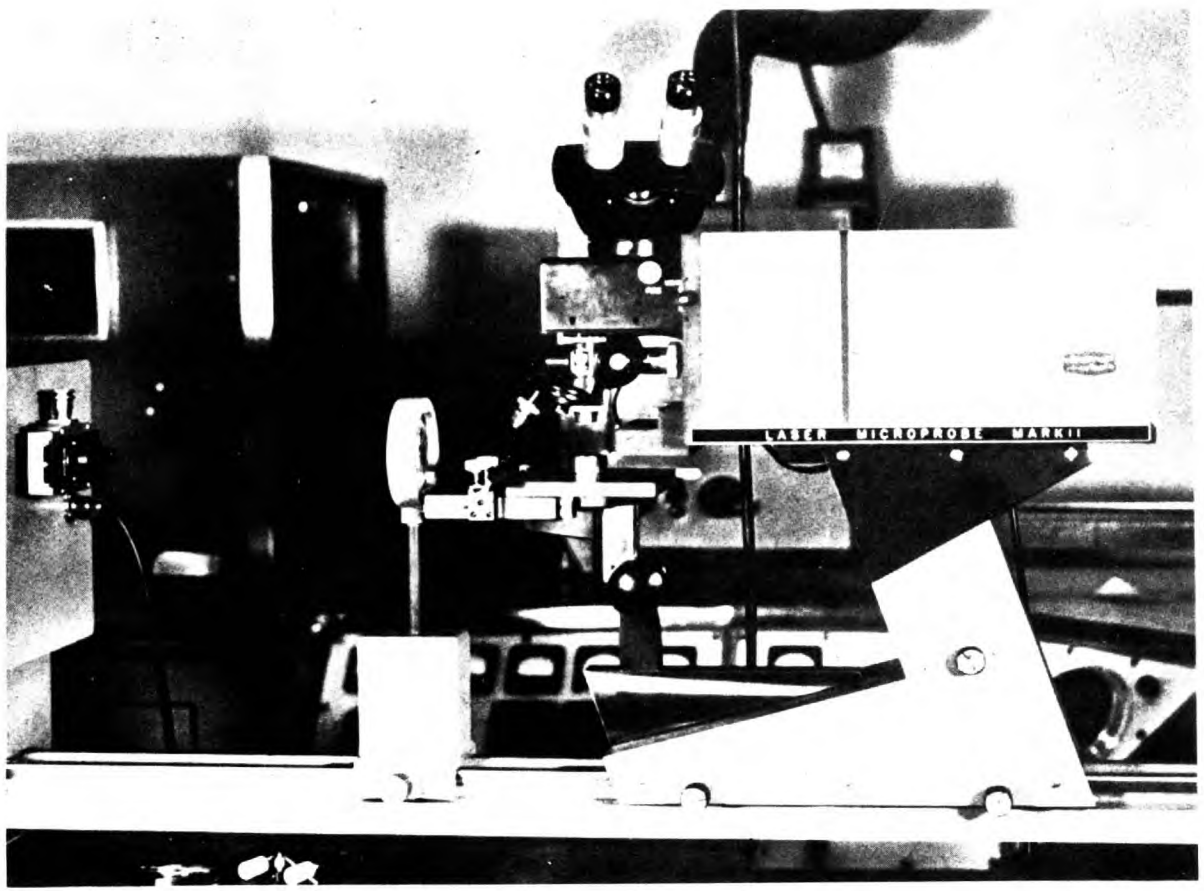


Fig 2.4 THE JARRELL-ASH MARK II LASER MICROPROBE

operating characteristics. A filter is fitted in the head in place of the Q-switching prism to improve control of beam divergence. The lifetime of the laser rod is extended, since an output energy of only 0.05-0.5 J is necessary. Stepwise control of the laser pulse power is available by variation of an aperture via a mode selector switch and further optional attenuation by a 50% filter. The voltage across the spark source can be varied similarly between 1.5 and 2.0 KV.

Selection of the target is aided by a binocular eyepiece on the microscope, and the laser and optical foci are parfocal. Other developments are the safety fitting of manual and electrical interlocks to prevent accidental firing, and an optical-bar mounting facility.

Overall reproducibility is said to be much enhanced

$$\left.\begin{array}{l}\pm\ 3\%\text{, firing at 15-second intervals} \\ \pm\ 10\%\text{, " " 5-second "}\end{array}\right\}\ \text{being}$$

quoted by the makers, and there is certainly some improvement compared to the ruby laser microprobe (12, 13, 14).

Applications to chemical analysis.

Signal detection.

In laser microprobe spectral analysis, the laser beam is focussed on a specific site and usually subsequent spectrographic analysis of the radiant plume provides qualitative elemental analysis of localised sites such as inclusions (15). The atomic absorption characteristics of the vapour cloud formed by the laser action have also been examined (16, 17).

Most recent advances have concerned the development of alternative methods of signal detection. An integrator provides direct readings with time resolution and integration of multiple samplings (27). Photo-electric time differentiation and recording of optical emission are also currently under investigation (28, 29).

Elements.

The instrument has been used in qualitative and semi-quantitative estimations of most common elements (10^{-4}-1% in general), except the noble gases, nitrogen and oxygen. Sensitivity is potentially high, but precision lacking (13). Most work has concerned metallic elements (e.g. 7, 9, 12), but boron, silicon, sulphur and phosphorus lines have also been identified (e.g. 9, 10, 24).

Environments.

Both conducting and non-conducting materials are volatilised: metals, alloys, ores, glasses, rocks and tissue, for example. Therefore, there are applications to metallurgical (12, 22), geological (4, 14) and biological fields (13, 21).

Sample form.

Polished solid sections are preferred to untreated metals or rock slices for comparison with standards (18), although material may be powdered with graphite and examined as pelleted homogeneous powders (19). Biological determinations can be carried out in living or resected tissue,

sectioned or *in situ* (10). Extensive sample preparation is unnecessary so the laser microprobe is a flexible tool. The greatest limitation to quantitative work beyond that imposed by the firing reproducibility is the possibility of matrix effects which may invalidate the comparison of a system to a standard series. Such interferences in metallurgical environments have been examined by several workers, but inconclusively (7, 8, 9, 16, 19, 20, 25). There is also a possibility of suppression of spectral emission in biological and inorganic systems (20, 21).

Specific applications.

The most valuable analytical applications of the laser microprobe have been the non-destructive qualitative identification of elements in inclusions. Examples include boron distribution in steel (22) and oxide defects in glasses (23), the examination of geological samples without extraction from matrix (14), and of specific sites in calcified tissue (10, 24). However, instrumentation requires development if further progress is to be made and useful quantitative results obtained (30). Current developments mainly concern improvement of signal detection (27, 29) and investigation of atmospheric influences on laser sampling and the resulting plumes (31, 32).

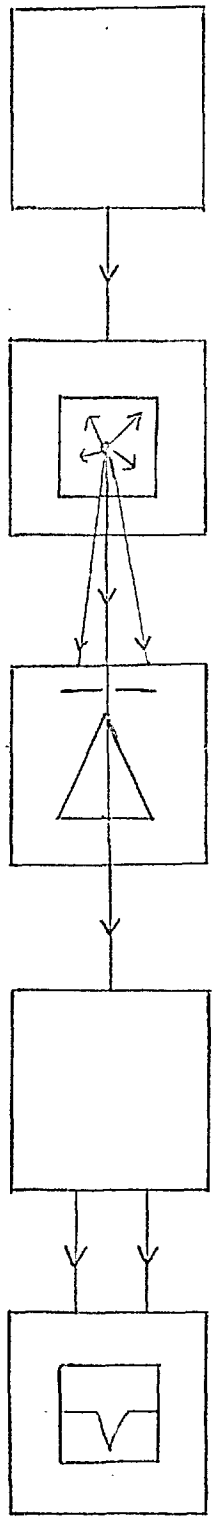
2.3 Instrumentation assembly.

A Jarrell-Ash Mark II neodymium-glass laser microprobe was available, comprising microscope, power unit and transformer. Auxiliary equipment was assembled to form a photoelectric signal detection and measurement system, in contrast to the normal laser microprobe-spectrograph layout.

For the emission spectroscopic measurements, the sampling position of the target on the microscope table was aligned to the entrance aperture of an Optica CF4 Grating Monochromator containing a Bausch and Lomb plane grating blazed for 300.0 nm. This grating was adjusted to diffract light of the wavelength of a chosen atomic line onto the dynodes of an EMI 6256 B photomultiplier. The photomultiplier was mounted perpendicular to one end of the monochromator and contained in a specially constructed light-proof metal housing. A Brandenburg Type PM 2500 R EHT power supply provided the high voltage necessary to measure the emission. Signals were fed into a Telequipment D 535 Storage Oscilloscope with JD Amplifier and TD 57 Time Base, using the 'single shot' facility to record emission against time traces.

It was necessary to trigger the oscilloscope sweep by the firing of the laser. This was achieved by deriving a pulse from the inductive coupling to the cable carrying the laser discharge current, which could be shaped up in voltage and form to meet the oscilloscope requirements for a trigger pulse. The triggering circuit was interposed between the laser power unit and oscilloscope.

Fig.2.5 OUTLINE OF INSTRUMENTATION FUNCTIONS FOR LASER MICROPROBE EMISSION SPECTROSCOPY.



POWER UNIT produces laser pulse.

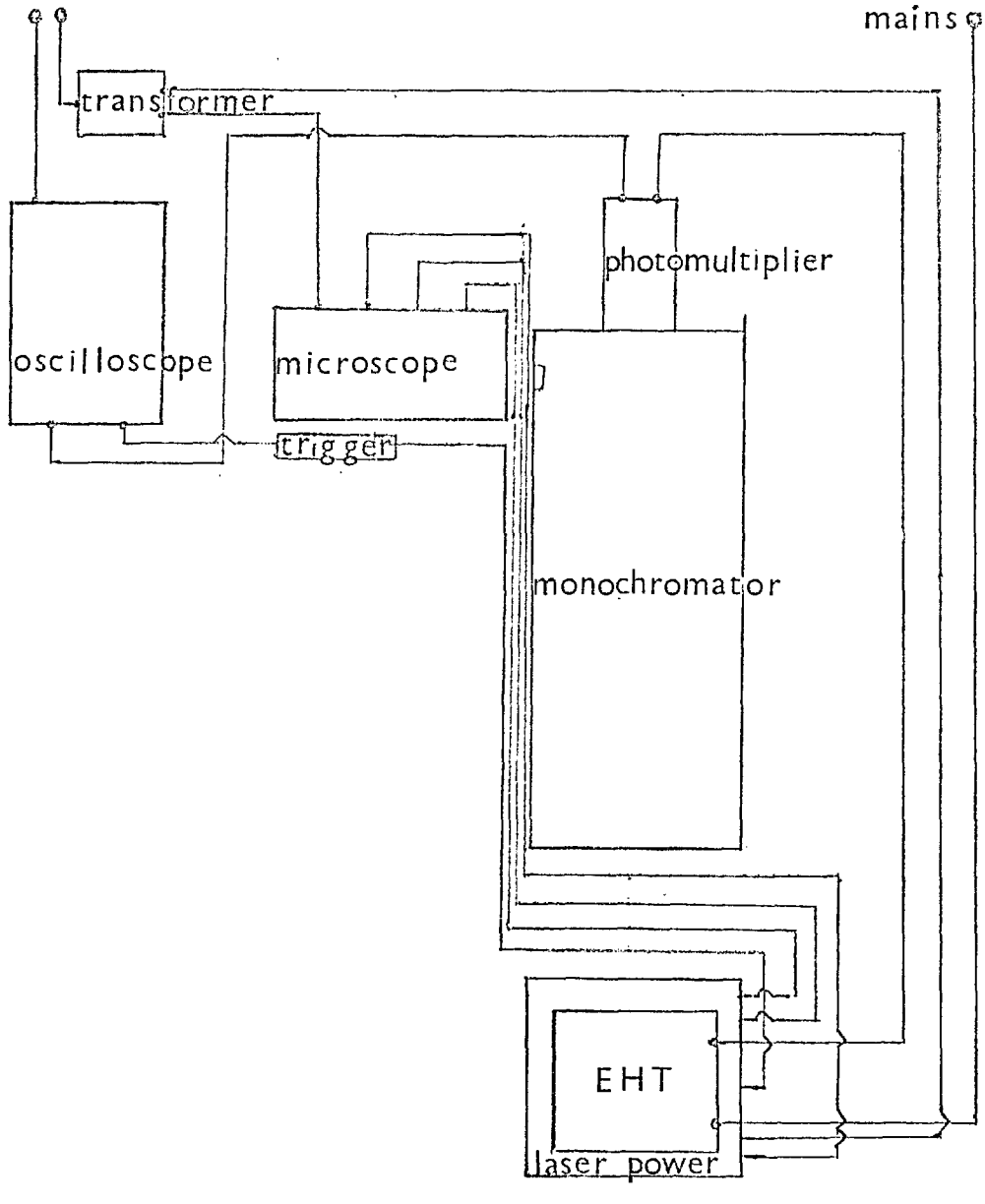
MICROSCOPE focusses beam on target, exciting atoms.

MONOCHROMATOR, via slit and grating selects specific wavelength.

PHOTOMULTIPLIER responds to light signal and magnifies the equivalent electrical signal.

OSCILLOSCOPE records the signal magnitude.

Fig.2.6 INSTRUMENTATION ASSEMBLY FOR LASER MICROPROBE EMISSION SPECTROSCOPY: EXPERIMENTAL ARRANGEMENT AND ELECTRICAL CONNECTIONS.



For safety the equipment was contained in a separate room and the operator's eyes were regularly tested.

2.4 Choice of working conditions.

Technique and normal parameters.

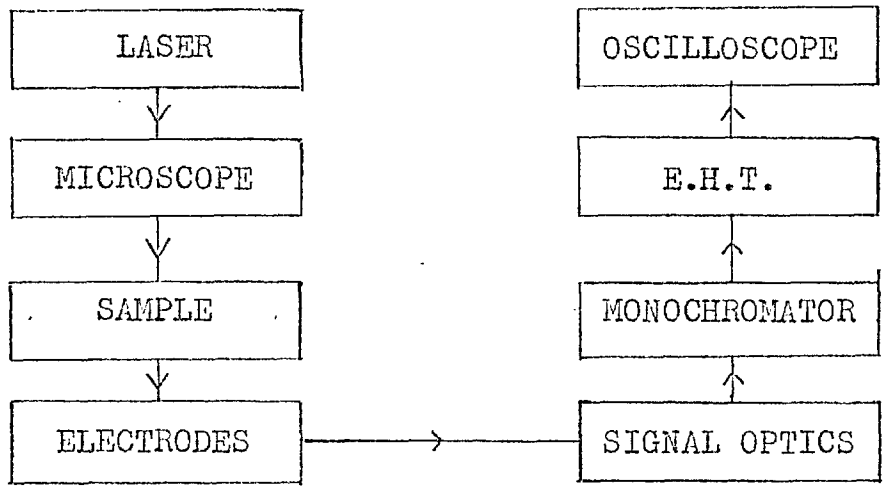
When the laser was fired on a specimen over a series of wavelengths including a spectral line of a component element, a graphical plot of oscilloscope signals against wavelength defined the line position. The following general conditions were used to achieve this and a high signal:background ratio.

With maximum laser power, 1 J, the beam was focussed down through a low power objective lens (32 mm focal length) onto a solid sample open to the atmosphere. As the specimen vaporised, discharge occurred between the two adjacent electrodes, which were separated by a 2 mm air-gap, and pre-set at the maximum cross-excitation voltage of 2000 V. Some of the light emitted reached the entrance aperture of the monochromator to pass through a 0.03 mm slit and be diffracted onto the photomultiplier. This was modified to respond to the final intense signal by the introduction of capacitators between the last four stages. The EHT power supply to the photomultiplier was 900-1000V, and the signals passed to the oscilloscope which was operated without y-scale expansion on a 200 μ sec/cm time base. The resultant emission trace was complex, consisting of a train of four or five peaks of decreasing amplitude occupying about 900 μ secs.

Results were plotted as the sum of the four most intense peak heights against wavelength, recording one or two shots per wavelength for a spectrum, and two or three shots per setting for a calibration. Precautions were taken to ensure reproducibility.

There are many variable components in this system and each was tested until a good working combination for laser emission spectroscopy with cross-excitation had been evolved. Specific aspects will be considered in turn from excitation through to detection as indicated below (Fig.2.7).

Fig.2.7 CHOICE OF WORKING CONDITIONS: CONTRIBUTORY COMPONENTS.



Laser.

Although four power variables were provided, for a range of 0.1 to 1.0 J output energy, only the top two settings were effective in cratering samples.

The choice of a suitable firing frequency is important. This must be high enough to allow work at a useful rate without over-stressing the electrical components (anti-surge fuses in the transformer 'blew' while firing one shot/minute), or the operator. On a given site, reproducibility of $\pm 2.5\%$ was obtained when firing at a steady rate of 1 shot/2 minutes through a determination.

Microscope.

The optical and laser beam focal points should coincide. Therefore, before firing, the microscope must be adjusted for coincidence of an indicator light spot with the cross-wires of the eyepiece, with the sample surface also in focus. Since the objective lenses became pitted by the continual passage of laser pulses, the higher power lens should not be used in conjunction with maximum laser power.

Sample.

Any variations in surface composition are reflected by the signals recorded, so that unless a sample is to be specifically examined for inhomogeneities it should be as homogeneous as possible. A ≈ 1 mm deep planar slice of material, with a shiny rather than matt surface, is easiest to handle and view.

Electrodes.

Signals are affected by the condition and positioning of the cross-excitation electrodes. Abnormally high signals were obtained for the first three or four shots with a new pair, after which signals gradually decreased and background increased as the electrodes wore away asymmetrically and the spark gap increased.

Although most measurements were made at the maximum cross-excitation voltage available, the intermediate 1750 V did give slightly better signal:background ratios.

It was hoped to measure emission signals without cross-excitation for high sensitivity without noisy discharge. The detection system should be adequate, and such usage might

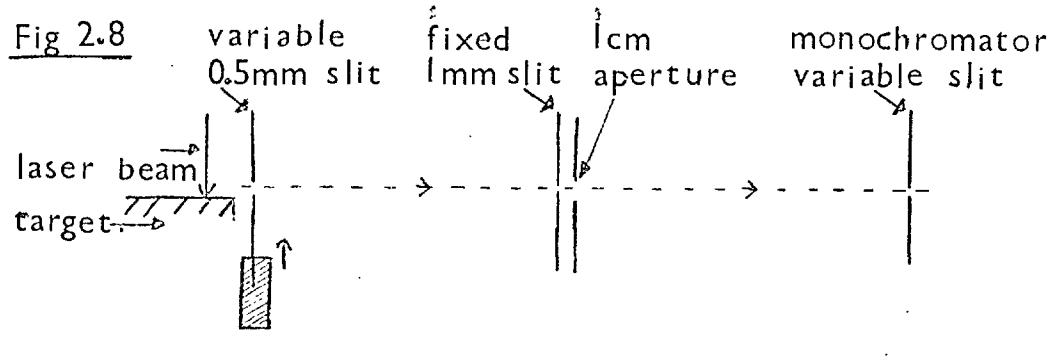
lead on to the laser microprobe's incorporation into AA and AF systems. However, better synchronisation between the laser pulse, triggering circuit and the detector, was required.

Signal optics.

The excited vapour plume emits light in all directions and the maximum amount due to atomic emission must be collected while excluding background as far as possible.

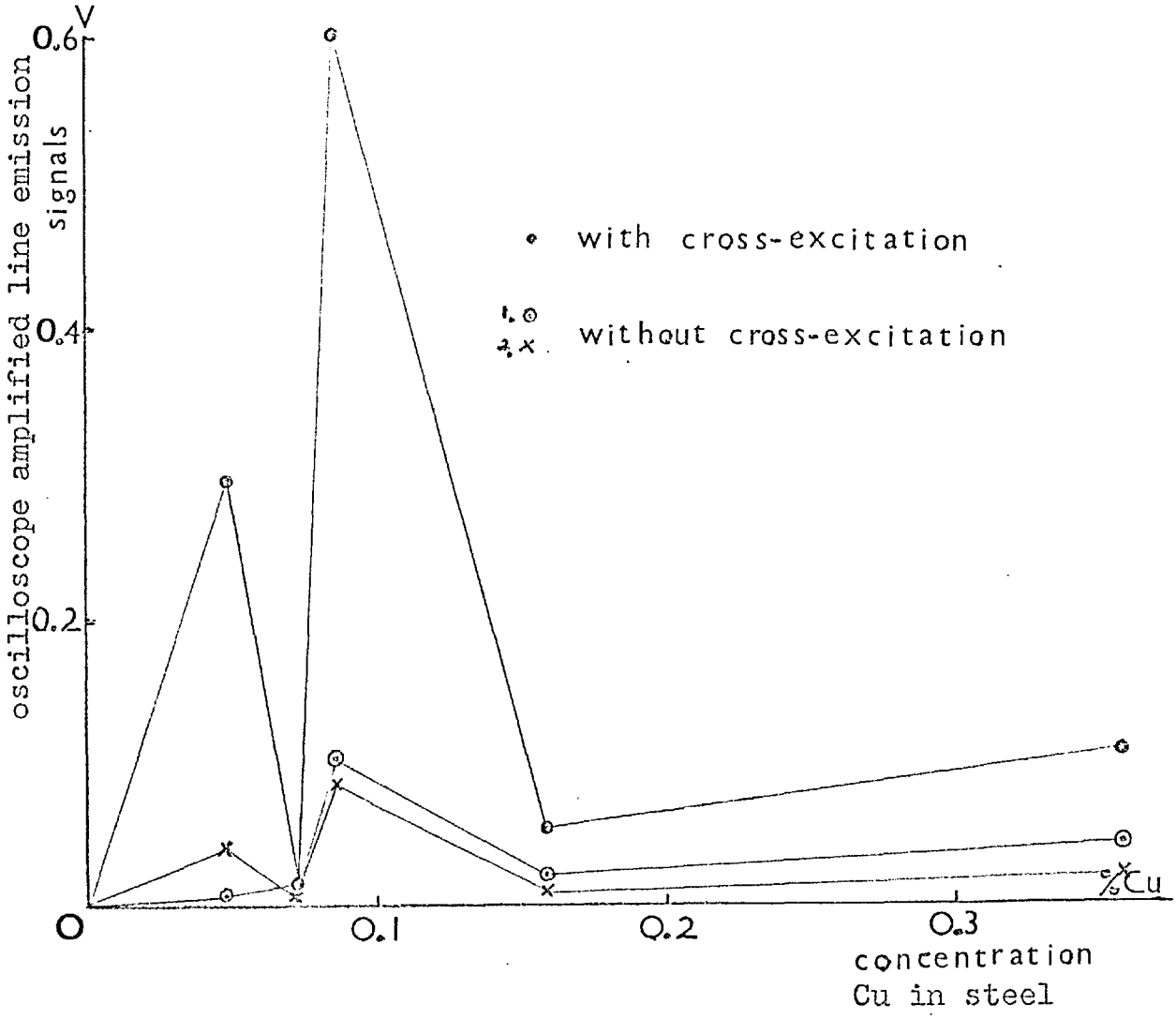
At first, lenses were used to focus emission onto the monochromator slit for a good oscilloscope response. Lenses of different diameters were tried, mounted singly, in doublets, or at either end of a tube, using a miniature bulb to find the best optical alignment for each. However, once the external triggering system was working reliably, it was generally possible to collect adequate emission without using lenses, so long as the microscope was brought as close as possible to the entrance aperture of the monochromator.

Next, an improvement in signal:noise ratios was sought, using a combination of horizontal slits to view only a selected part of the vapour plume and exclude most background emission. One 1 mm slit was mounted across the centre of the monochromator aperture, and a second 0.5 mm slit positioned immediately in front of the target. The height of the latter was varied with respect to the mounted slits (Fig.2.8):



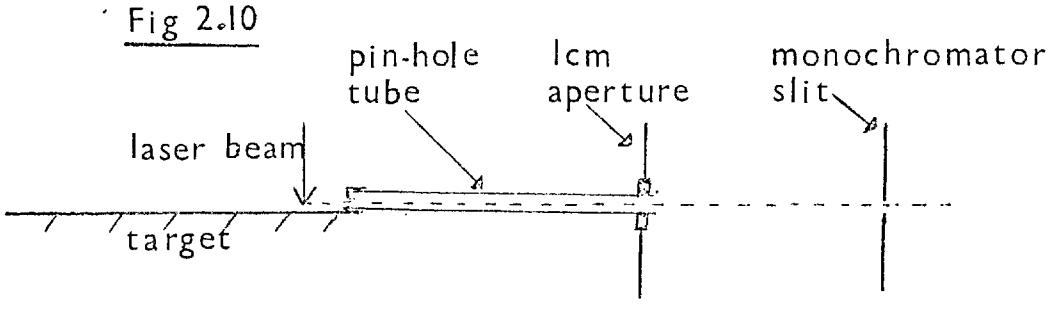
The best viewing positions were with the slit 0.5-1.5 mm above the sample surface. Although signals were small, spectral lines for copper were slightly narrower than without the slit system, signal:noise ratio marginally better and the oscilloscope trace less complex, comprising just one firm peak. However, when such conditions were reproduced in an attempt to obtain a linear calibration for a series of traces in BCS steels (0.047-0.36% copper) the resultant low signals could not be measured with sufficient precision, so the determination was not considered to be successful (Fig.2.9).

Fig 2.9 COPPER AE 327.4 nm



In a further attempt to define the best viewing position precisely, vertical and horizontal 'emission profiles' were obtained for several elemental lines. The microscope was moved with respect to a steady horizontal blackened cupro-nickel collimator tube of length 12.7 cm. and internal diameter 0.5 cm. with alternative screw-in pin-holes of 0.5, 1.0 or 2.0 mm diameter. (Fig.2.10):

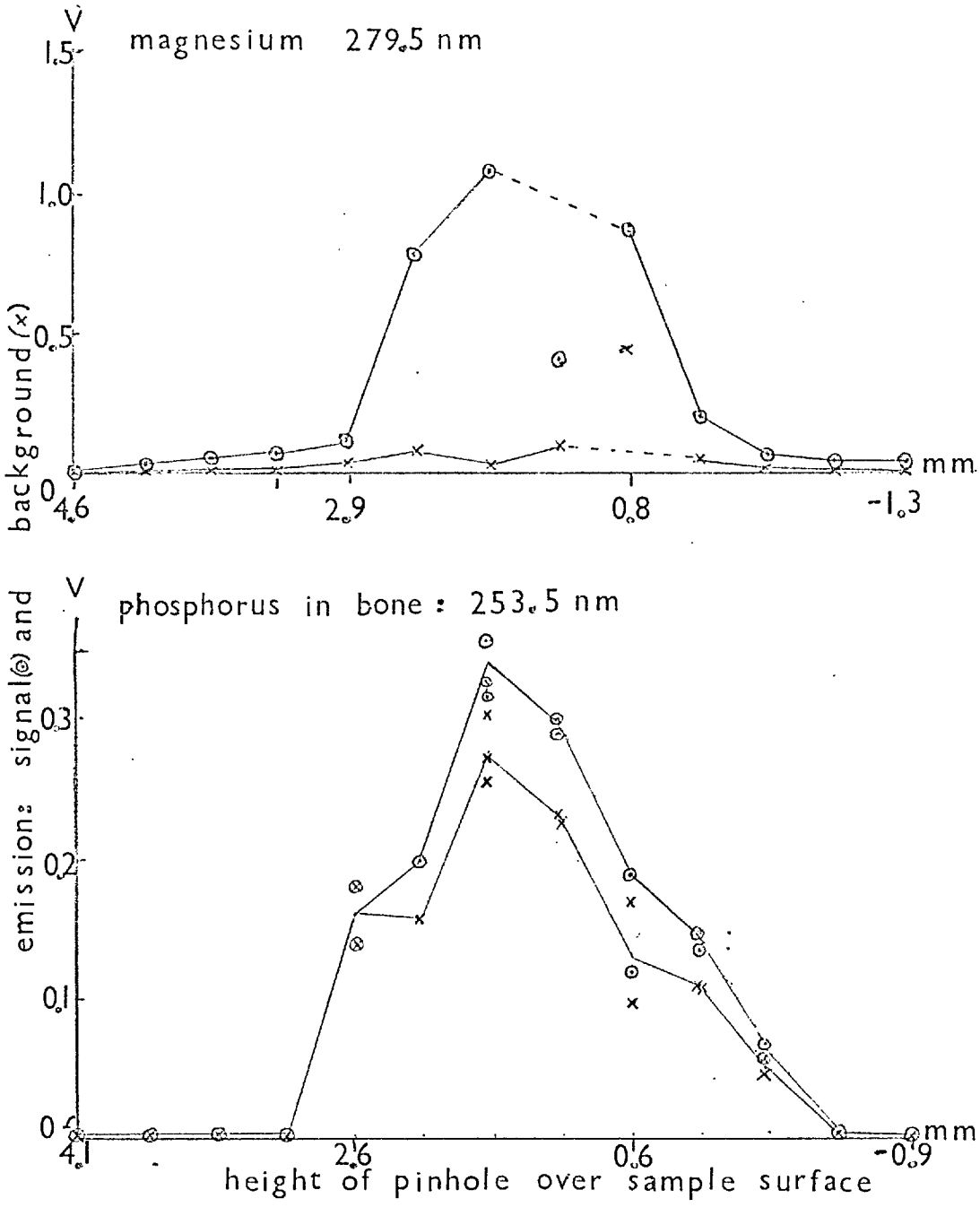
Fig 2.10



For the accuracy in positioning obtainable, the 1mm pin-hole was the best to use. Although it was difficult to handle the low signals and adjust to the different positions, it did seem again that the best viewing position was 0.5 to 1.0 mm over the sample surface for both ionic and atomic lines. This is just below the electrodes but above the target surface.

Examination of the horizontal profile with the same pin-hole system did not show conclusively that any region other than the plume centre provided a better viewing condition. It was therefore preferred to work at higher light levels without any form of collimator in most tests.

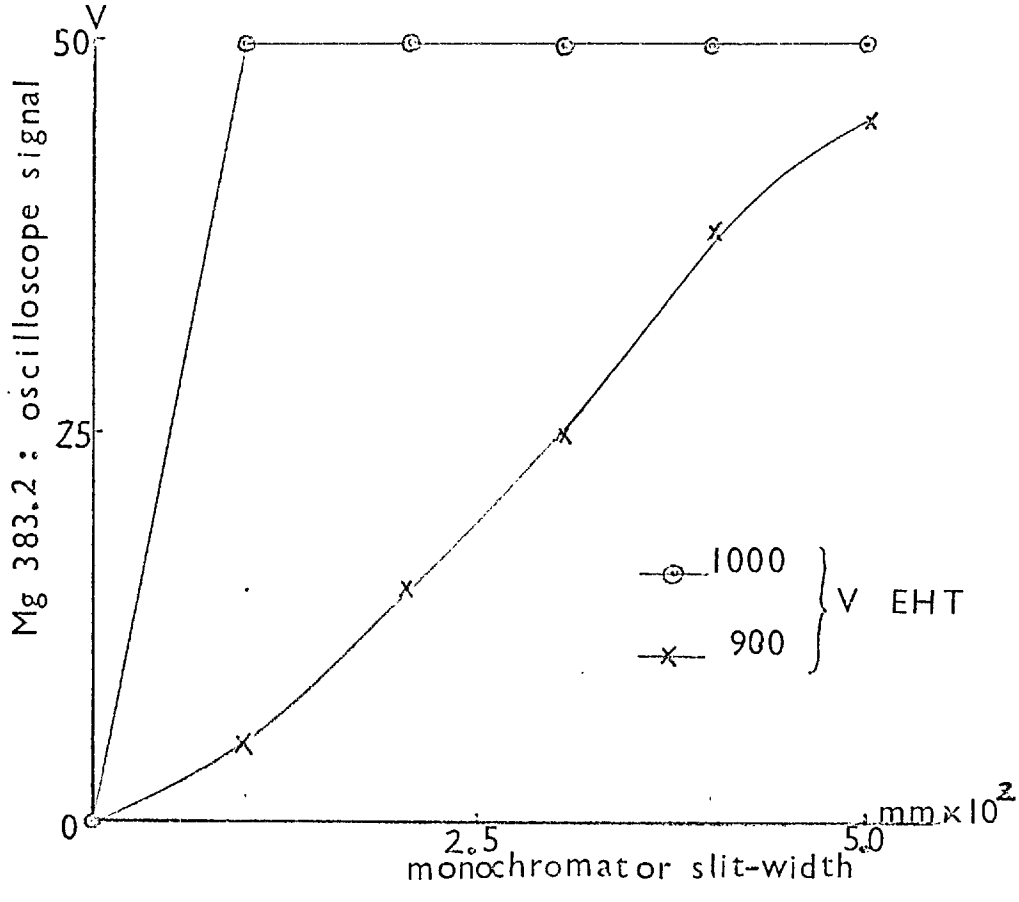
Fig 2.11 CHOICE OF BEST VIEWING POSITION



Monochromator.

The final reproducibility of results is partly related to the precision attainable in setting the monochromator slit-width and wavelength: normally within 0.3 nm of wavelength sought.

The slit-width must be small enough to provide a narrow spectral line, although wide enough to locate it reproducibly. The band-pass of the Optica monochromator is 1.6 $nm.mm^{-1}$, and usually a slit-width of 0.02-0.03 mm was used (Fig.2.12).



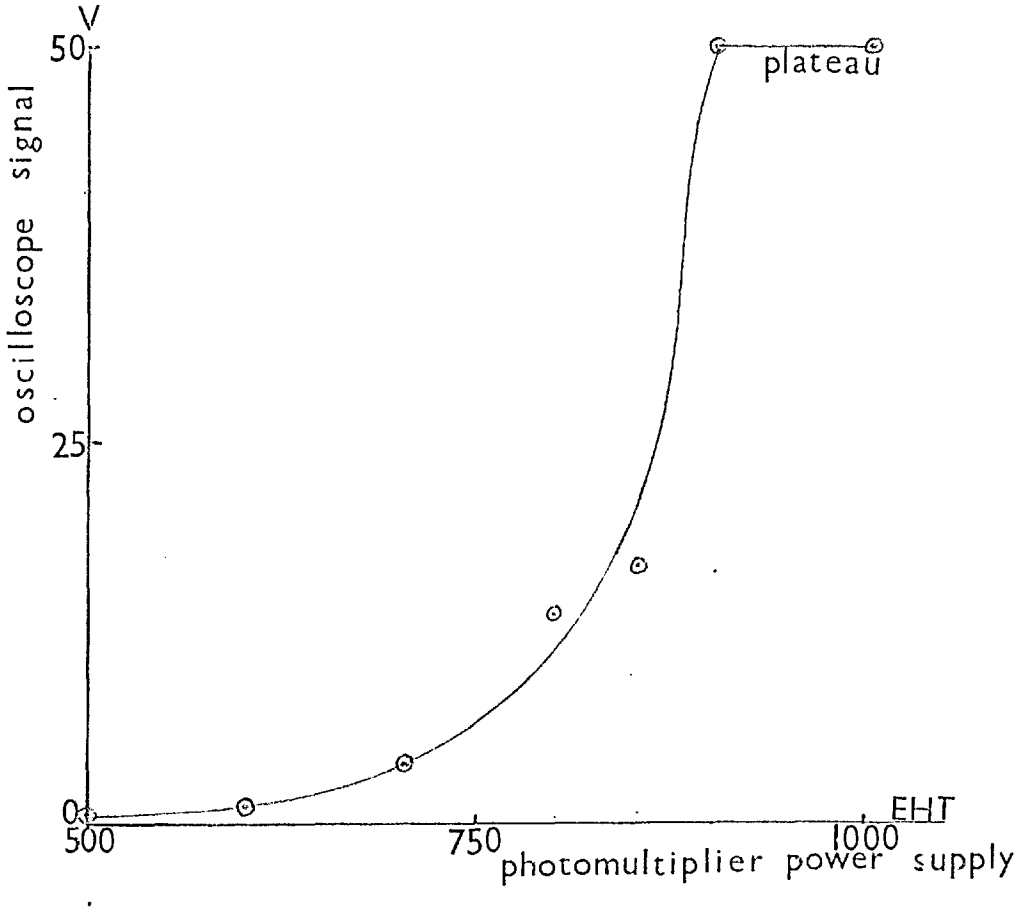
Most elements are best detected at their strongest emission line if this is within the most sensitive region for the monochromator and photomultiplier: 200.0-500.0 nm, and without interferences, especially by carbon, air or iron lines.

EHT

The Brandenburg power supply has a large voltage range available: 0-2500V, but was usually used at 900 ± 100V, to give good signal:background ratios without using unnecessary power.

Five minutes were allowed for initial stabilisation, and it was checked that no drift occurred during determinations.

Fig 2.13 SIGNAL DEPENDENCE ON EHT (Mg 383.2)



Oscilloscope.

With other components correctly calibrated and pre-set, accurate signals should be reproducibly obtainable. For precise quantitative results, an integrator should be used to record areas of the oscilloscope traces, and replace peak-height measurements.

2.5 Analysis.

Aims.

Current applications of the laser microprobe to chemical analysis have been summarised in the review (2.2). Further developments should aim to improve the instrument's performance or apply the technique to situations where alternatives are awkward or unavailable.

Therefore, after the assembly and practical assessment of the laser microprobe when metallic spectral lines were identified, it was proposed to attempt to recognise and estimate non-metallic traces.

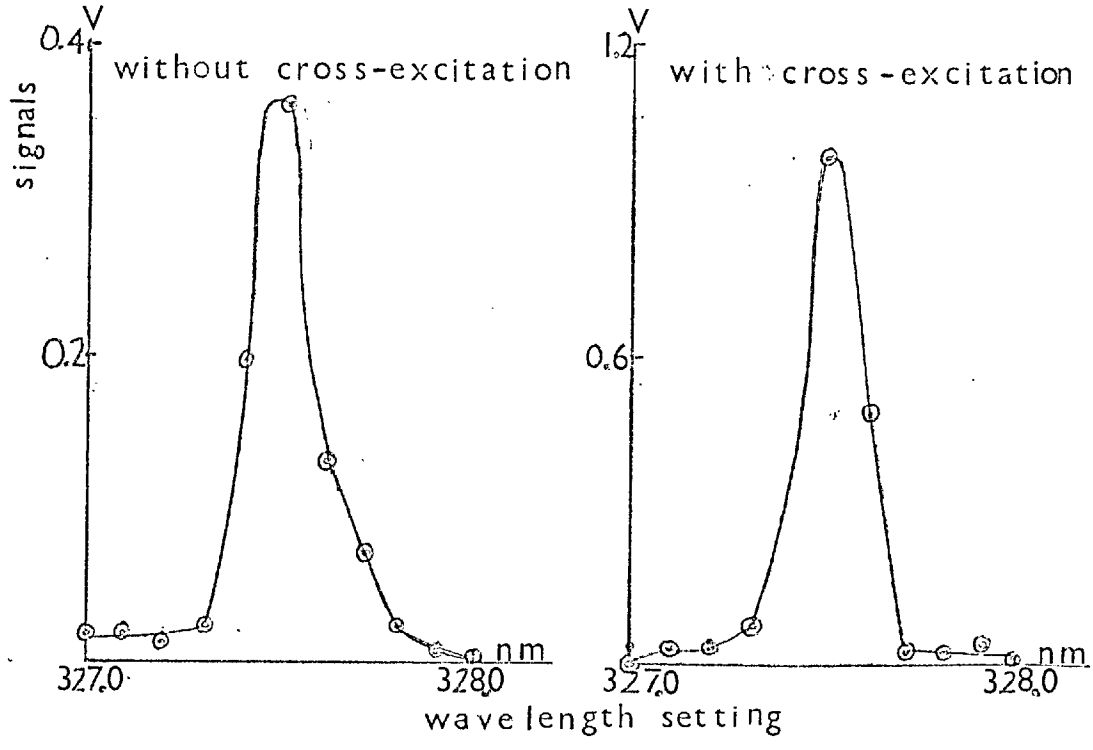
Such non-metals can affect brittleness, ductility and hardness properties of their matrix materials so that it is important to know the order and range of the concentrations present.

For the analyses 'wet chemical' methods are often lengthy. Instrumental methods can be rapid but are usually costly (33). Vacuum fusion extraction and inert gas fusion require subsequent manometric, mass spectrographic or chromatographic determination of oxygen, hydrogen and nitrogen. Combustion methods for carbon and sulphur require further titrimetry, conductimetry or gas chromatography. Electron probe or fast neutron or γ-ray activation analyses are effective, but complex calculations are necessary and there may be matrix interferences. Spark source mass spectrometry is recommended for sensitivity, precision and convenience, but needs sensitive spectral line detection techniques as the best non-metallic emission lines lie in the vacuum uv region (34).

Approach.

With the laser microprobe, the first emission signals recorded were obtained by firing onto a copper target, and were independent of the monochromator wavelength setting. After decreasing the monochromator slit-width to 0.03 mm, 'on' and 'off' spectral line conditions were distinguishable. Cross-excitation was usually used, to provide large signals and narrow spectral lines.

Fig 2.14 SPECTRA : COPPER 327.3 nm AE



The optimisation of instrument settings and a working knowledge of the system were mainly achieved by examining signals from steels and from pure metal samples: copper, zinc, manganese and magnesium. Then lower concentrations of these metals in alloys were detected and phosphorus and sulphur sought in several environments.

Metals.

Pure metal targets were used to locate sensitive elemental emission lines before attempting to detect or determine low concentrations as alloy constituents.

Signal against wavelength spectra were plotted for the pure elements. This was repeated at lower concentrations and finally for metallic traces in BCS standards down to 0.084% copper in steel. Lines were clearly defined except from one stainless steel where background continuum and strongly emitting adjacent lines apparently marked those sought for iron and chromium. As the instrumentation was developed, qualitative definition of the atomic lines became easier and more reproducible:

ELEMENT & FIGURE	ENVIRONMENT	EMISSION LINE nm Key (--most intense —preferred)	ELEMENT CONCEN-TRATION %
COPPER	copper	324.7,327.3	100
(2.15)	brass	324.7	70
	duralumin	324.7	4
	BCS steel 326	324.7	0.36
	BCS steel 328	324.7	0.084
ZINC	zinc	213.9,328.2	100
(2.16)	brass	213.9,328.2	30
MANGANESE	manganese	403.1,403.3,403.4	99
(2.17)	BCS steel 328	403.1,403.3	0.43
IRON	stainless steel	248.3	74
CHROMIUM	stainless steel	357.9,425.4	18
MAGNESIUM	magnesium	(279.5,280.2,285.2)	100
(2.18)	Mg/zirconium	(382.9,383.2,383.8) (516.7,517.2,518.3)	95

Fig 2.15 COPPER AE AT SEVERAL CONCENTRATIONS

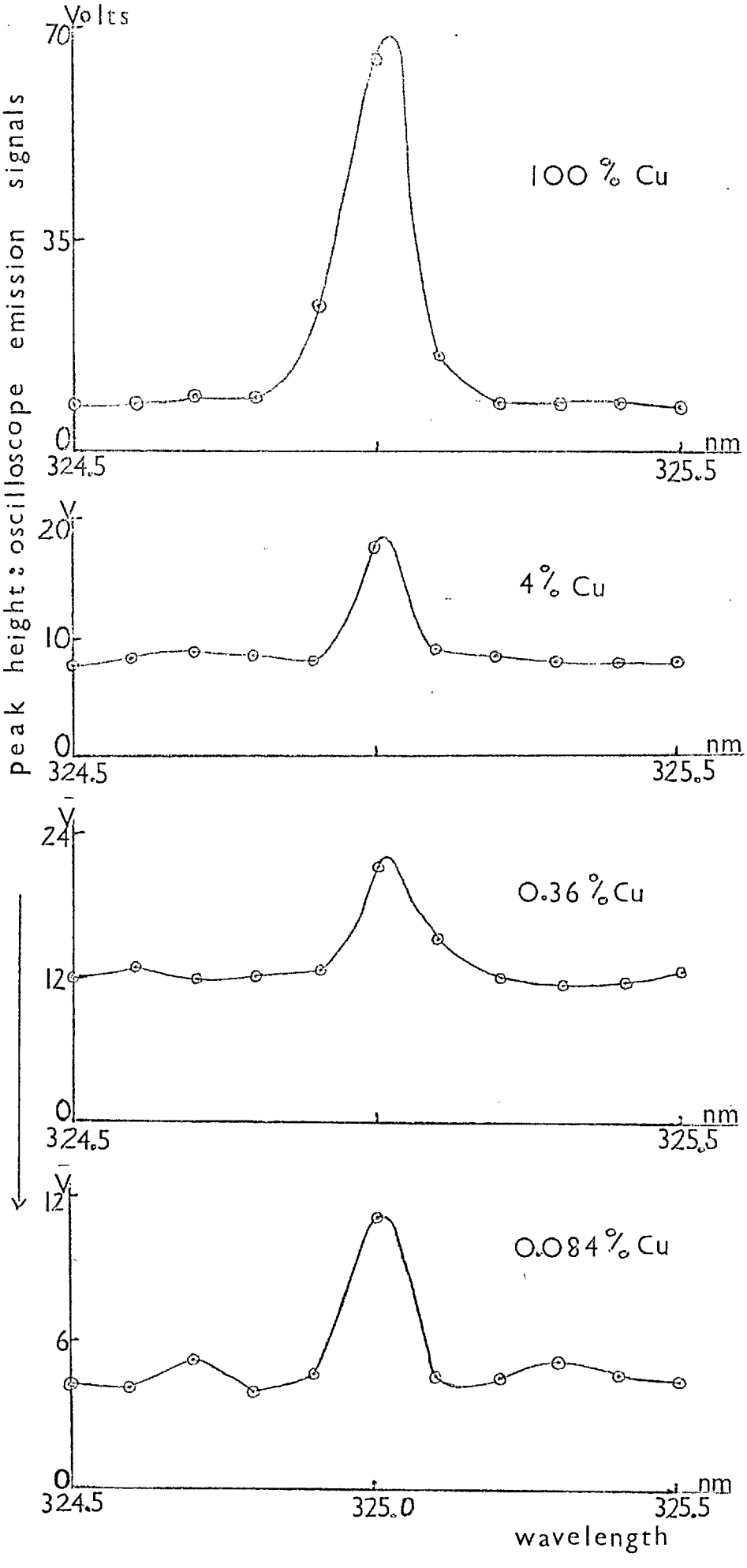


Fig 2.16 ZINC AE AT TWO ATOMIC LINES

brass target Zn : Cu — 3 : 7

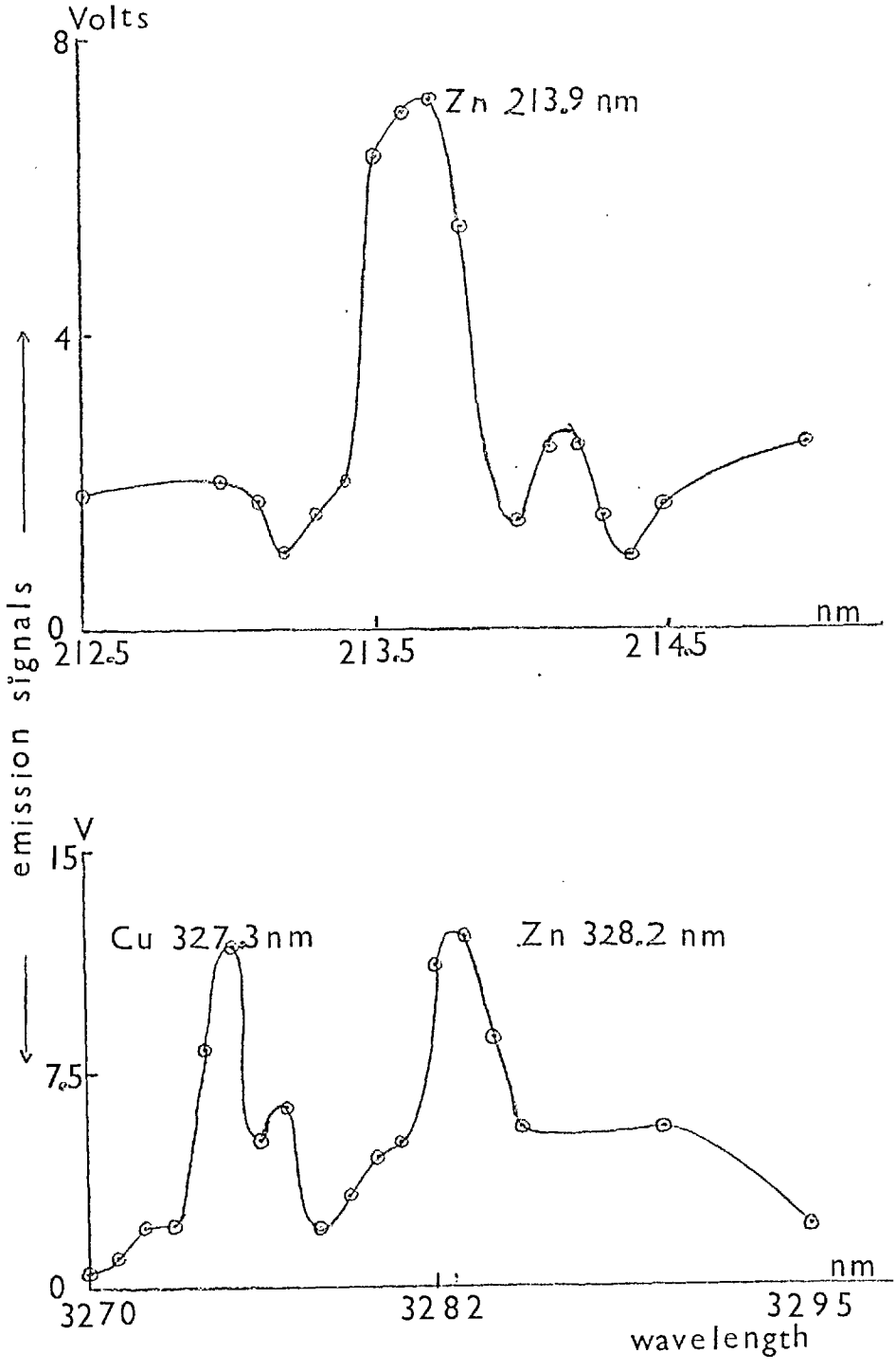
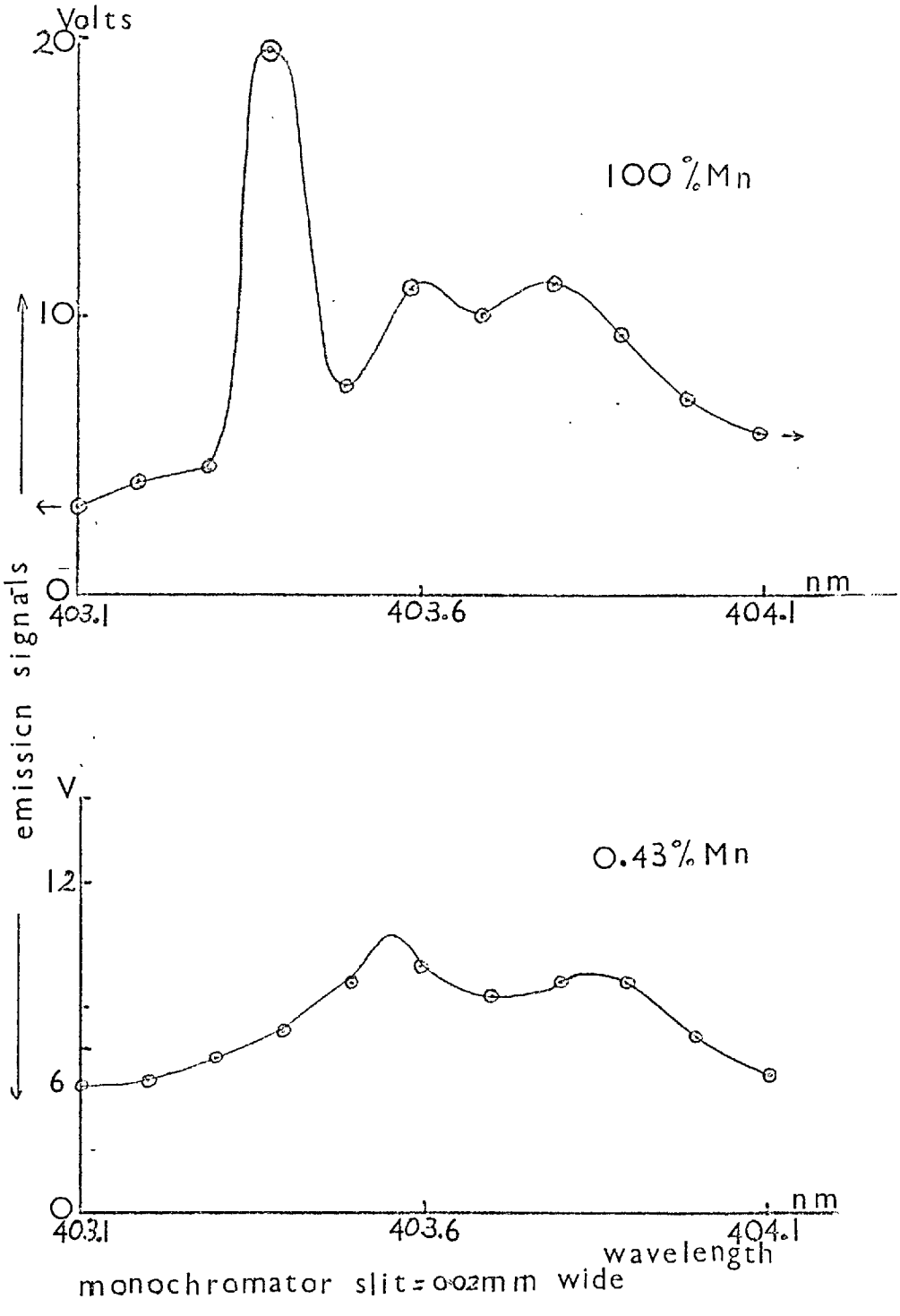
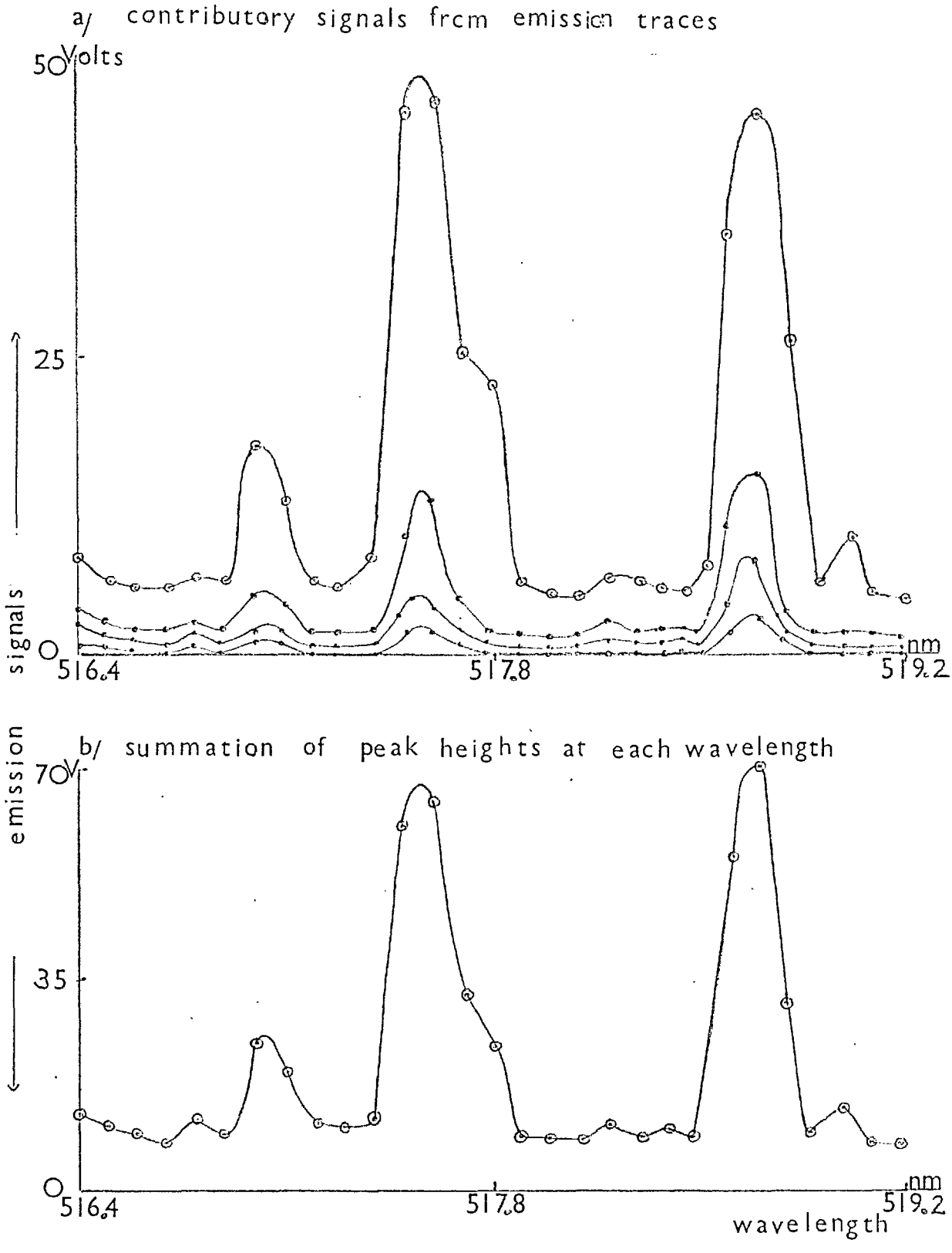


Fig 2.17 MANGANESE AE : PARTIAL RESOLUTION OF ADJACENT EMISSION LINES



monochromator slit = 0.02mm wide

Fig2.18 MAGNESIUM AE : 516.7, 517.2, 518.3nm LINES



Magnesium was examined in more detail. Nine sensitive atomic and ionic emission lines were tested in turn, to find the best, and an order of sensitivity (Fig.2.19). For general use, the best atomic line must be easily distinguished as well as intense, and 285.2 nm was chosen. The experimental order of sensitivity followed neither the reported arc nor the reported spark sensitivity orders (35).

Fig.2.19: THE SENSITIVITY OF MAGNESIUM EMISSION LINES.
This table compares the order of intensity of nine lines tested with the laser microprobe to their excitation potentials (ev) and a spectrographic designation of their relative emission intensities (35).

EXCITATION POTENTIAL			RELATIVE INTENSITIES					
			ARC EMISSION		LASER EMISSION		SPARK EMISSION	
nm	ev							
516.7	5.1	U	518.3	50	383.8		279.5	30
517.2	5.1	U	285.2	30	383.2		280.2	30
518.3	5.1	U	383.8	30	382.9		518.3	30
285.2	4.3	U	383.2	25	285.2		383.2	20
383.8	5.9	U	517.2	20	280.2		383.8	20
383.2	5.9	U	279.5	15	279.5		382.9	15
382.9	5.9	U	280.2	15	518.3		285.2	10
279.5	12.0	V	382.9	10	517.2		517.2	10
280.2	12.0	V	516.7	10	516.7		516.7	5

decreasing intensity ↓

Key: U: atomic line
V: ionic line

The magnesium systems exhibited both arc and spark discharge properties. Some general properties of arc and spark spectra (33) were compared to the 'laser microprobe and cross-excitation' spectra:

PROPERTY	CONDITION	DESCRIPTION	DESIGNATE LASER
Spectral intensity	Arc (A) / Spark (S)	Neutral atom spectra most intense. Ionic spectra most intense.	S
Reproducibility	A	Poor reproducibility by non-random sampling of electrode.	S
	S	Better reproducibility.	
Self-reversal	S	Line self-reversal common.	S
Sensitivity	A	High sensitivity because high temperature.	A
	S	Lower sensitivity because poorer sample volatilisation.	
Background	A	Moderate background.	A/S
	S	High continuum background.	
Electrode influence	A	Result not highly dependent on electrode type and position.	A/S
	S	Result dependent on electrode separation and nature and pressure of ambient gas.	

Non-metals.

Although latter measurements were promising for the semi-quantitative determination of metallic traces, it was next necessary to begin tests for non-metals. The same approach was used as for the recognition of metallic traces, and phosphorus and sulphur were sought at various concentration levels:

ELEMENT & FIGURE	ENVIRONMENT	EMISSION LINE nm	ELEMENT CONCEN-TRATION %	LINE DEFINI-TION
PHOSPHORUS	bone	253.6(U2)	25	Yes
(2.20,2.21)	cast iron	253.6	0.6	No
	cast iron	255.3(U3)	0.6	No
	phosphor bronze	253.6	0.5	Yes
SULPHUR	sulphur	216.6,217.0	100	Yes
(2.22)	sulphur	469.4/5/6 (U7, 8, 9)	100	Yes
	sulphur	190.0	100	?
	chrome alum	921.3 (U4)	25	No

The phosphorus lines were located and working conditions found using bone as the target material. 0.6% phosphorus in cast iron could not be distinguished due to interfering iron, air and carbon lines, but 0.5% phosphorus in phosphor bronze was defined with a monochromator slit width of 0.02 mm. The phosphorus emission was confirmed by running a spectrum of copper (phosphorus free), in the same range.

Sulphur lines were located using the pure solid element as target, and signals confirmed by running comparison spectra for

copper or manganese. Low value lines: phosphorus 177.5, 178.3 and 178.8 nm, or sulphur 190.0, 191.5, 180.7, 182.0 or 182.6 nm could not be tested at this stage. Most of these values were outside the monochromator wavelength range, (185.0 nm:minimum reading), and since the system was neither evacuated nor nitrogen-purged, it was unsuited to vacuum uv measurements.

Working with the low intensity signals of less sensitive lines, 1500V EHT was required to work without y-scale expansion on the oscilloscope in pin-hole work, to obtain good emission profiles (cf.Fig.2.11).

Fig 2.20 PHOSPHORUS AE: 253.6 nm

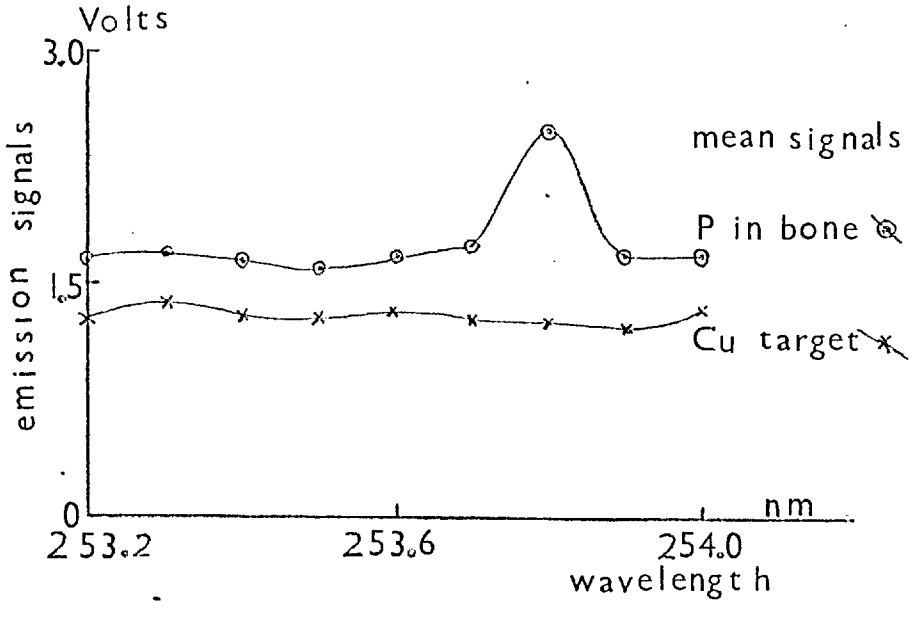


Fig 2.21 PHOSPHORUS AE: EFFECTS OF MONO-CHROMATOR SLIT-WIDTH VARIATION (0.5% P)

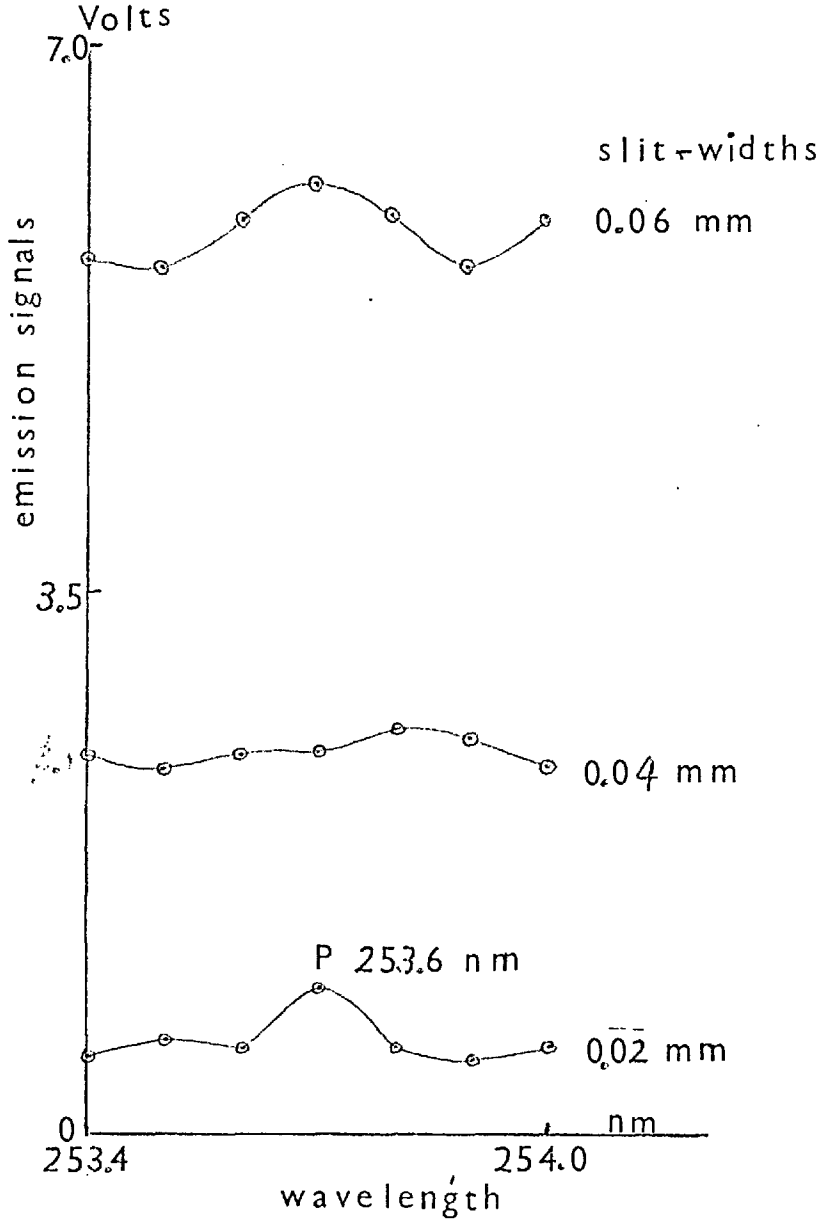
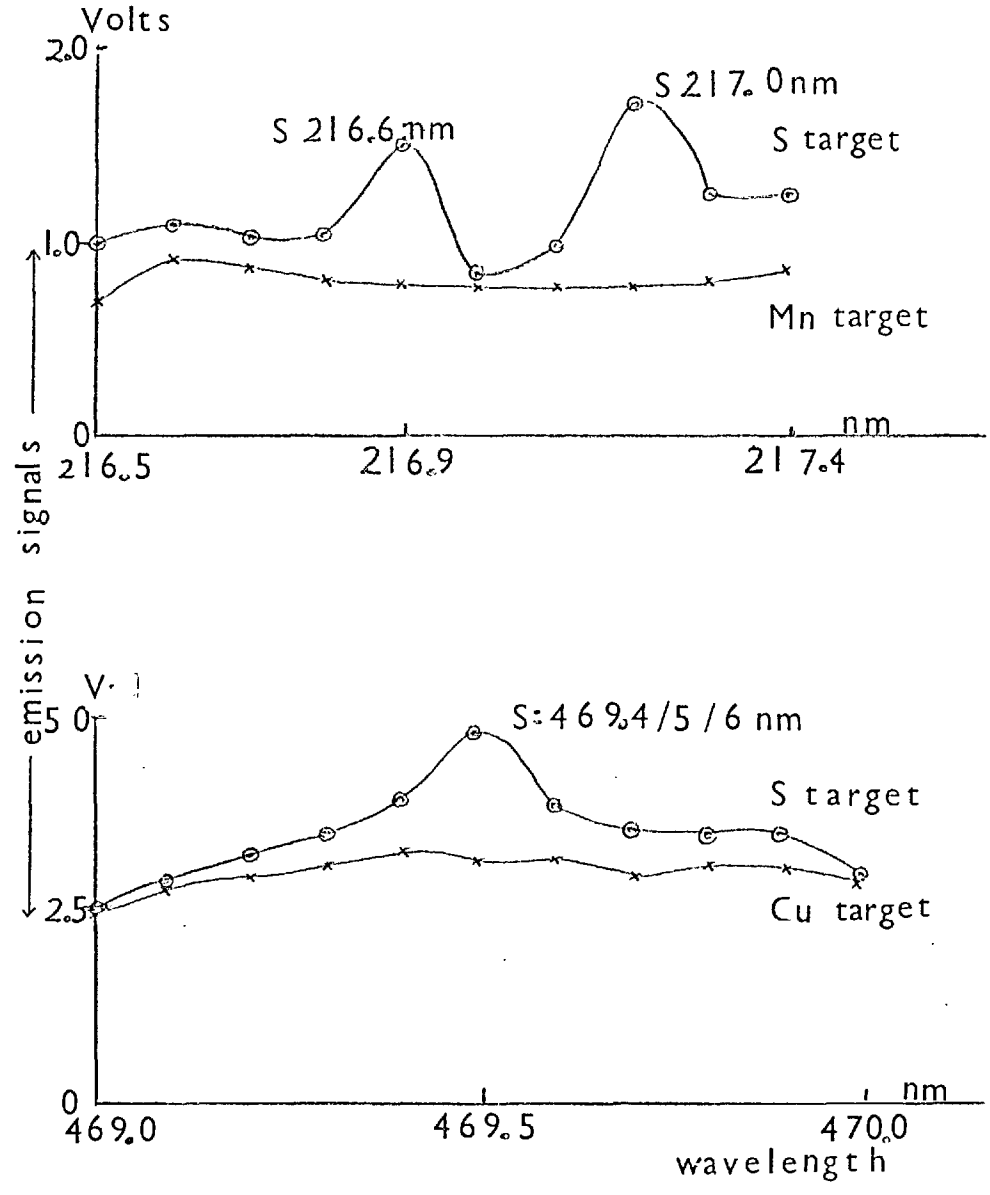


Fig 2.22 SULPHUR AE AT >200.0 NM



Termination.

The gradual deterioration of performance of the laser unit hindered the later experiments. Faults included deterioration of reproducibility, severe degradation of microscope objectives, failure of cratering at low laser powers and lack of alignment between laser axis and the axis of the microscope objectives. As a result, the crater positions did not coincide with the cross-hairs and when the firing position was centralised the surface was only slightly disturbed, if at all. Then cross-excitation could not be used. These faults could not be corrected and the instrument was returned to Jarrell-Ash for overhaul. Negotiations were protracted and the instrument has not been available for further experimental work.

2.6 Evaluation and future prospects.

Although the laser has been unavailable, further experimental work has been proposed to follow upon reassembly and checking.

In its performance, the laser microprobe, although a sensitive qualitative and reasonable semi-quantitative tool, has not yet fully justified its complexity and cost. Therefore, only a few general and quantitative tests are suggested. Qualitative detection of non-metals is recommended as the next aim, rather than extended metal determinations which by now have been well tested elsewhere (2.2) and are most usefully investigated as specific problems.

On the present system an integrator could be incorporated in the circuit for quantitative signal measurements (36). Then precise results should be obtainable for copper and other metallic traces in spectrographic standards, to make a statistical reproducibility check for ten shots on and off each line found, with calculation of the standard deviation. The triggering circuit should be checked for reliability with and without auxiliary excitation. The signal:background ratio might be improved in the latter condition, and adaption to AA, AF or resonance monochromator detection may be possible (37). The provision of an alternative ambient atmosphere might also be examined (29,30).

Perhaps the investigation of non-metallic traces in spectrographic standards using cross-excitation and seeking the most sensitive emission lines will be more rewarding. After the usual preliminary location of the lines by examining high concentrations, the standard steels containing incremental traces of carbon, sulphur and phosphorus (0.01-1.0%) would be tested (38) (Fig.2.23).

Fig.2.23 CONDITIONS PROPOSED FOR EXPLORATORY TESTING OF NON-METAL EMISSION.

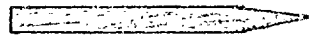
ELEMENT	ATOMIC LINES nm	ELEMENTAL ENVIRONMENTS and % CONCENTRATIONS	
		HIGH	INTERMEDIATE
PHOS-PHORUS	167.5,168.0,171.9 177.5,178.3,178.8 253.5,255.3	bone(25%) red phosphorus	phosphor bronze (0.5%)
SULPHUR	180.7,182.0,182.6 190.1,191.5 469.4,469.5,469.6	sulphur	potassium pyro-sulphate (23%)
CARBON	156.0,156.1 165.6,165.7,165.8 247.9	graphite	carbonates (as marble)
HYDROGEN	<125.0 486.1,656.3	paraffin wax (14%)	sodium bicarbonate (1.2%)
OXYGEN	<140.0 777.2,777.4	stable light metal oxide or salt	heavy metal oxide
NITROGEN	<120.0 174.3,174.5 410.0	nitride or ammonium com-pound	nitrate

Specific sensitive lines in the 155.0-200.0 nm region are quoted (39). Sensitive atomic lines are quoted for>200.0 nm, but are always less intense than the former (35). Target materials are of suitable physical form.

Before attempting measurements at <200.0 nm (vacuum uv) the monochromator must be purged with argon or oxygen-free nitrogen (OFN), to prevent absorption of short-wave radiation by oxygen and water vapour. A 200.0 nm blazed grating should be fitted in the monochromator, and its wavelength scale offset and the calibration extended to read 185.0 nm.

Alternative electrodes have been designed for the cross-excitation examination of carbon samples and at wavelengths where carbon lines could interfere. These have been prepared from pure copper and silver rods, diameter 3 mm, cold drawn for easy working into tapered electrode form (Fig.2.24).

Fig 2.24 SCALE ILLUSTRATION OF AN ELECTRODE



actual size

Working conditions and qualitative results must be thoroughly considered before attempting quantitative measurements on nickel and niobium alloys. The aims of continued tests should then be clarified, enumerating the traces, the range of concentrations and degree of accuracy sought, the importance of small concentration variations and the feasibility of alternative analytical techniques. Results might then provide evidence of segregation: localisation of the traces on an atomic scale, and relate usefully to the macro properties of the material.

CHAPTER 3

THE CARBON-FILAMENT ATOM RESERVOIR (CFAR)

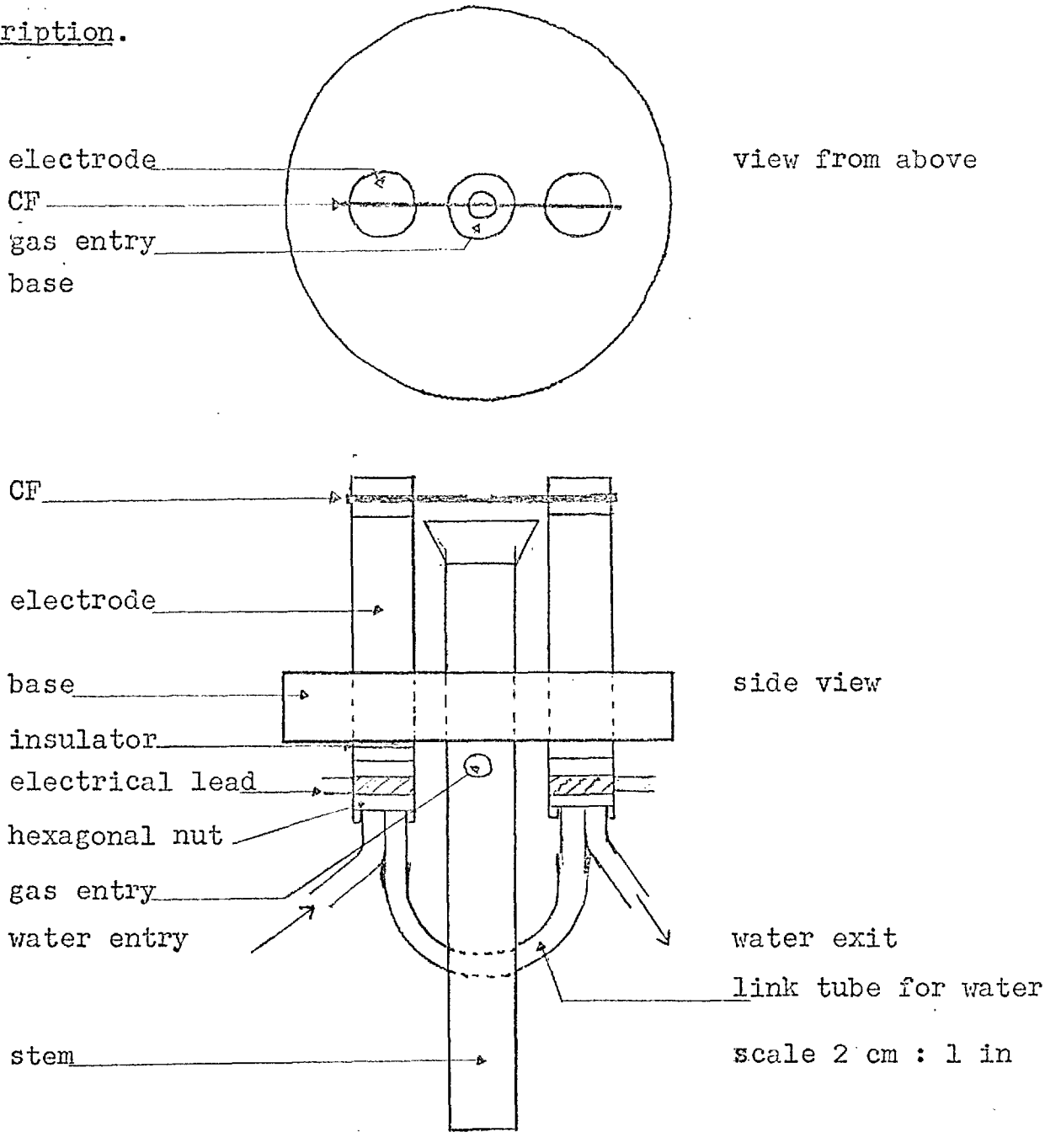
3.1 Introduction to the CFAR and its application in this project.

The CFAR provides a flameless method of atom production for atomic absorption and atomic fluorescence spectroscopy. Sample solution is atomised from a notched carbon filament into the light-path between a radiant source and a light detector. This filament, which is surrounded by a flowing stream of inert gas, is resistively heated by the application of an AC voltage across its ends, first gently to evaporate the solvent, then to white heat to atomise the sample. The basic method, design of equipment and some applications have been fully described recently in a series of papers from Imperial College (40,41).

The use of a CFAR was not originally intended in this project, but began while the laser microprobe was away for repair. It was hoped to provide CFAR atomic absorption or atomic fluorescence methods for non-metal determinations, making preliminary tests with metals, before adapting to vacuum uv measurements and attempting to detect non-metallic elements.

3.2 Description of the CFAR and the assembly of the analytical system.

Description.

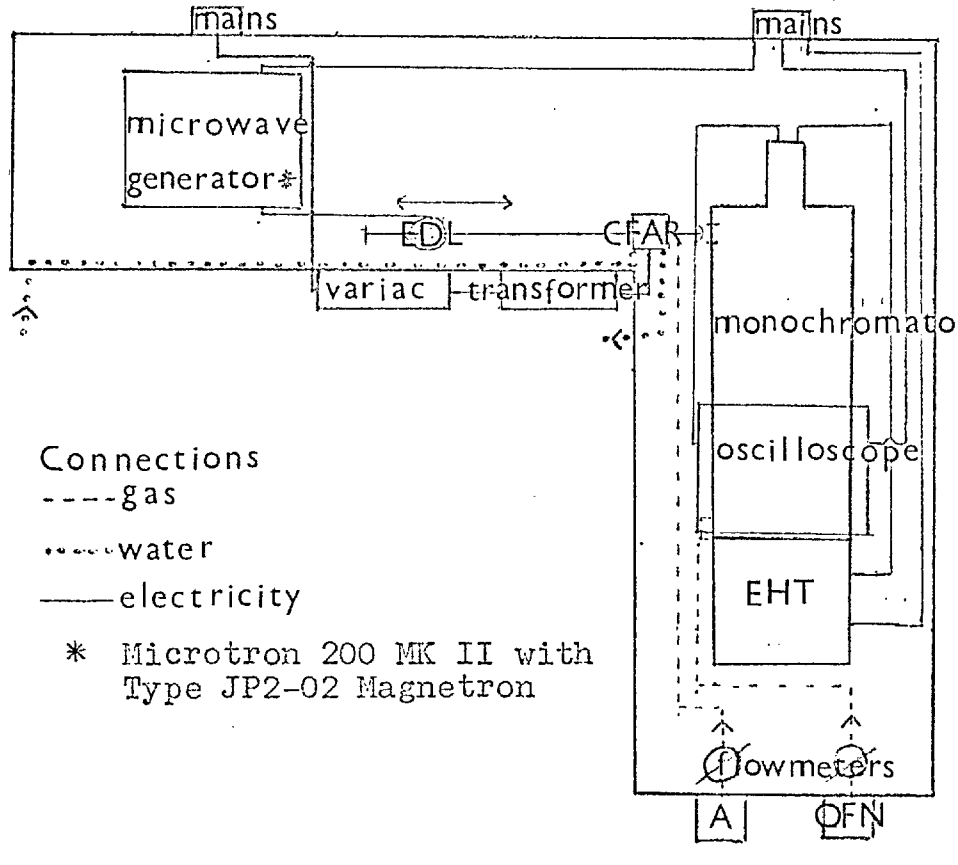


Note: This CFAR, although very similar to those used previously (40,41), was the first of several made with modified electrodes, water-cooling and gas-supply methods, so preliminary tests included an assessment of these changes.

Assembly.

This system used the same basic components and arrangement of equipment as had been required for the laser microprobe. For atomisation, the CFAR and its power supply replaced the laser microscope and power units. Electrodeless discharge lamps (EDLs), operated in $\frac{1}{4}$- or $\frac{3}{4}$-wave resonant cavities powered by a 2450 MHz Microtron microwave generator, provided the additional atomic line sources necessary to make AA or AF, rather than direct AE measurements. The fast response auxiliary triggering system required with the laser was unnecessary, as the response of the normal time-base storage facility of the oscilloscope was fast enough to record the CFAR signals.

Fig.3.2 ASSEMBLY OF THE CFAR ANALYTICAL SYSTEM.



Conversions.

The basic layout used was similar to the laser microprobe assembly, but several additions and changes were necessary. These included the electrical connection of the CFAR and auxiliary equipment and the provision of an optical bar and appropriate gas and water supplies.

CFAR

For some early tests, an uncooled CFAR was used (40:I), but at considerable disadvantage due to unevenness of electrode heights and poor electrical contacts. Then an early water-cooled model (40:II) was repaired and modified to provide a CFAR with new water and gas-supply methods to be assessed. A CFAR built to the latter specification with renewable filament mountings has been used for most of the subsequent tests (Fig.3.1).

Electrical connections

A step-down transformer and Variac control supplied current to the filament to provide continuous variation of voltage across it. The same photomultiplier, EHT supply and oscilloscope were used for signal detection and measurement as in the laser system.

Gas and water supplies

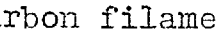
The CFAR electrodes are hollow and water-cooled and the filament is heated in an inert atmosphere of argon. Polythene tubing was fitted to supply water to the operating room. Argon for the filament and oxygen-free nitrogen (OFN) to purge the monochromator were supplied *via* calibrated flow meters.

Optical system

EDLs were made after instruction in the preparative technique (42). A rigid rod was clamped to the bench as an optical bar to

mount the CFAR and align the related lenses and light sources.

Sampling

Sample solutions were delivered from 1 µl repelcoted glass capillaries contained in teat syringe pipettes (43), onto notches filed in 2 mm diameter carbon filaments:  Solvent was evaporated by warming the filament: 1-2 V for 5-10 seconds, before heating to white heat: 7-9 V, on/off, to atomise the sample into the path of the light beam.

3.3 Preliminary analyses.

Aims and approach.

After the assembly of the apparatus, it was necessary to obtain a working system and become familiar with its operation and the practical technique, while assessing the modifications made on the CFAR itself.

To achieve this, brief studies of zinc and thallium AA were carried out. Concentrated solutions of the test elements were used to identify signals before optimising signal detection conditions. Calibration curves and graphs illustrating the variation of other parameters were then prepared.

Preparatory to the proposed non-metal AA experiments, EDL line sources were used, although in metal AA greater sensitivities should be attainable using the hollow-cathode lamps usually available.

Zinc.

The AF determination of zinc at 213.9 nm with a CFAR and a hollow-cathode lamp had previously been examined (40:II). The high reported sensitivity, together with the ready availability of zinc salts and EDL sources, recommended the choice of zinc as a test element here.

An aqueous 100 ppm stock solution of zinc sulphate was prepared, and the 213.9 nm line examined. 1 µl of 20 ppm zinc solution was used to locate an absorption signal on the oscilloscope screen.

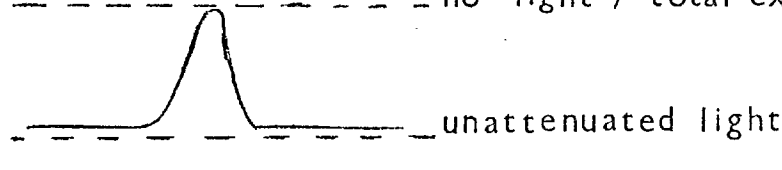
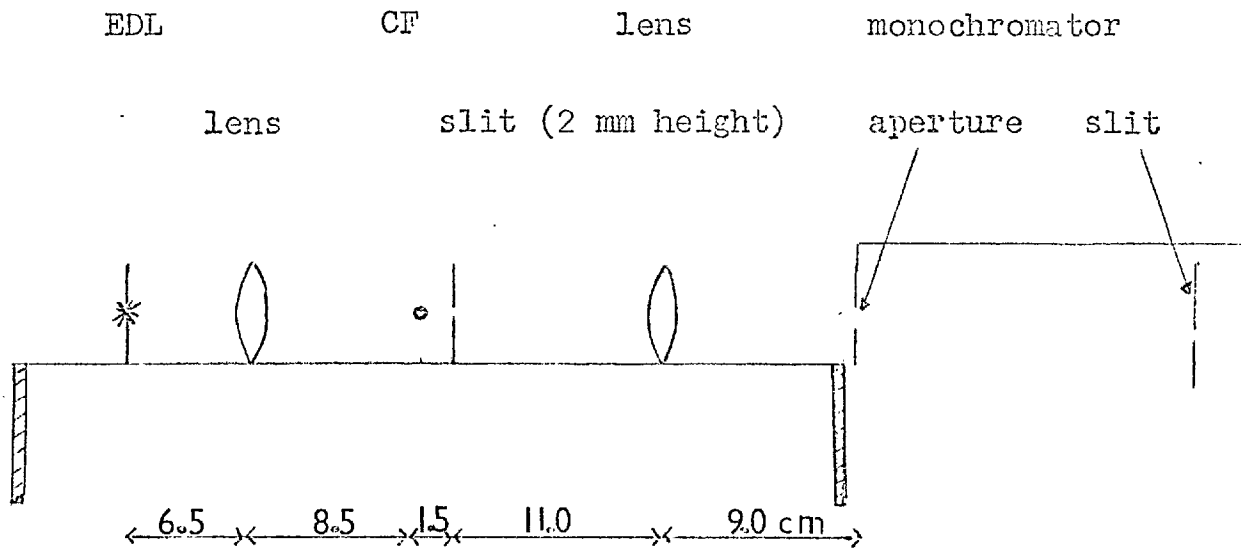


Fig 3.3
ABSORPTION
SIGNAL
(time-base 1sec/cm)

This was obtained using a simple lens and slit optical system as outlined below, and by adjusting the monochromator slit, EHT value (1500V) and oscilloscope y-scale to provide 3-4 cms unattenuated light signal on the screen, with signal:background ≥ 10:1.

Fig 3.4 OPTICAL SYSTEM: ZINC AA



optical bar

scale: 0.1 in represents 1.0 cm

Next, sensitivity was increased by using narrower slits and improving the optical alignment. It was then possible to prepare a calibration graph for 0-10 ppm zinc (Fig.3.5), and to measure the dependence of AA signals on argon sheathing gas flow-rate using 5 and 10 ppm solutions of zinc (Fig.3.6).

Fig 3.5 ZINC AA

(detection limit = 0.7 ppm Zn, 7 x 10^{-10} g Zn)

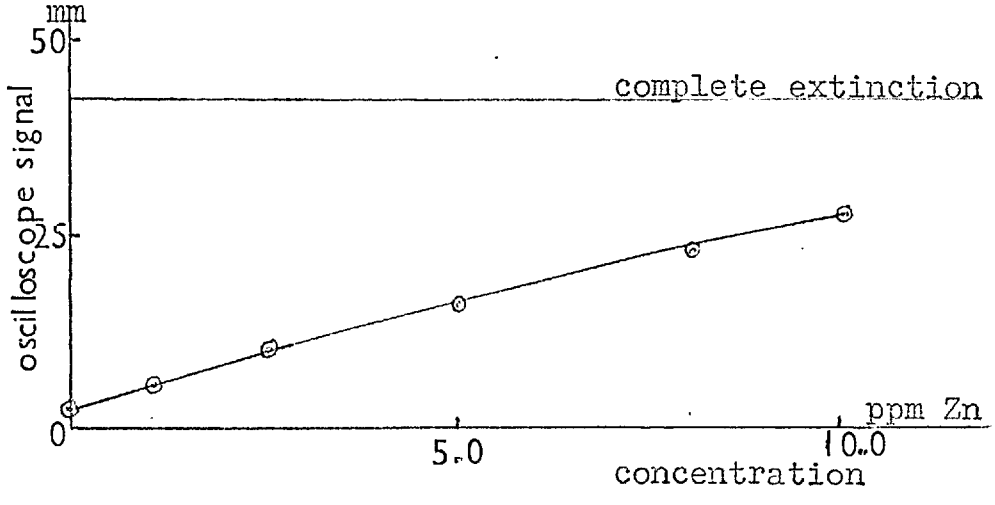
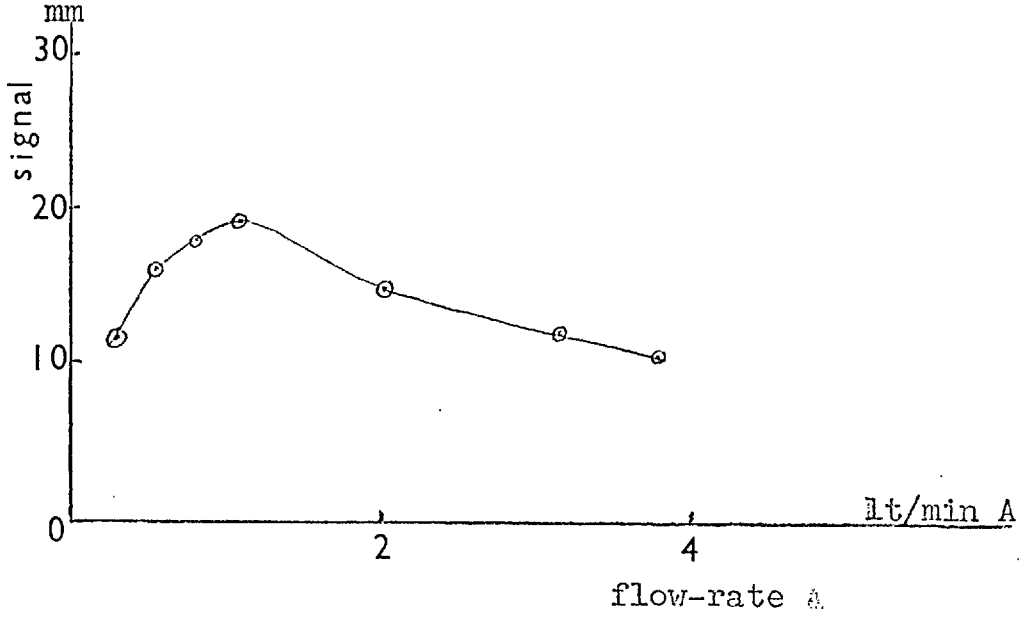


Fig 3.6 AA SIGNAL DEPENDENCE ON ARGON FLOW-RATE FOR 5 PPM ZINC



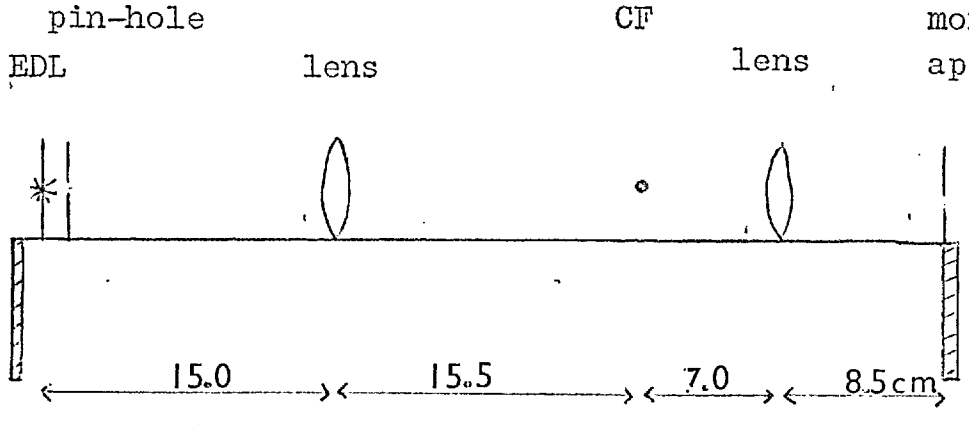
Thallium.

The AF determination of thallium at 377.5 nm with a CFAR had also been examined, but was limited by the use of an inadequate EDL. A 10^{-2} x 5 ppm thallium detection limit was attained compared to 10^{-5} x 2 ppm zinc detection limits (40:II). Here, thallium was chosen for AA testing because an intense EDL source was available and there was no previous knowledge of any AA detection of thallium with the CFAR.

An aqueous 100 ppm stock solution of thallous chloride was prepared since this slightly soluble thallous salt was available. The 276.8 nm thallium line was chosen as appropriate for AA, being a ground-state transition resonance line. Results could be compared to a reported flame sensitivity of 0.8 ppm thallium, and detection limits of 0.2 ppm and 0.05 ppm for specific determinations with an absorption tube (44). 1 ml of 100 ppm thallium solution was used to locate the first AA signal.

The thallium EDL was sufficiently intense to be attenuated at source with a pin-hole. Then subsequent alignment to illuminate a small volume over the filament notch could be more precise than when using an open tuning cavity (Fig.3.7).

Fig 3.7 OPTICAL BAR: THALLIUM AA



0 to 8 ppm thallium and 0 to 3 ppm thallium calibrations were prepared (Fig.3.8). The dependence of AA signals on argon flow-rate was measured at 8 and 20 ppm. The optimum flow-rate was low: 1 lt/min, and enhanced by covering the CFAR. A best viewing position for this system of ca 1 mm above the filament notch surface was demonstrated by varying the former with respect to the fixed light source (Fig.3.9). Reproducibility was satisfactory: EDL performance and argon flow-rate were the most critical variables for the thallium determination.

Fig 3.8 THALLIUM AA
(detection limit = 0.2 ppm Tl, 2 x 10^{-10} g Tl)

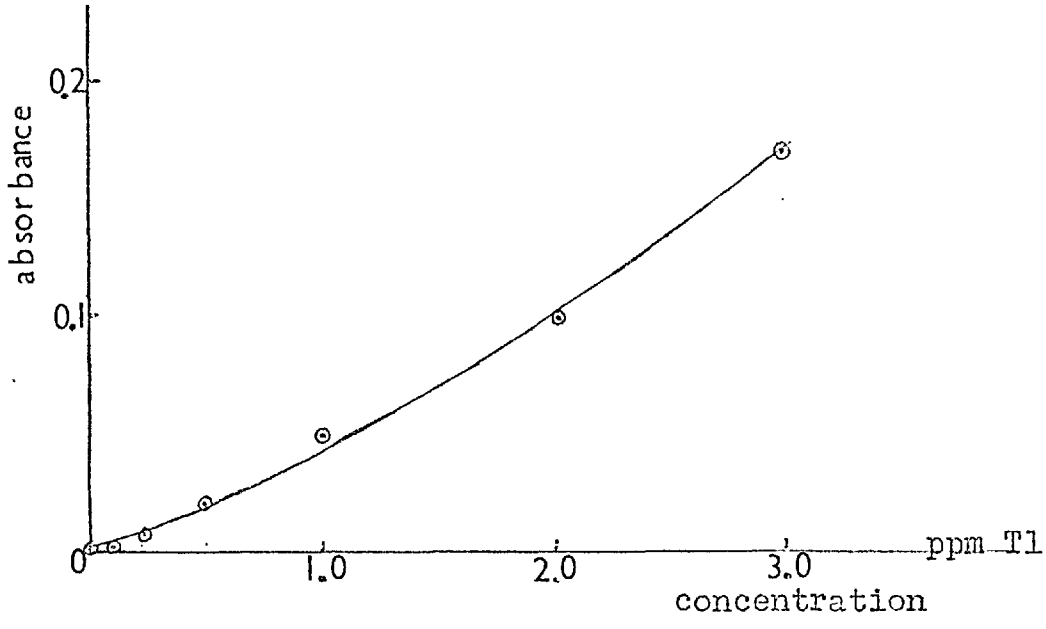
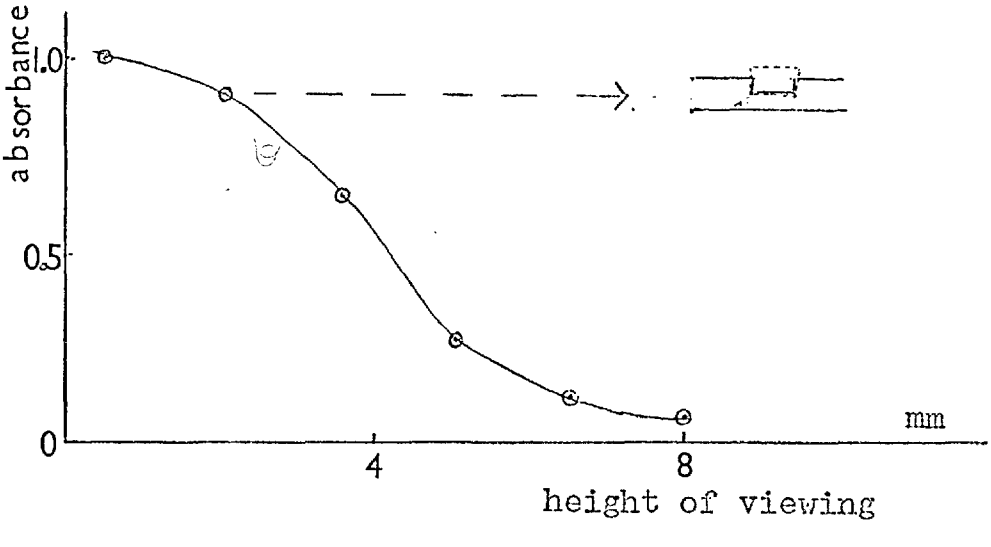


Fig 3.9 AA SIGNAL DEPENDENCE ON VIEWING POSITION FOR THALLIUM



Assessment of CFAR modifications.

As already indicated, the aims of the preliminary analyses included an assessment of the modified CFAR used (Fig.3.1). On this model, the water-cooling supply inlet, outlet and connecting pipes were all situated below the electrode platform, whereas previously the connector link between the electrodes had been above the platform. Also on this model the argon supply tube, entering at the centre of the platform, extended to just below the filament where it opened out through a T-piece to make a 2 mm slit parallel with the filament. This replaced more complex circular or rectangular argon entries of greater cross-section.

The bore of the copper pipe which carried the water supply, although fine (2-3 mm diameter), maintained an adequate flow-rate. The electrodes did not overheat and the ends of the filament did not wear unduly. Cooling after heating the filament to white heat was rapid. Less than one minute was necessary between samples. No leakages were detected at any joints or where the plastic tubing joined copper tubes, although this had sometimes occurred on previous models.

The streamlined argon entry, although a simple unit to construct, and leaving space on the CFAR platform to mount slits close to the filament, was often inadequate. The relation between argon flow-rate and sensitivity is similar to that of alternative entries, with best signals at low flow-rates (Fig.3.6).

However, filament deterioration occurred too rapidly, within thirty 'shots', unless it was operated with a cover over the CFAR. Such a cover is suited to non-metal determinations at low wavelengths, but should be unnecessary for ordinary metal determinations. For these, a wider, laminated gas-entry is required.

3.4 Choice of conditions for the AA detection of sulphur. Problem.

With the laser microprobe, the in situ AE detection of phosphorus, carbon, nitrogen, oxygen, hydrogen or sulphur constituents of metallic matrices was sought. Of these elements, sulphur and phosphorus are most suited to CFAR analysis since air and carbon spectroscopic interferences can be excluded. The CFAR method uses AA or AF determinations for samples supplied in the form of dilute solutions. Some general problems must be overcome to extend its application from metal to sulphur and phosphorus analyses.

Since the most sensitive AA lines for the latter elements are in the vacuum uv, it is necessary to use a monochromator with a special grating and adapt to a short argon/OFN-purged or evacuated optical path, with lenses and windows which can transmit radiation at less than 200.0 nm.

Where hollow-cathode lamps are unavailable, EDL sources must be prepared to provide identifiable atomic lines of adequate intensity and good signal:background ratios.

When the atomisation region is adequately illuminated, other conditions must be selected to ensure a maximum concentration of atomic species there, so that AA detection is effective. Typically, for sulphur, salts must first be decomposed.

$$M_2SO_4 \xrightarrow[C]{\Delta} M_2S \xrightarrow{\Delta} 2M + S$$

$$M_2S \xrightarrow[O]{\Delta} SO_2 \xrightarrow[C]{>1000^{\circ}C} S_1$$

With the CFAR, a high flow-rate of inert sheathing gas around the filament will maintain a reducing atmosphere and cause cooling. Since some oxygen must oxidise the sulphide ions initially, and high temperature is necessary for atomisation, a

low flow-rate may be chosen. The carbon filament can attain 2500°C, which may be necessary since elemental sulphur tends to persist primarily as molecular chains. The formation of S starts at ca 1000°C and reaches only 45% at 2000°C.

$$S_8 \xleftarrow{750^\circ C} 4S_2 \xleftarrow{1000^\circ C} 8S$$

$$S_8 \xleftarrow[55\%]{2000^\circ C,\ 45\%} 8S$$

Further support and guidance for the proposed CFAR approach to sulphur analysis was sought from the literature. Few reports of any kind of atomic spectroscopic determinations of sulphur are available, but two workers have summarised the problem for sulphur, halogens and other non-metals, including references to some practical analyses (45,46).

Sulphur has been determined by molecular emission from S_2 in a cool flame (47), but flame AA is unsuitable for measurements at the principal sulphur resonance lines where strong absorption by flame gases, atmospheric oxygen and quartz optical components, occurs.

L'vov and Khartsysov report AA detection of sulphur using their argon-purged graphite cuvette atomiser in conjunction with a vacuum monochromator, lithium fluoride lenses and windows, and spherical, thin-walled (0.2 mm) quartz high frequency lamps containing the pure element (48).

Summary of reported conditions (48).

Element	Source	Temperature	Atomic line nm	Sensitivity for 1% absorption	
SULPHUR	$3CdSO_4.8H_2O$ $CuSO_4.5H_2O$	1600°C	180.7	5.4×10^7	<8
			182.0	4.2×10^7	7
			182.6	1.4×10^7	2

A CFAR assembly was modified to attempt the AA detection of sulphur at these wavelengths.

Approach.

After defining the problem, several basic changes were made to the experimental system before attempting any specific CFAR analyses for sulphur. These will be described next. Further changes were made during the practical tests, to examine alternatives or to develop the method.

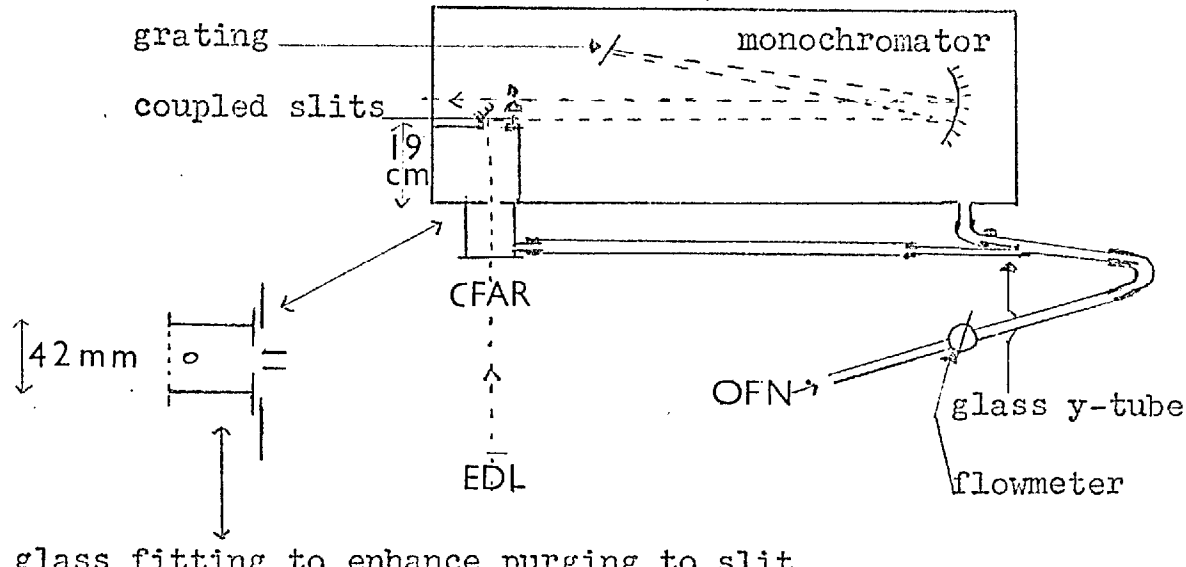
Optics.

Argon was used along the enclosed optical path and in the CFAR to maintain an inert atmosphere and transmit short wavelength radiation.

No vacuum monochromator was available, but a purging system was made for the Optica model using OFN to displace absorbing oxygen and water vapour, (Fig.3.10).

The monochromator wavelength scale was offset, and an extended calibration marked from 185.0 down to 155.0 nm.

Fig 3.10 MONOCHROMATOR PURGING SYSTEM AND LIGHT-PATH

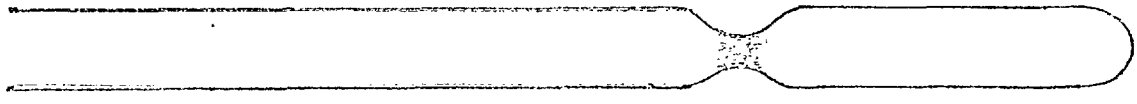


The optical path-length was minimised by positioning the EDL close to the CFAR. Generally, slits were used to produce a light-profile which closely resembled the form of the sulphur plume: —⌒— The short path then made best use of the consequent low light intensity, while a slit positioned between the EDL and filament aided alignment of the light spot over the notch.

Initially, any lenses used were of biconvex quartz (1.0" diameter and 1.5" focal length), and the windows of thin Vitreosil silica (1 mm).

The preparation and evaluation of sulphur EDLs was necessary. Silica tubing of 8 mm internal diameter and 1 mm wall thickness was used to make the lamps, forming a 4-5 cm bulb at the end of a 9-10 cm stem (Fig.3.11). The sealed bulbs contained minimal sublimed sulphur (< 1 mg) and argon filler gas to a pressure of 1.0-2.5 T . Such lamps were prepared with about 50% success and tested to locate sulphur lines.

Fig 3.11
EDL



Sulphur EDLs: Summary of atomic lines sought (35,49).	
Wavelength nm, and atmosphere	Atomic lines nm
> 200.0 air	217.5 469.4(U7), 469.5(U8), 469.6(U9) (but S_2 bands 270.0-600.0)
≐ 200.0 OFN	190.0, 191.5 (intensity 2:1)
« 200.0 OFN	180.7, 182.0, 182.6 (principal resonance lines; most sensitive for AA is 180.7, nickel interferes at 182.6.)
Key: U7, U8, U9 : AE order of decreasing intensity.	

At this stage, little was known about the operation of sulphur EDLs, so three were tested, trying various conditions with the aim of locating the sulphur atomic lines. With each lamp adjacent to the monochromator, lines were sought by monochromator slit, Magnetron power and lamp position variation.

Operation of sulphur EDLs.

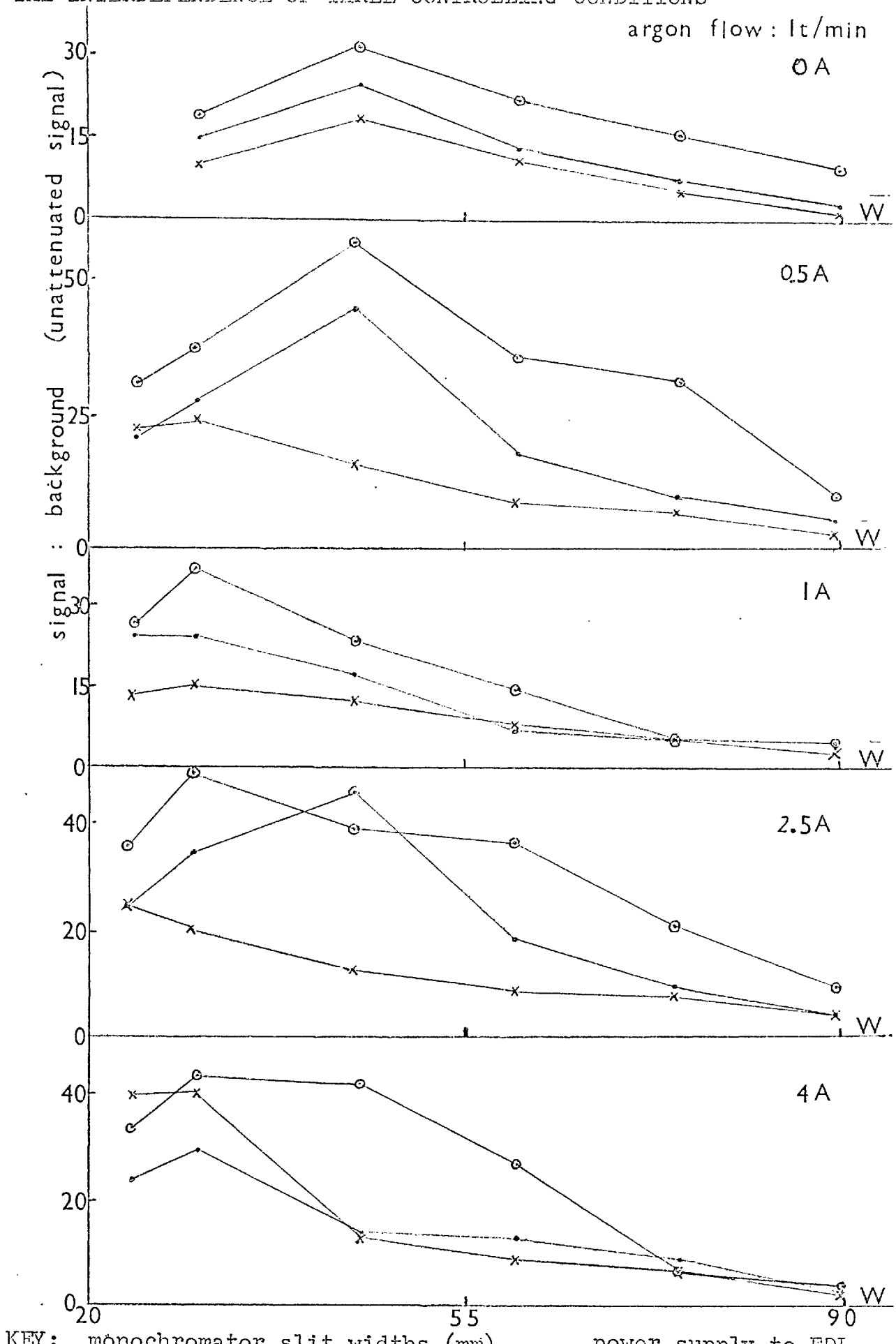
Conditions compared and most intense lines located.

Conditions	Unit	Magnitude
EHT	V	1500
power to EDL	W	45, 100
monochromator slit-width	mm	0.05, 0.1, 0.5, 1.0
oscilloscope y-scale	V/cm	1, 2, 5, 10
monochromator atmosphere	-	OFN, air
lines located	nm	(180.7-182.6) 190.0 217.0

Each EDL has its own particular running characteristics. The interdependence of these can be found and used to choose promising AA running conditions. Hence the 180.7-182.6 nm lines were chosen for sulphur, running the EDLs cool for atomic lines (45W), and selecting intermediate monochromator slit-widths (0.5-1.0 mm), for reasonable on-line light levels without undue introduction of noise.

A description of the extensive tests made on one particular lamp will illustrate this approach. The interdependence of three monochromator slit-widths, five alternative power supplies to the EDL and five different flow-rates of argon through the $\frac{3}{4}$-wave tuning-cavity was investigated to define good working ranges (Fig.3.12).

Fig 3.12 CHOICE OF WORKING RANGES FOR AN EDL BY MEASUREMENT OF THE INTERDEPENDENCE OF THREE CONTROLLING CONDITIONS



CFAR

Two particular aspects were considered at this stage: the choice of operating with or without a cover around the filament, and the most suitable sample solutions.

For metal determinations, an unenclosed CFAR has generally been favoured due to similar sensitivities but increased light transmission and accessibility compared to an enclosed system. However, on the CFAR used here, with a modified argon-flow entry, best responses were obtained on an enclosed system when it was possible to work at low argon flow-rates without undue filament deterioration or absorption of radiation along the light-path.

Prototype covers were constructed for the early tests since the 1-2 cm diameter windows of available glass covers gave insufficient flexibility for exploratory variations in the optical system. Cylindrical wire frameworks were superseded by rigid cubical Meccano covers with 4 cm diameter windows and separate lids. These allowed the introduction of samples without disturbance of optical path or extensive loss of argon from the purged cavity.

Development.

It was decided to start with sulphur powder on the filament, then to use sulphide solutions for approximate work and sulphate for greater accuracy. Aqueous solutions of sodium sulphide and sulphate were prepared (100 to 1000 ppm sulphur), and sulphur-free solutions of similar concentration to aid signal identification.

The trials were inconclusive, as unequivocal AA signals for sulphur were not obtained. However, definite improvements

were made to the experimental assembly. These provided an efficient metal detection system of suitable form for subsequent tests with other non-metals, while limitations were increasingly understood. Here some of the aspects considered will be described under the same general headings as in the previous section.

Optics.

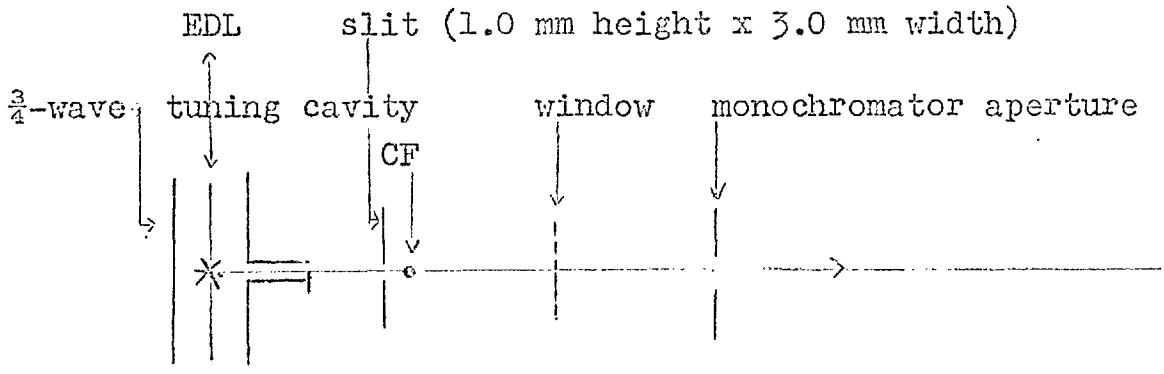
The nature and flow-rates of the sheathing and purging gases were examined. A short test using OFN in place of argon as sheathing gas was not promising. Nitrogen is less dense than argon, and vacuum uv atomic line signals from EDLs were smaller and deteriorated rapidly without the quenching of any unwanted signal background by the nitrogen (40:III).

The efficiency of purging the monochromator was greatly improved by tape-sealing all joints. Then signals were maintained using $\leq$ 1.5 lt/min OFN after preliminary displacement of air at $\triangleq$ 5 lt/min.

Passage of the OFN through a silica gel drying-column before use was found unnecessary, and required increased gas flow-rates to maintain a stable signal. Argon, denser and more costly than nitrogen, gave no advantage for purging.

An illumination system was evolved so that with 2000 V EHT an EDL atomic line source signal of $>$1.5 cms and $<$4.0 cms might be displayed on the oscilloscope screen, using the 5 or 10 V/cm y-scales. Its suitability for AA was confirmed by detecting cadmium and zinc easily at low concentrations: 0.004 ppm cadmium and 1 ppm zinc respectively. Sulphur AA was not detected, only attenuation of the light-beam by concentrated sulphur solutions: $>$ 1000 ppm.

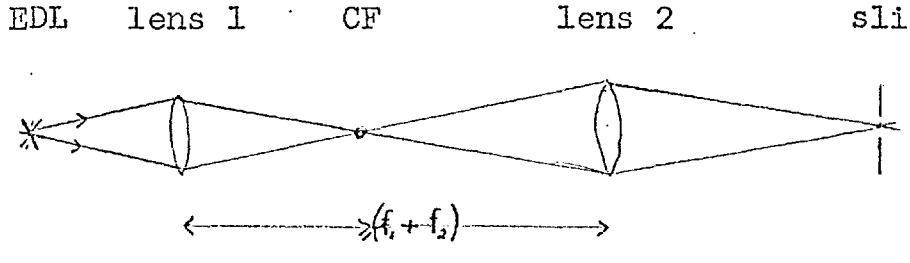
Fig 3.13 OPTICAL SYSTEM FOR AA TESTING OF CADMIUM, ZINC AND SULPHUR



All components along the optical bar were touching (Fig.3.13). This was because light losses by absorption can be high in the vacuum uv, and light levels were low, since illumination was restricted to the sample vapour region.

Alternative optical systems included lenses: long 'ideal' optical paths (Fig.3.14), or shorter paths with light concentrated over the filament by a short focal length lens doublet.

Fig 3.14 AN IDEALISED OPTICAL PATH USING TWO BICONVEX LENSES TO COLLECT AND FOCUS LIGHT



However, since the quartz lenses available transmitted only 50% of incident radiation at 182.0 nm, and alternative fused quartz or expensive fluoride lenses were unavailable, it was necessary to use windows and collimators only.

Window material, thickness and number were chosen. At 182.0 nm, transmission by 1 mm Spectrosil was more than 10% better than by 1 mm Vitreosil silica windows. Finally, just one Spectrosil window interrupted the light beam. Signal diminution by this window was offset by the greater purging efficiency obtained by operating two separate gas-tight units. Several collimating slits of 0.5, 2.0 and 5.0 mm height x 0.5, 1.5 and 2.0 mm width were positioned in turn immediately in front of the filament, to approximately determine the best shape and area for slits. Then three rectangular slits in duralumin, of 0.5, 1.0 and 2.0 mm height and 3-4 mm width were tested particularly. Best responses occurred for 0.5 mm slit height, but 1 mm was usually necessary to provide a practicable light intensity. The preliminary alignment by tube collimation of light leaving the tuning-cavity enhanced precision. The original monochromator diffraction grating was exchanged for one blazed at 200.0 nm.

Light sources.

Both the general operation of the EDLs, and the recognition of specific sulphur lines, were examined. Signal:background for the three unresolved sulphur lines was ca 10:1 for the restricted viewing system evolved. High electronic noise levels were associated with the amplification of the low light levels. These were minimised by use of 2000 V EHT and by adjusting the monochromator slit-width to use $y \geqslant 5$ V/cm for the oscilloscope ordinate scale,

rather than using a lower EHT and more y scale-expansion.

The type and position of the tuning-cavity was also considered. A $\frac{1}{4}$-wave cavity might produce marginally greater signal intensity than $\frac{3}{4}$-wave, but at this stage, better preliminary collimation was obtained from the latter. It was tested variously: open, open with a pin-hole over the exit, end-on, or turned to allow light to emerge from the side-arm. The last condition was selected.

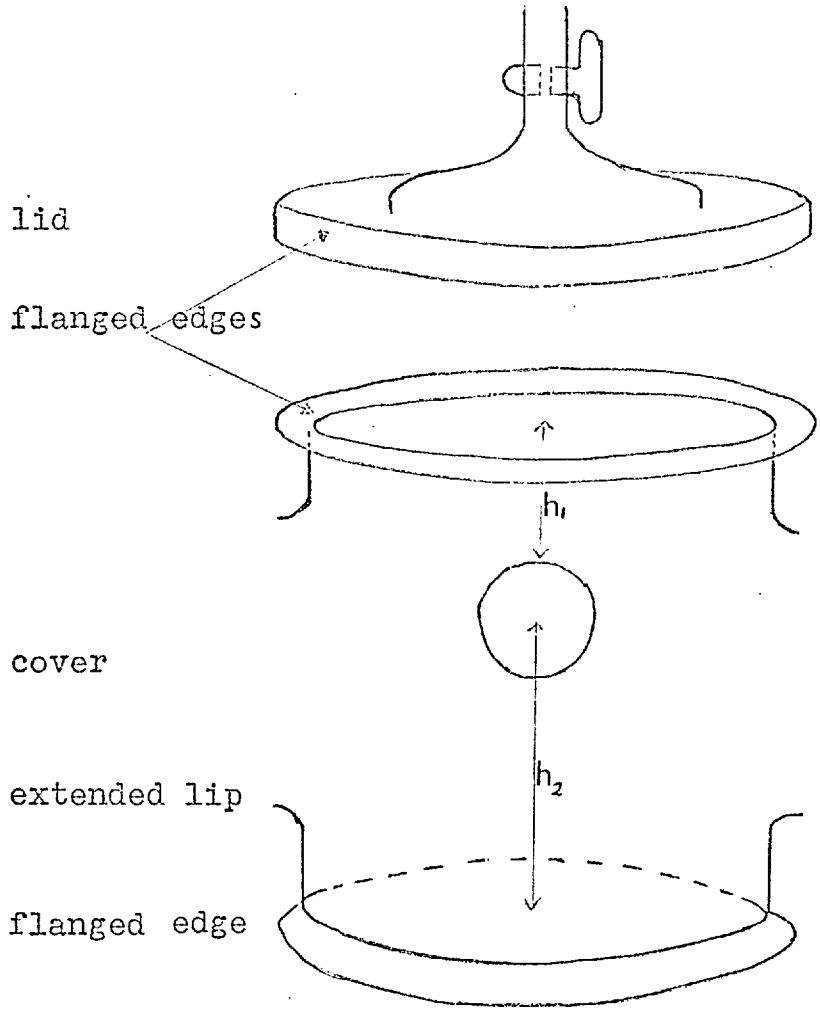
Several more sulphur EDLs were prepared and tested to characterise the individual tubes and select those of high intensity output of the three unresolved atomic lines: 180.7, 182.0 182.6 nm. Typically, signal:background for the unresolved lines was measured with monochromator slits 0.5, 1.0 and 1.5 mm at power supplies of 30, 50 and 70 W in turn. Low power and narrow slit was the best condition and practicable for intense sources.

Later, the separate sulphur lines were resolved. In AA measurements, a primary aim is the provision of a concentrated light beam of adequate intensity. The original monochromator slit was too wide to resolve the three adjacent lines, 0.5 mm wide being equivalent to 0.8 nm band-pass. The component lines were resolved by a 0.2 mm slit. Comparative emission intensities for 180.7, 182.0, 182.6 nm were 1 : 5 : 9. L'vov reports the first as most sensitive in AA but since this emitted least strongly, all were tested here (48).

CFAR

The simple prototypes were successful and a useful outcome of these experiments was the design and construction of a glass

Fig 3.15 GLASS LID AND COVER FOR CFAR



internal diameter	6.2 ± 0.2 cm
external diameter	7.2 ± 0.2 cm
flanging depth	0.8 ± 0.2 cm
lip	0.5 ± 0.2 cm
large window diameters	4.3 ± 0.3 cm
side-entry diameter	1.8 ± 0.3 cm
h_1	1.5 ± 0.2 cm
h_2	3.0 ± 0.2 cm

cover for the CFAR which has subsequently been used advantageously for AA of metals at >200.0 nm as well as for this application (Fig.3.15).

The glass cover has large windows which provide flexibility in optical alignment. The side-entry and separate lid allow filament exchange and sample introduction respectively without disturbance of a tight optical alignment. This basic dome is adaptable to many applications. For example, AF is feasible, with illumination from the side or above, and side arms can be added at the main windows to extend an enclosed optical path.

Also the chemical source of sulphur, and its solvent, concentration and volume, were considered further.

Water-soluble sources are inorganic alkali metal and ammonium salts, inorganic acids or organic sulphonic acids. Sulphate, sulphide, thiosulphate, thiocyanate and thiourea were all tested.

Organic solvents for solid sulphur or organic compounds which contain sulphur were considered: benzene, carbon disulphide, toluene and cyclohexane. The former are very poisonous, and toluene an insufficiently good solvent, but cyclohexane evaporates off the filament well, and can dissolve >200 ppm solid sulphur.

In practice, most 1 µl x 1000 ppm sulphur solutions volatilised from the filament would attenuate signals, but unspecifically. 100 ppm solutions gave no attenuation although AA should have been detectable on the system at this level.

10^{-10} g is the sulphur sensitivity quoted by L'vov, who used 10^{-8} g sulphur samples from copper and cadmium sulphates at 180.7 nm (48). Relating this to the CFAR approach, where 1 µl of 1 ppm sulphur solution contains 10^{-9} g, 1 µl x 100 ppm sulphur solution should give definite AA signals.

Therefore tests for sulphur AA continued using aqueous solutions of copper, sodium and cadmium sulphates, sulphuric acid and saturated solutions of sulphur in cyclohexane (<500 ppm sulphur).

Interim conclusions.

The foregoing survey of practical tests shows some of the theoretical disadvantages of sulphur AA reflected in practice. Even with the final experimental assembly, sulphur AA was not certain. Typically, 1 µl of concentrated solution (1000 ppm sulphur), volatilised after evaporation of solvent, attenuated the light source signal on the oscilloscope, but not selectively. The effect occurred at several wavelengths, and with sulphur-free solutions of similar concentration such as those of zinc salts. Less concentrated solutions (100 ppm sulphur) did not attenuate the signal.

Such unwanted optical interference, occurring as light passes through a turbid medium, is manifest as non-selective absorption. L'vov comments that this may occur in AA when there are foreign substances present ≥ 4-5 times the amount of element being determined (45 p.230). He distinguishes 'molecular' and 'particulate' non-selective absorption. High temperatures for atomisation, 2000°C compared to 1700°C for example, decrease the former by encouraging molecular dissociation. The scattering of light is especially prevalent in the vacuum uv and is related to the ratio of wavelength to diameter of the scattering particles.

The interference effect can usually be eliminated by using slits to view only the region where atomic absorption is the

major contribution. Then a signal is measured which is the difference between one due to a line source and a reference beam from a continuous source. This method assumes a negligible AA contribution from the latter source.

Here, a narrow horizontal slit (1 mm) was positioned in front of the filament, because low light levels are inherent with the ideal viewing condition of 0.5 mm over the filament (40:I,IV,V). It was still hoped to detect sulphur at moderate concentrations.

Next tests should show whether lack of sulphur AA was due to insufficient formation or concentration of atoms, or inadequacies in the illumination or signal detection methods. It is necessary to produce an absorption signal attributable solely to the atomisation of sulphur, and detectable because due to the interruption by a hot concentrated atom cloud of a suitably intense line source light beam of adequate intensity.

The degree of atomisation obtained will still be uncertain, but other aims should be attainable by continued improvement of the experimentation assembly and by seeking AA of similar elements while continually checking for sulphur AA.

Increased light levels might result from making new thinner walled EDLs and operating these in a $\frac{1}{4}$-wave tuning-cavity, at minimum power or with attenuation of the power supply, and comparing the use of resolved and unresolved lines. Perhaps different filament materials such as tungsten should be used, or atomic fluorescence, where beam collimation is less important.

After the previous success in detecting cadmium and zinc, the examination, on the improved system, of other elements with vacuum uv sensitive lines was chosen as the most promising

development. After preliminary collection of data for elements, light sources, atomic lines, sample salts and working conditions, several elements were selected for testing at exploratory levels.

3.5 Alternative vacuum uv analyses.

Approach.

It was decided that it was first necessary to test the suggested modifications to the analytical system and confirm its potential sensitivity by demonstrating the AA of cadmium at low concentrations. This would be followed by a general survey of the current state of AA detection of elements with sensitive absorption lines in the vacuum uv. After a consideration of the physical and chemical characteristics of several such elements, vacuum uv analysis of those most suited to the CFAR assembly was tried.

Modifications to the analytical system.

Light sources.

Sulphur, phosphorus and iodine EDLs prepared from thin-walled quartz tube: 8.6 mm external diameter, 7 mm internal diameter, showed no significant advantage over those made previously.

Dimensions of silica tubing used to prepare EDLs.

	Internal diameter mm	External diameter mm	Wall thickness mm
Normal	8.0	10.0	1.0
Thin-wall	7.0	8.6	0.08
	7.4	8.8	0.07

50-60% of the lamps made would light, although sometimes only in a $\frac{1}{4}$-wave cavity. The nature of the sulphur-argon filler gas was more important than wall thickness.

Tuning cavities.

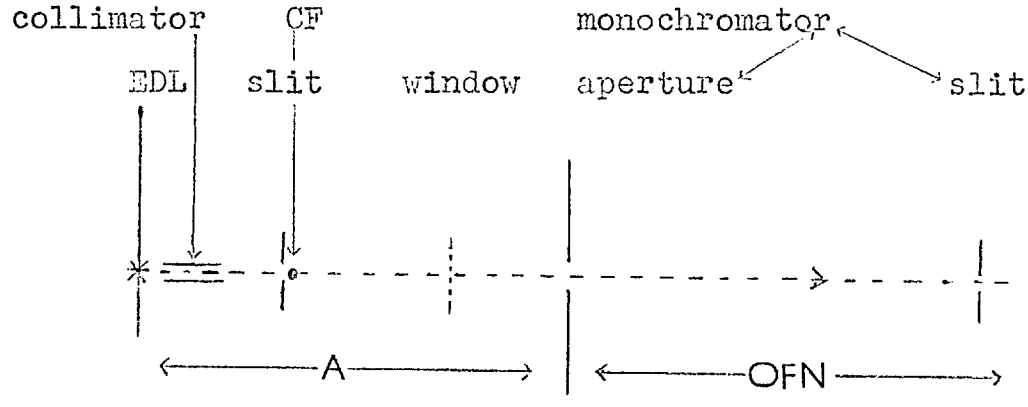
After evaluation, the EDLs were run under such conditions as best suited individual lamps. $\frac{1}{4}$- or $\frac{3}{4}$-wave tuning cavities were used, often operated at low power ≤ 30 W, for maximum line

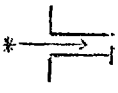
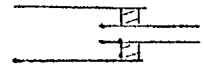
intensity and minimum associated noise. Sometimes it was possible to use minimum Magnetron power: 18 W, and still maintain a stable discharge. However, the imposition of further attenuation by incorporating an electronic attenuator in the coaxial cable or by running the lamps untuned would only very occasionally be worthwhile.

Collimation.

Collimator tubes and slit sizes were chosen to suit particular lamps and cavities.

Fig 3.16 GENERALISED OPTICAL ARRANGEMENT FOR TESTS

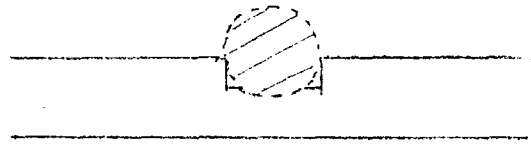


With the $\frac{3}{4}$-wave cavity, the collimator tube was the side-arm of the cavity with a semi-circular exit aperture:  .
For the $\frac{1}{4}$-wave cavity a series of 5 cm collimator tubes of various internal diameters were tested:  , with 1 cm overlap of outer (0.9 or 1.9 cm diameter) and inner (2.0, 3.5 or 4.0 mm diameter) tubes. As with the auxiliary CFAR and monochromator slits, minimum diameter provided maximum sensitivity, but it was

usually necessary to compromise with intermediate dimensions compatible with the EDL intensity.

CFAR slit

A 1.0 mm height CFAR slit was generally preferred to 0.5 mm. It was easier to position in front of the filament, and had associated good light levels, sensitivity and viewing range. However, to extend detection limits in specific determinations with an intense EDL it is worth testing the narrower slit after minimising the monochromator slit-width. AA signals were measured for various heights of both slits, with respect to filament and monochromator, up to 5.0 mm over the filament notch. Highest sensitivities were associated with the region immediately over the notch, which should therefore be the main illuminated region.



Servicing.

At this stage, several electrical faults developed in the instrumentation. Faulty rectifiers were replaced in the Brandenburg EHT after approximately one month of running at 2000 V and eighteen months at 1000-1500 V. The oscilloscope JD amplifier also failed, and the transformer heavy duty 2-pole rotary switch. The latter was attributed to the frequent large current surge to which it is subject.

Cadmium.

The optical system evolved for vacuum uv measurements was sensitive for the AA detection of cadmium (3.4). In these tests cadmium was continually used as a convenient standard against which to check slit sizes and positions and to locate lines. Absorption traces obtained from various conditions of volatilisation of cadmium also assisted the recognition of various effects produced in subsequent experiments with different elements of uncertain behaviour.

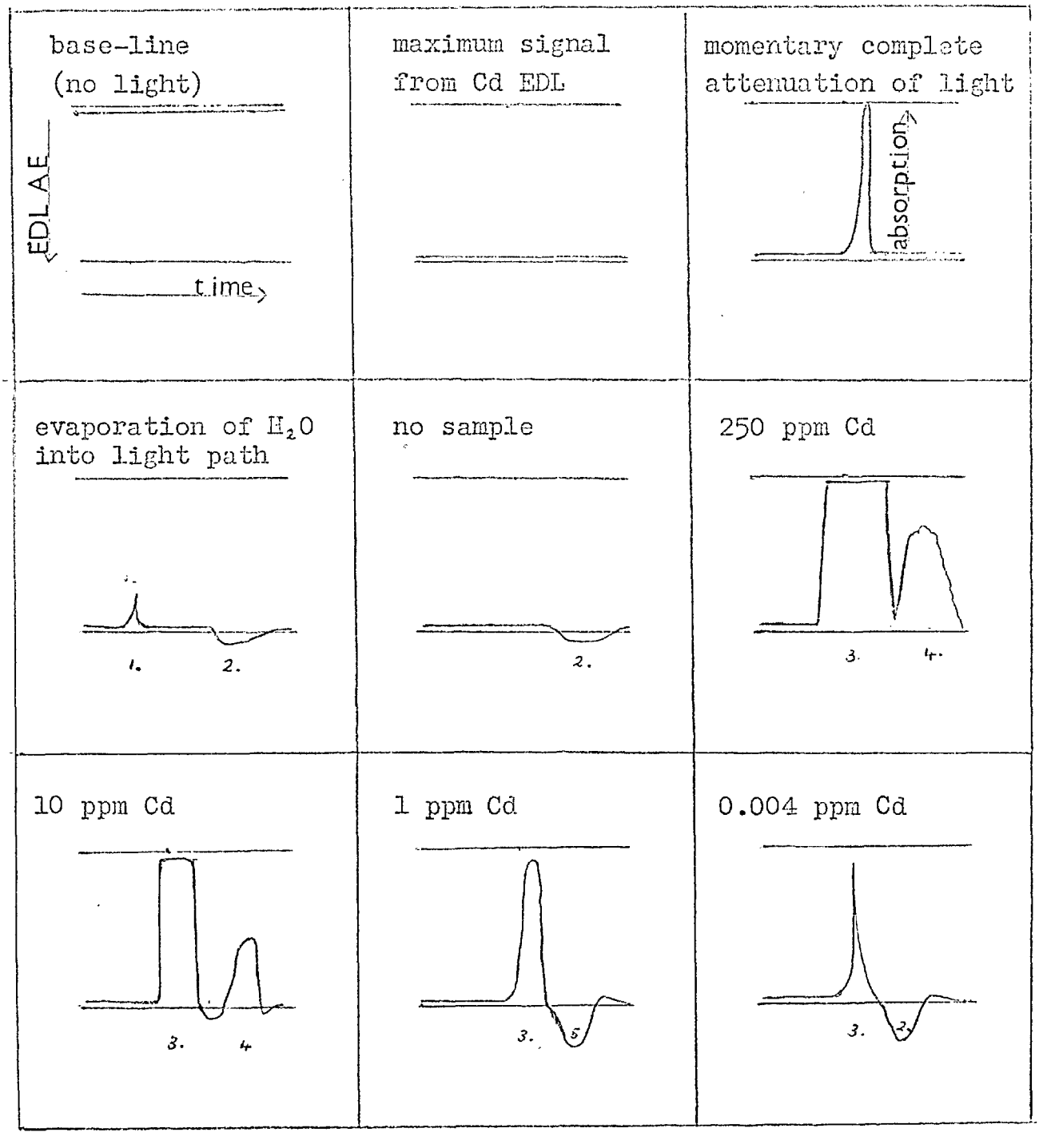
Working conditions and results for cadmium AA.

Condition	Value
power to EDL	50 W
monochromator slit-width	0.2 mm
EHT	2000 V
oscilloscope y-scale	10 V/cm
oscilloscope time-base	1 sec/cm
EDL source signal (y)	2-3 cm
noise on signal trace	< 0.5 cm
variac to evaporate solvent	±7 sec/2V
variac to atomise Cd	on/off/±9V
argon flow-rate	1 lt/min

Results

Atomic line nm	Salt	Concentrations ppm	Low concentration absorbance	
228.8	$3CdSO_4.8H_2O$	0.004 0.4 20 250	0.001 ppm	0.05

Fig 3.17 CADMIUM AA USING CFAR: ILLUSTRATIONS OF TYPICAL OSCILLOSCOPE ABSORPTION TRACES WITH DESIGNATIONS OF EFFECTS



Interpretation of traces
1. molecular absorption by solvent at low variac voltage
2. Cf emission at low variac voltage
3. cadmium AA signal
4. light scattering after atomisation of high Cd concentrations
5. CF emission at high variac voltage

Cadmium samples were atomised after evaporation of water.

Choice of elements for vacuum uv analyses.

A reasoned consideration of the situation and prospects preceded CFAR exploratory experiments for AA detection of sulphur (3.4). This survey was extended before choosing further elements for testing.

These elements, which have sensitive absorption lines at < 200.0 nm, were mercury, selenium, phosphorus, arsenic, the halides, oxygen, nitrogen and the inert gases.

Some high wavelength atomic lines exist for the inert gases. All the vacuum uv gas resonance lines are at >105.0 nm except for helium, neon and fluorine, but the majority at <135.0 nm. Atomisation can be obtained by heat or electrical discharge, or sometimes molecular absorption measurements are made (45). This extremely low wavelength range is inaccessible with the Optica monochromator. Also gases may be unsuited to the CFAR technique, especially at the vacuum uv exploratory level.

More promising, with accessible sensitive lines, preparable EDL sources and likelihood of atomisation were mercury, arsenic, selenium, phosphorus and iodine. There are comparatively few reports of AA determinations of any of these. Vacuum flameless methods or the use of unusual transitions are generally recommended. Sensitivities for 1% absorption are usually ten to one hundred times greater than those obtained for sulphur, however.

Mercury, arsenic and selenium have all been determined in flames at > 200.0 nm (44), but such modifications as separated flames (50), or sampling cups (51), are necessary to achieve high sensitivities.

L'vov and Khartsysov report the determination of mercury,

phosphorus and iodine as well as sulphur, using the graphite cuvette atomiser in conjunction with a vacuum monochromator, and resonance lines 175.0-185.0 nm (48). Alternatively, a sputtering cathode method has been described for the vacuum determination of phosphorus (52).

There are also reports of flame or flameless determinations of phosphorus and iodine using favoured transitions of metastable states at >200.0 nm (53,54,55(P),56(I)).

Here it was decided to attempt the AA detection of mercury, arsenic, selenium, phosphorus, iodine and sulphur on the CFAR analytical system.

Exploratory tests: mercury, arsenic, selenium, phosphorus, iodine and sulphur.

To select promising conditions for the detection of each element, the analytical lines available, and the literature conditions and results for their detection on a related atomising system, usually L'vov's graphite cuvette, were surveyed (Fig 3.18)

Further consideration concerned the likelihood of atomisation of particular elements, and the changes necessary to convert various combined forms to uncharged monatomic species (Fig.3.19).

With these results in mind, chemicals of adequate solubility were selected from those available, and source solutions of suitable type and concentration were prepared and tested at appropriate wavelengths. Aqueous solutions of inorganic chemicals were used for these initial tests, but the alternative approach of using solid solutes in organic solvents was recognised

It was also necessary to assemble a range of working EDLs. New phosphorus and iodine lamps were made containing red

phosphorus-argon and iodine-argon respectively. All lamps were tested to find the order of intensity of emission for the preferred AA lines, best operating wattage and good CFAR slit alignment and monochromator slit-width. The optical system was as previously described (3.5 'modifications'), with $\frac{1}{4}$- or $\frac{3}{4}$-wave tuning cavities as suited the characteristics of individual lamps (Fig.3.20).

The trials were carried out using cadmium AA as the standard for comparison. They included preliminary and confirmatory tests with mercury, arsenic and selenium, preliminary tests with phosphorus and iodine, and regular tests for sulphur.

The comparison of oscilloscope traces for absorption against time for the various samples vaporised from the carbon filament confirmed results indicated by cadmium (Fig.3.17). Then, solvent, molecular condensation, particulate scatter and AA peaks could generally be distinguished (Fig.3.21).

After checking the specificity of absorption to line and element, exploratory absorbance against concentration graphs were prepared for mercury, arsenic and selenium in the 0-1-10-100 ppm range (Figs.3.22,3.23,3.24). Phosphorus and iodine were also detected, but improved EDL emission for sensitive lines, or higher temperature atomisation was necessary before calibration graphs could be meaningful.

The best sensitivities usually required a low oscilloscope time-base: 1 sec/cm, a high variac setting: 8-9V, low argon flow-rate: <1.0 lt/min, narrow monochromator slit: 0.2 mm ($\equiv$ 0.26 nm band-pass) and a low Magnetron wattage: $\leq$30W (Fig.3.25).

Fig 3.18 CONDITIONS FOR EXPLORATORY TESTS (Reported in 45,46,47,53,55).

Element	Source	Atomisation temperature °C	Designation of transitions A	E	f	Order of absolute detection limit, g
MERCURY	$Hg(NO_3)_2$	700	184.9	0	1.2	10^{-9}
			253.7	0	0.03	10^{-10}
ARSENIC	-	1700	189.0	0	-	10^{-9}
			193.8	0	0.095	
			197.3	0	-	
SELENIUM	-	1600	196.0	0	0.12	10^{-10}
			204.0	>0	0.26	
			206.0	>0	0.30	
PHOSPHORUS	$NaH_2PO_4.2H_2O$	1600	177.5	0	-	10^{-10}
	H_3PO_4		178.3	0	-	10^{-9}
			178.8	0	-	10^{-9}
			213.5	>0	-	10^{-10}
		2700	214.8	>0	-	
IODINE	NaI	1500	183.0	0	-	10^{-9}
		2700	206.2	>0	-	10^{-8}
SULPHUR	$CuSO_4.5H_2O$	1600	180.7	0	-	10^{-8}
	$3CdSO_4.8H_2O$		182.0	0	-	10^{-7}
			182.7	0	-	10^{-7}
			190.0	0	-	10^{-5}
CADMIUM	$3CdSO_4.8H_2O$	1500	228.8	0	1.2	10^{-14}

KEY A Atomic line, nm
E Energy of lower level, cm
f Oscillator strength of line

Fig.3.19 ATOMISATION

ELEMENTS	E N V I R O N M E N T S		
	Some combined forms available	Elemental forms	Atomisation
MERCURY	Hg^{I} $X^{-}\cdot\cdot Hg^{+}-Hg^{+}\cdot\cdot X^{-}$ Hg^{II} X-Hg-X	$Hg_2 \rightleftharpoons 2Hg$ liquid	$Hg_2 \rightleftharpoons 2Hg^{\circ}$ liq. → gas ⇅ Hg_2 (gas)
PHOSPHORUS	PO_4^{3-}	P_4 : △ solid	$4PO_4^{3-} \xrightarrow{c} P_4$
	P-X, P-O-X, P=O, HP=O, MP=O	P_4 : in CS_2	$P_4 \rightleftharpoons 2P_2$
IODINE	IO_3^- , I^- , I^+ $I_2 + KI \rightleftharpoons KI_3$ I- X	I_2 : I-I solid I_2 in CS_2 , CCl_4 $S \leftrightarrow I_2^{-} \cdots S^{+}$ in C_6H_6 liq. SO_2 , alcohols, unsaturated hydro-carbons	$IO_3^- \xrightarrow{c} I^-$ $I^- \xrightarrow{o} I$

KEY: X = halogen

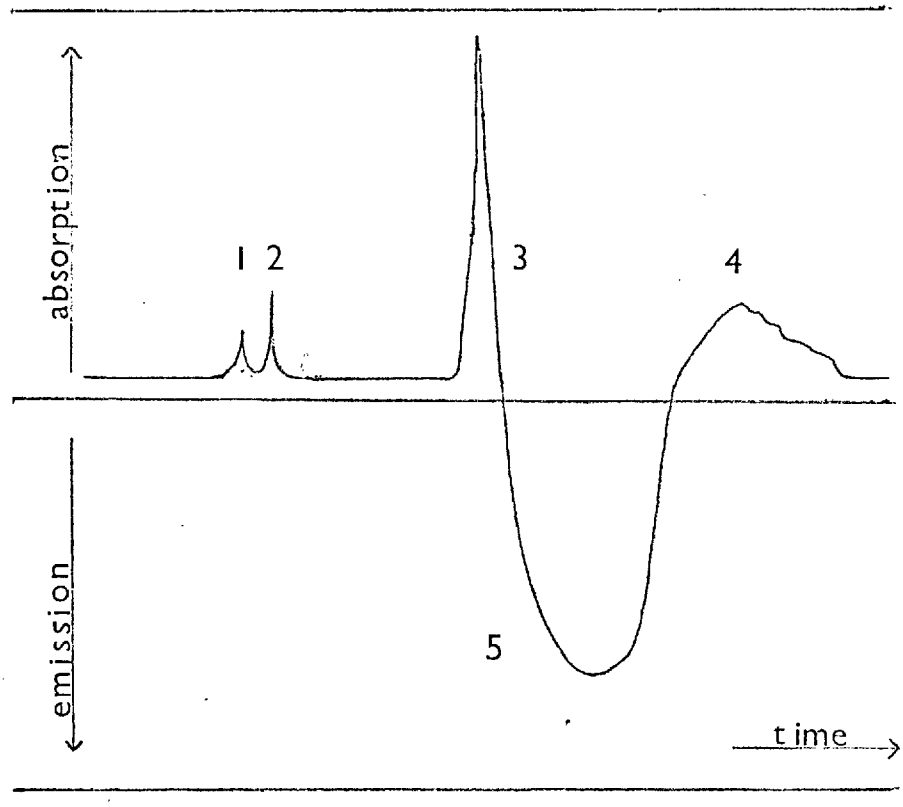
S = solvent molecule

N.B. cf. sulphur atomisation (3.4)

Fig 3.20 SUGGESTED WORKING CONDITIONS

Element	Source	Power to EDL W	Atomic line nm	Monochromator slit-width (MS)	Oscilloscope y-scale V/cm	EHT V
MERCURY	$HgCl_2$	<30	184.9	0.2	10	2000
			253.7	0.1	20	1750
ARSENIC	KH_2AsO_4	35	189.0	0.2	10	2000
			193.8	0.2,0.4	10	2000
			197.3	0.2,0.4	10	2000
SELENIUM	$(NH_4)_2SeO_4$	40	196.0	0.2	10	2000
			204.0	0.2	10	2000
			206.0	0.2	10	2000
PHOSPHORUS	$NaH_2PO_4 \cdot 2H_2O$	70	177.5	-	-	-
			178.3	-	-	-
			178.8	-	-	-
			213.5	0.3	10	2000
IODINE	KI	35	183.0	0.4	2	2000
			206.2	0.2	10	1700
SULPHUR	$CuSo_4 \cdot 5H_2O$	<30	180.7	0.3	2:0.3MS	2000
	$3CdSO_4 \cdot 8H_2O$		182.0	0.3 } 0.8	5:0.8MS	2000
	S/C_6H_{12}		182.7			2000

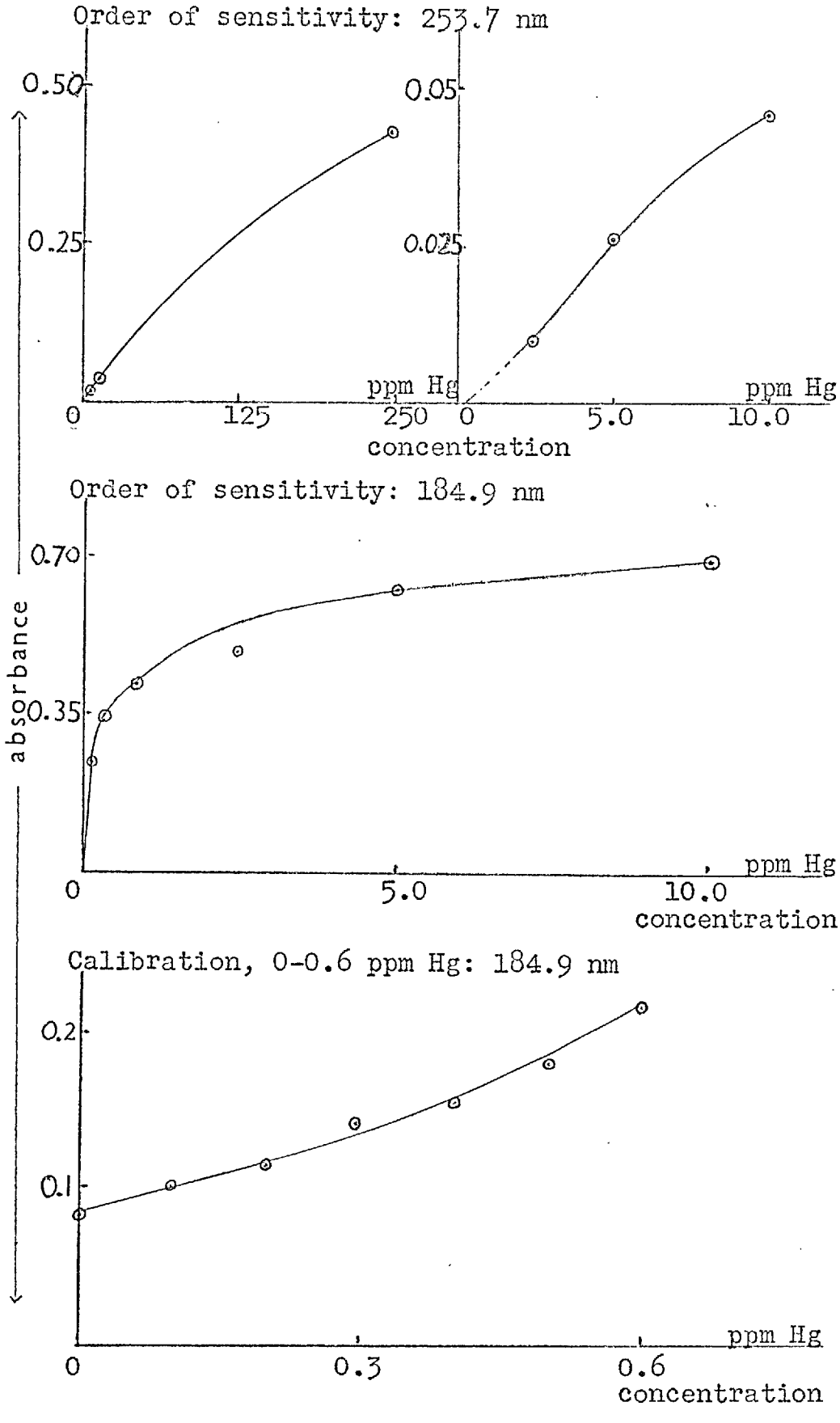
Fig 3.21 DESIGNATION OF PEAKS AND TROUGHS ON THE OSCILLOSCOPE TRACES (cf. Fig 3.17)



Interpretation of traces

1. solvent absorption
2. molecular absorption
3. atomic absorption
4. scatter absorption
5. filament emission

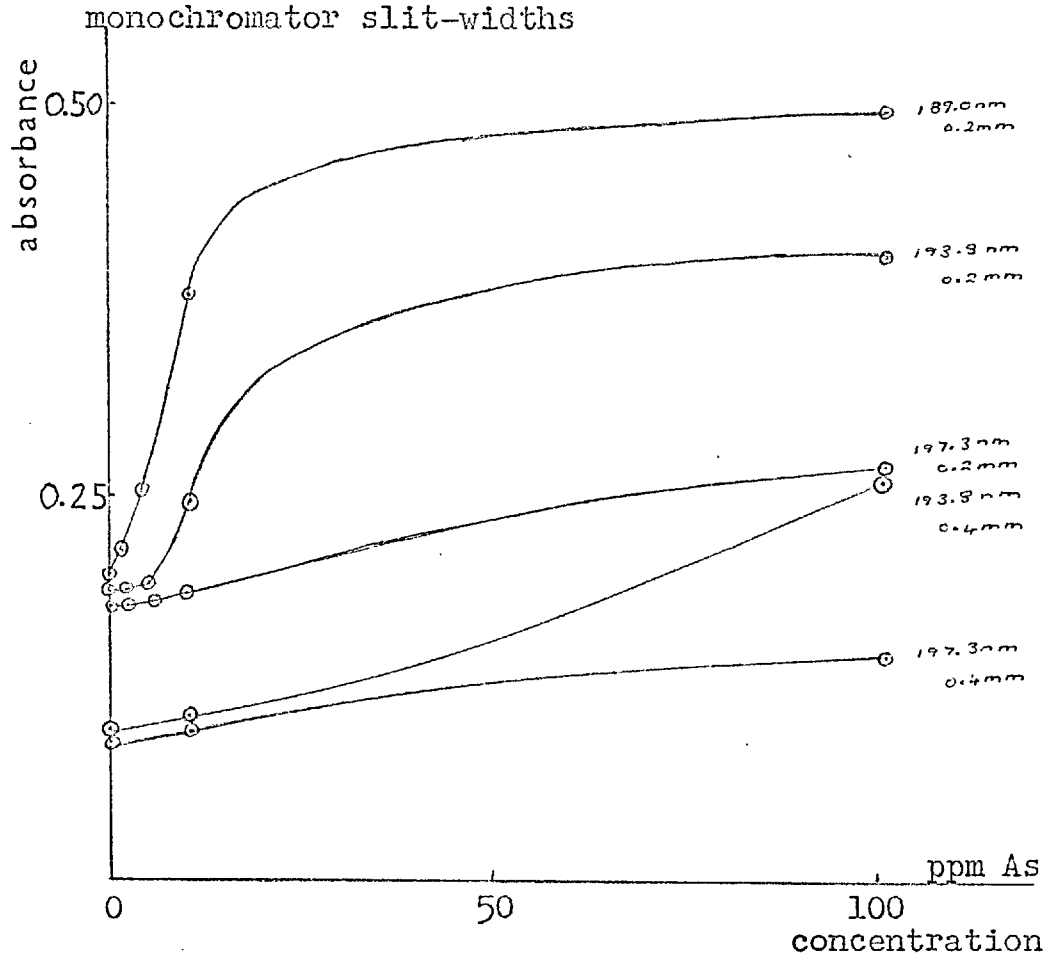
Fig 3.22 MERCURY AA



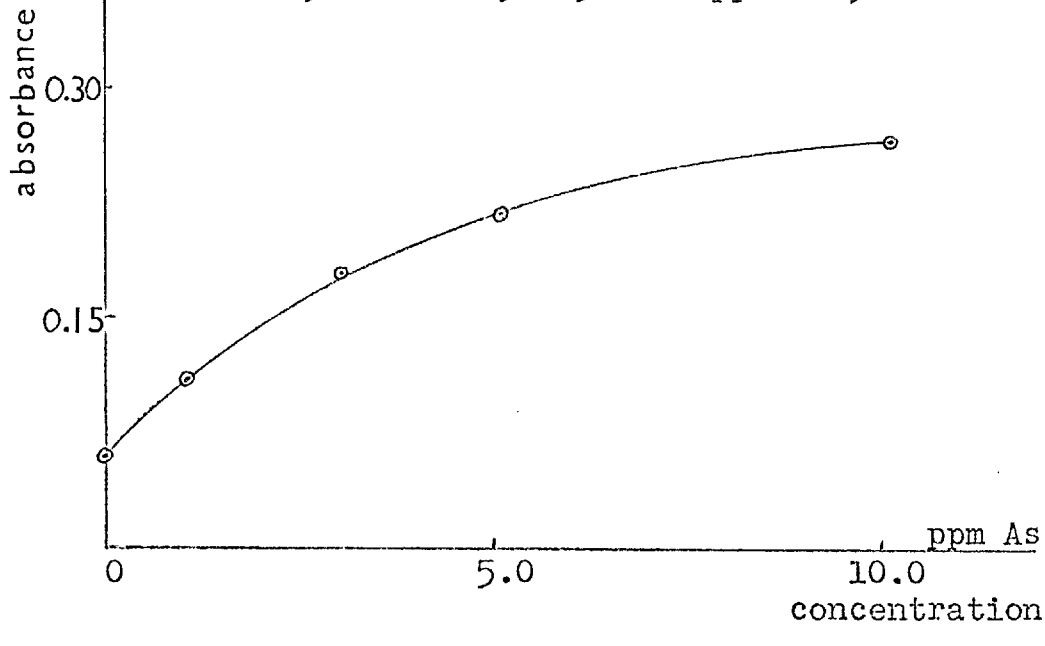
detection limit ≏ 0.25 ppm

Fig 3.23 ARSENIC AA

Comparative sensitivity of atomic lines and monochromator slit-widths

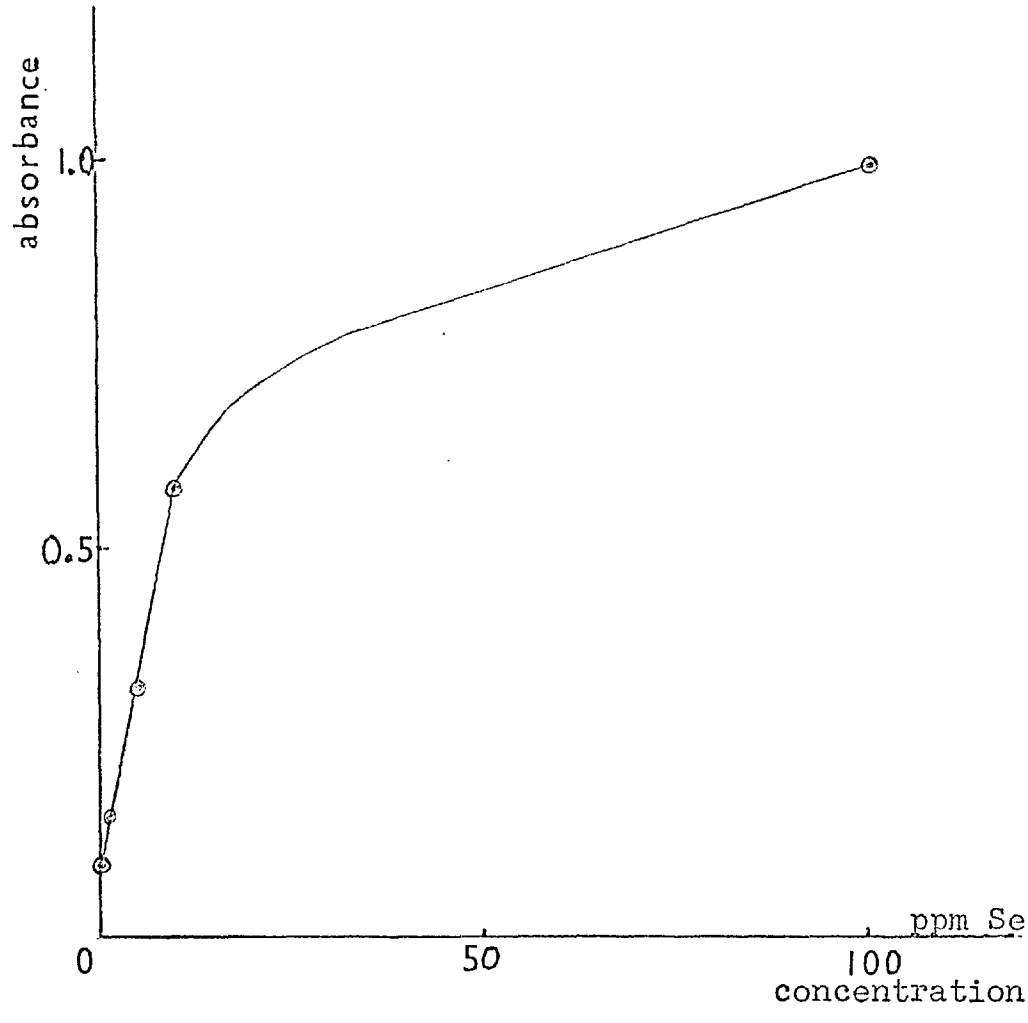


Calibration, 0 - 1 - 3 - 5 - 10 ppm: 189.0 nm



detection limit ≐ 1 ppm

Fig 3.24 SELENIUM AA : 196.0 nm



exploratory calibration: 0 - 1 - 5 - 10 - 100 ppm

detection limit ≐ 1 ppm Se

Fig.3.25 SUMMARY OF SOME RESULTS OF AA TRIALS USING EDL LINE SOURCES AND A CFAR.

Element	Atomic line nm	Typical relative EDL intensity	ppm detected	Order of absorbance	Development recommended
MERCURY	184.9	2.9 strong	0.1	0.08	Yes
	253.7	4.9 strong	1.0	0.10	-
ARSENIC	189.0	1.5	1.0	0.20	Yes
	193.8	1.3	10.0	0.10	-
	197.3	1.3	10.0	0.05	-
SELENIUM	196.0	2.5	1.0	0.05	Yes
	204.0	2.0	-	-	-
	206.0	2.0	-	-	-
PHOSPHORUS	177.5	0.0	-	-	Yes
	178.3	0.0	-	-	-
	178.8	0.0	-	-	-
	213.5 / 214.8	1.8	100	0.04	-
IODINE	183.0	1.0	100	1.0	Yes
	206.2	2.0 strong	1000	0.10	Yes
SULPHUR	180.7	0.5 } or 2.5 unresolved	1000	0.08	Yes
	182.0	1.3 }			Yes
	182.7	1.8 }			Yes
CADMIUM	228.8	2.5 strong	0.001	0.05	Standard

Comment on results.

In the foregoing tests, atomic lines more sensitive in terms of oscillator strength were compared to those normally accessible which are used for flame AA. It was also hoped to demonstrate the suitability of the CFAR for atomisation of the elements concerned, and to achieve detection of sulphur atoms. In these first trials, sensitivities were poor, especially compared to those obtainable for most metals. However, these elements are always awkward to determine, and here atomisation had to be successful, and also initially unknown optical conditions had to be arranged. From this starting-point, developments can be made to extend the detection ranges considerably.

Fig.3.25 has summarised specific results and provides a basis for an evaluation of prospects. Adequate atomisation was obtained except for sulphur. The value of the individual determinations varies. It would be necessary to use dilute solutions and ideal optical conditions to make quantitative measurements. Comparisons are possible, however.

For mercury, 184.9 nm is ten times more sensitive in absorption than 253.7 nm, and source emission, although less intense, provides an adequate signal. With focussing in the vacuum uv, 184.9 nm could give a high sensitivity compared to 253.7 nm. However, unfocussed, and requiring a purged or evacuated environment, the 184.9 nm line may not always be preferred in practice.

For arsenic and selenium, however, all AA lines are enhanced in an oxygen- water- free atmosphere. The lowest wavelength lines are the most sensitive in absorption as well as the strongest emitted by EDLs. Therefore, both arsenic 189.0 nm and selenium

196.0 nm are worth exploiting further on the CFAR system, especially the latter.

Although several phosphorus and iodine EDLs emitted strongly in some regions, iodine 183.0 nm was only a very weak signal and phosphorus ca 177.5 nm lines were undetected. Iodine 183.0 nm was very strongly absorbing, so should be examined further with alternative light sources, and the intense iodine 206.2 nm line might have application in emission work. With silica lenses for focussing in the >200.0 nm region, and the use of a hotter filament, perhaps of a more resistant material than carbon, it might be possible to evolve and detect atoms efficiently at the metastable transition lines: 206.2 nm for iodine, 213.5 nm for phosphorus. Use of favoured transitions of vacuum uv lines would be preferable, however.

Sulphur AA was undetected. Probably insufficient atomisation of sulphur occurs or the response time of the oscilloscope is too long to detect atoms before recombination. The only sulphur solutions to give absorption were of such high concentration that the non-specific absorption was attributed to scatter, not AA.

In development it is imperative to ensure sample atomisation and ascertain detection of atoms produced. The lines from the EDLs are certainly due to atomic transitions. Problems are the high associated noise levels, and the need to maintain an oxygen-water-free environment. Even small air leaks can significantly reduce signals.

Some form of focussing is necessary: fluoride lenses or front-silvered reflectance microscope objectives are suggested to concentrate available light within the atomisation region.

The consequent attenuation of oscilloscope y-scale will decrease the effect of signal noise. With improved light levels and collimation, lines should be more clearly defined, and vacuum uv calibrations possible at lower concentration ranges, by working with narrower slits.

Cadmium will continue as a useful standard, while developing AA detection of the various elements. Different chemical sources and alternative solvent systems should also be tried. Improved fine adjustment of the vertical and horizontal displacement of the CFAR should aid alignment.

The major problem that remains is the long light-path between the EDL source and the photomultiplier, along which considerable light-losses will occur. The photomultiplier itself, EMI 6256 B, is a tube with a 2" diameter Spectrosil end-window, 10 mm cathodes and 13 'venetian blind' dynodes. It should be adequate as the sensitivity range extends to 165.0 nm. However, a solar blind photomultiplier, which acts as a visible/uv cut-off filter and should ignore continuum radiation from the hot filament, may be used in a short-path optical system without a monochromator.

It was decided to use this latter approach next, in conjunction with the alternative technique of AF: inherently more sensitive than AA. Focussing by front-silvered mirror objectives should provide intense illumination within short light-paths.

3.6 Non-dispersive atomic fluorescence.

Technique.

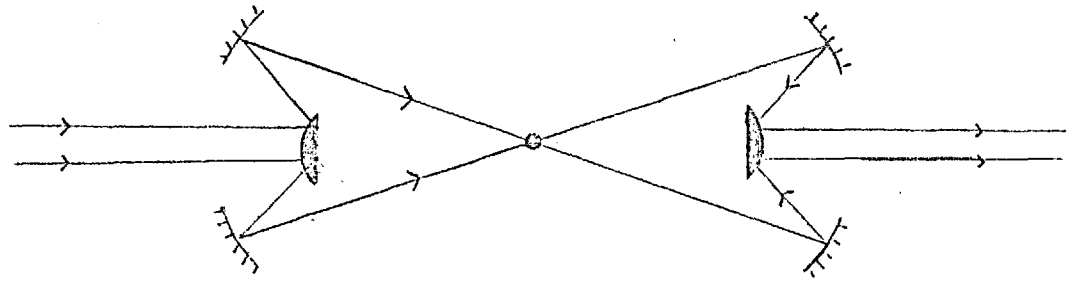
The CFAR can be used for atomic fluorescence as well as atomic absorption analysis. The AF determinations of silver, magnesium, lead, zinc, bismuth, thallium, gallium, cadmium and gold, on the CFAR, have all been reported (40:I-IV). This thesis includes descriptions of the AF technique (Introduction, 1.1, 1.4) In this section, the AF determination of sulphur, iodine and metals having their principal resonance lines low down in the uv or the vacuum uv, was sought. It required the design, construction and trial of a new AF system for measurement of short-wavelength and vacuum uv emission.

AF differs from AA in the necessary practical arrangement and operating characteristics (57). The fluorescence detector subtends a right angle with the source of excitation at the atom reservoir. Instead of measuring a small difference between two fairly large signals, an absolute measurement of the fluorescence signal is made, which may be amplified in a way not possible in AA. Specificity of analysis can be retained by using a high-intensity line source (EDL). Also, an increased sensitivity compared to AA is sometimes obtainable due to the linear dependence of fluorescence on the line intensity of the source.

There may be limitations to sensitivity due to the nature of AF signals. These are recorded with respect to zero light levels, and a small emission signal must be distinguishable from the noise-level on the zero-light baseline. In contrast, the AA difference measurement of an absorption signal is only limited by noise associated with emission from the atomic line source.

For this particular vacuum uv application, a minimum light path-length is desirable. Since the atoms in the atom reservoir act as their own monochromators, it is possible to eliminate the grating monochromator, thus allowing higher light intensities to fall on the photodetector. It is not feasible to eliminate the monochromator in AA because the source which irradiates the detector continuously also emits non-resonance lines and the filler-gas continuum. Silica lenses have to be avoided, as are glass lenses in the uv range, because they appreciably absorb radiation below 200.0 nm. For this reason it was decided to use a pair of reflectance objectives instead of silica lenses. Such objectives rely on convex hemispherical and concave torroidal mirrors to focus incident parallel light (Fig.3.26).

Fig.3.26 FOCUSSING BY REFLECTANCE OBJECTIVES



The mirrors are front-silvered, and since no dependence is placed on the use of refractive index as in silica or glass lenses, the focal length of a reflectance objective is independent of the wavelength. This is particularly useful for it is therefore

possible to fix the focal distance exactly, whatever atomic line is being used.

For this application, non-dispersive fluorescence using an atomic line source and a solar blind photomultiplier in conjunction with reflectance optics, was proposed, with the components contained within a small argon-purged glove-box.

A solar-blind photomultiplier was chosen since it responds to radiation only below 300.0 nm. This, although responsive at the atomic lines to be examined, is inactive towards white light and can be used DC in ordinary daylight. The non-dispersive approach allows all the fluorescent lines of the element that fall within the range of the photomultiplier to be used, not just the one isolated line available in conventional dispersive AF techniques.

After planning this experimental approach, several references to non-dispersive AF flame spectroscopic methods were examined (58,59,60,61). These were optimistic, so encouraged development of the proposed vacuum uv-CFAR application. For example, cadmium, zinc and mercury were determined, using spherical mirror focussing, EDLs, and a solar-blind photomultiplier.

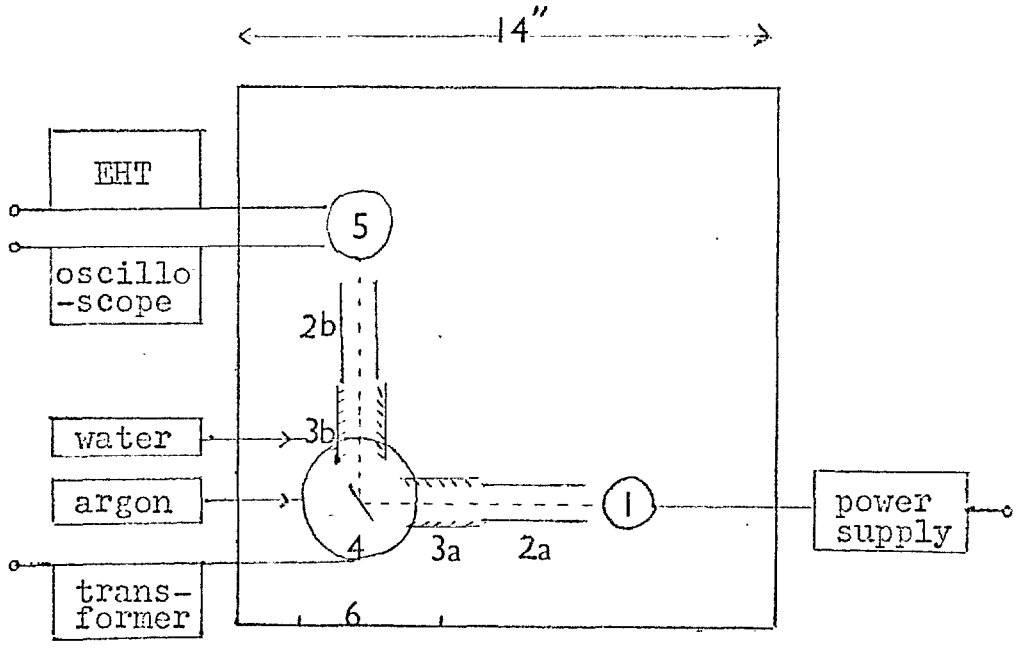
Components.

Fig.3.27 and Fig.3.28, overhead and side-views respectively, illustrate the design of the optical bench used for non-dispersive AF with the CFAR.

The lamps were operated in a $\frac{1}{4}$-wave tuning cavity because of its small size and suitability for most EDLs. The high line intensities available from such sources were another advantage.

The mirror objectives were Beck 1-inch focal-length, front-silvered, curved mirrors, mounted in threaded cylindrical tubes.

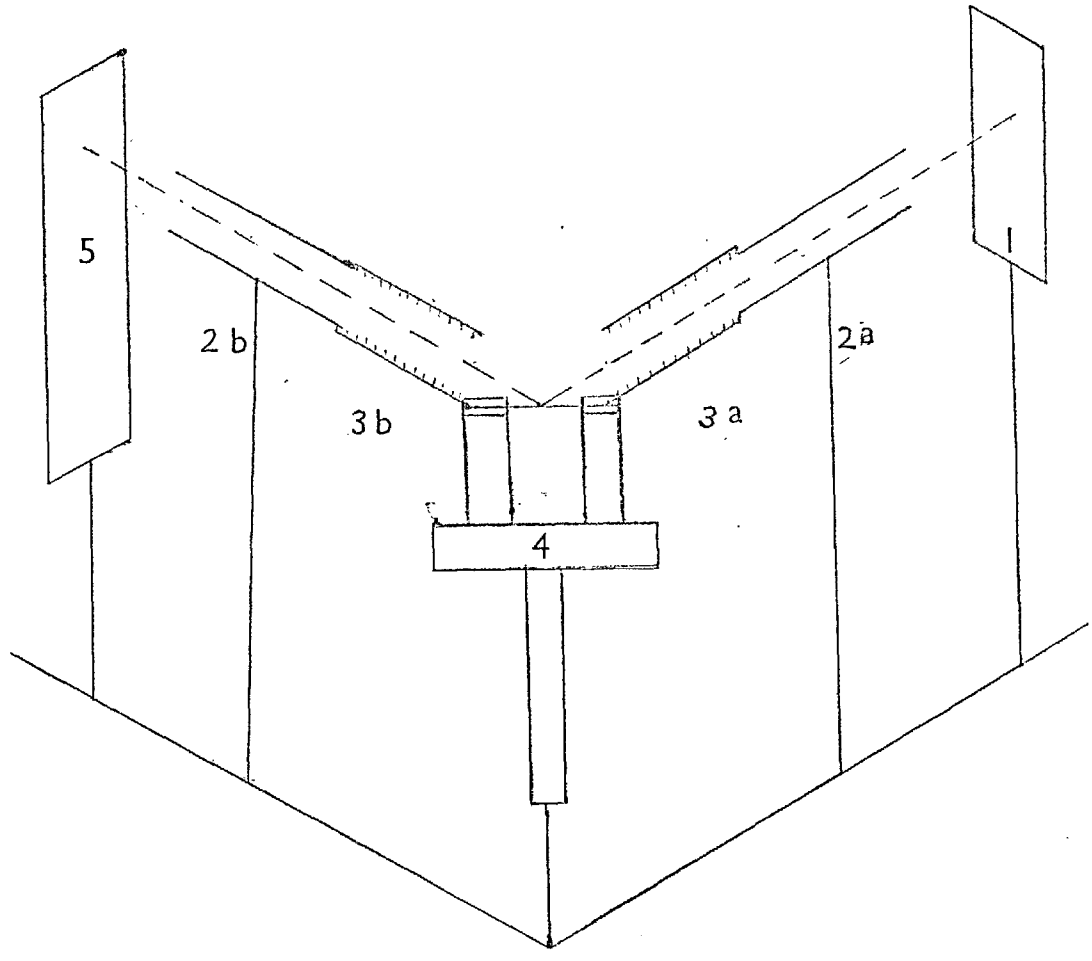
Fig 3.27 NON-DISPERSIVE AF WITH A CFAR: DIAGRAM OF THE ASSEMBLY AND OVERHEAD VIEW OF THE OPTICAL SYSTEM



Components are mounted to allow horizontal and vertical variation of their positions.

KEY
1. EDL in $\frac{1}{4}$-wave tuning cavity
2. collimator tubes to mount reflectance objectives (a & b)
3. reflectance objectives to focus light from source to CF notch and then to photomultiplier (a & b)
4. CFAR
5. solar-blind photomultiplier
6. side-entry to glove box

Fig 3.28 NON-DISPERSIVE AF WITH A CFAR: DIAGRAMMATIC SIDE VIEW OF THE OPTICAL SYSTEM



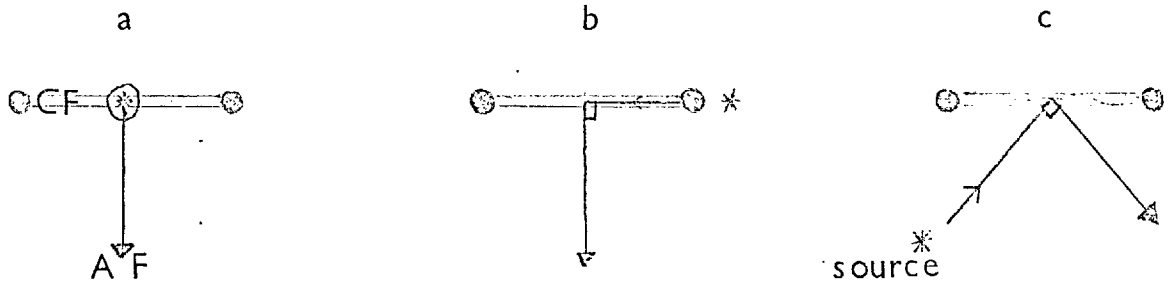
Components are mounted to allow horizontal and vertical variation of their positions.

KEY
1. EDL in $\frac{1}{4}$-wave tuning cavity
2. collimator tubes to mount reflectance objectives (a & b)
3. reflectance objectives to focus light from source to CF notch and then to photomultiplier (a & b)
4. CFAR
5. solar-blind photomultiplier

Their focussing effect is equivalent to lenses, but with maximum optical speed, zero absorbance of short-wave radiation compared to silica lenses, and action without refractive dispersal of different wavelengths (Fig.3.26)

In AF, there must be a right angle subtended between the light source and detector. The CFAR position used here was chosen after a consideration of three alternative arrangements (Fig.3.29).

Fig 3.29 ALTERNATIVE OPTICAL ARRANGEMENTS FOR AF WITH A CFAR

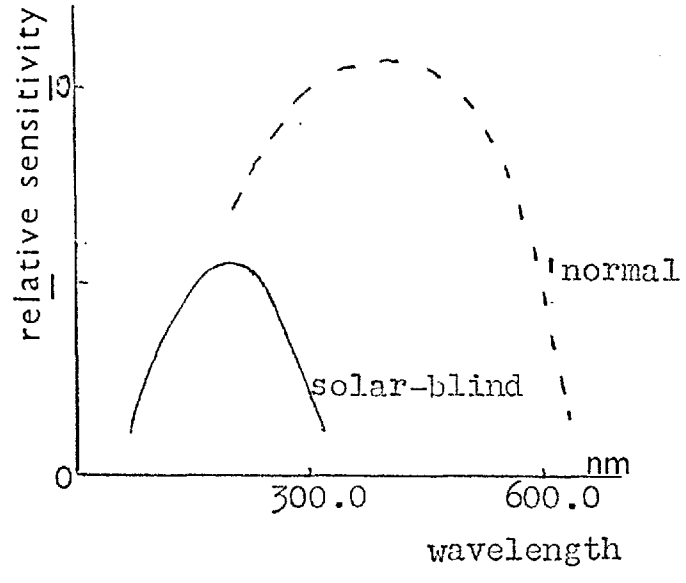


Illumination from above was not considered practical because of the risk of objective mirrors becoming stained by carbon particles, etc. (Fig.3.29a). Also alignment of illumination from above would be more difficult than along an optical path where all light travels in the same horizontal plane. Condition (Fig.3.29b) was impracticable as the height of the electrode caps restricts the passage of a light beam parallel and tangential to the carbon filament surface. Therefore the transverse approach was used (Fig.3.29c).

The photomultiplier was a Hamamatsu TV Ltd. solar-blind R166 model, for which ca |900V| is the recommended operating voltage.

It has a side-window, and a caesium-tellurium photocathode detector. The sensitivity is low, but the response range is from 160.0 nm to 320.0 nm with a maximum at 220.0 nm. This compares with the 300.0 nm to 600.0 nm normal range and higher sensitivity of most photomultipliers (62, Fig.3.30).

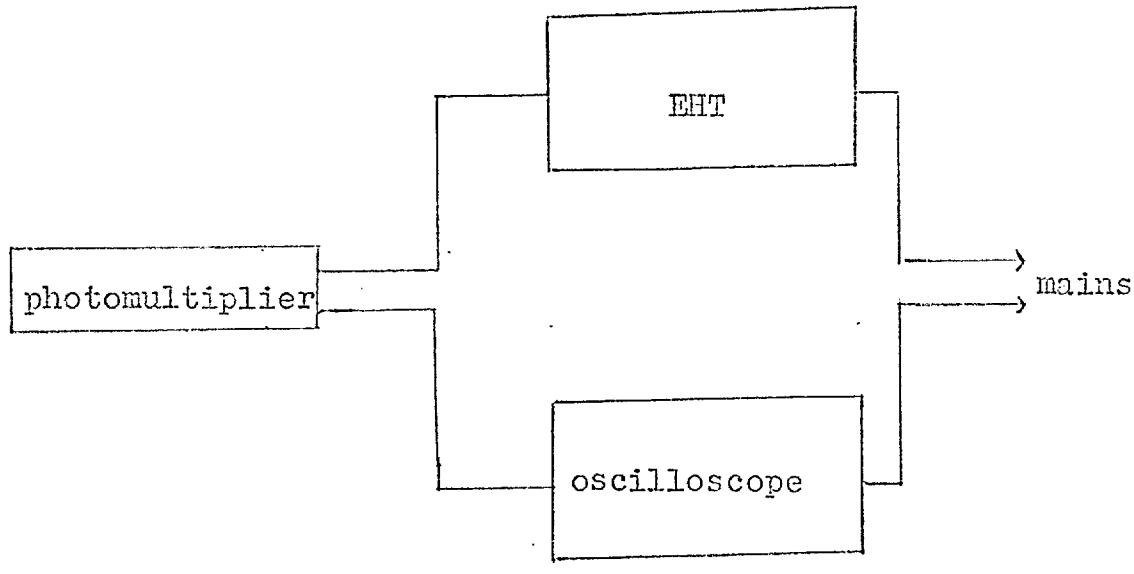
Fig 3.30 COMPARISON OF SPECTRAL SENSITIVITY CURVES FOR SOLAR-BLIND AND NORMAL PHOTOMULTIPLIERS



The completed optical system was mounted in a cubic perspex glove-box, so that analyses could be carried out in any chosen atmosphere, usually argon. The gas entered via the CFAR gas entry, and electrical cables and fluid tubes passed through split rubber bungs mounted in appropriate holes in the raised base of the box.

The Brandenburg EHT power supply, operated at 850 ± 50V , was used in conjunction with the storage facility of the Telequipment Type D535 oscilloscope, to amplify and record the current obtained by response of the photomultiplier to light signals (Fig.3.31).

Fig 3.31 SIGNAL DETECTION FOR NON-DISPERSIVE AF



Assembly.

Assembly followed the construction of the basic components of the non-dispersive AF system. First the electrical connections to the CFAR and photomultiplier were made. Matt-black Klingerite ring shields protected the faces of the objectives from heat and tarnish. The condition of the partially exposed mirror surfaces should be checked regularly. The objectives were aligned, using an EDL to produce a 1-2 mm diameter focussed light-spot ca. 1.5 mm above the base of the carbon filament notch. The focal point position of the second objective was adjusted to coincide with the first over the filament. A simple cover was made to surround the EDL and minimise glare and unwanted reflections. AF testing then began.

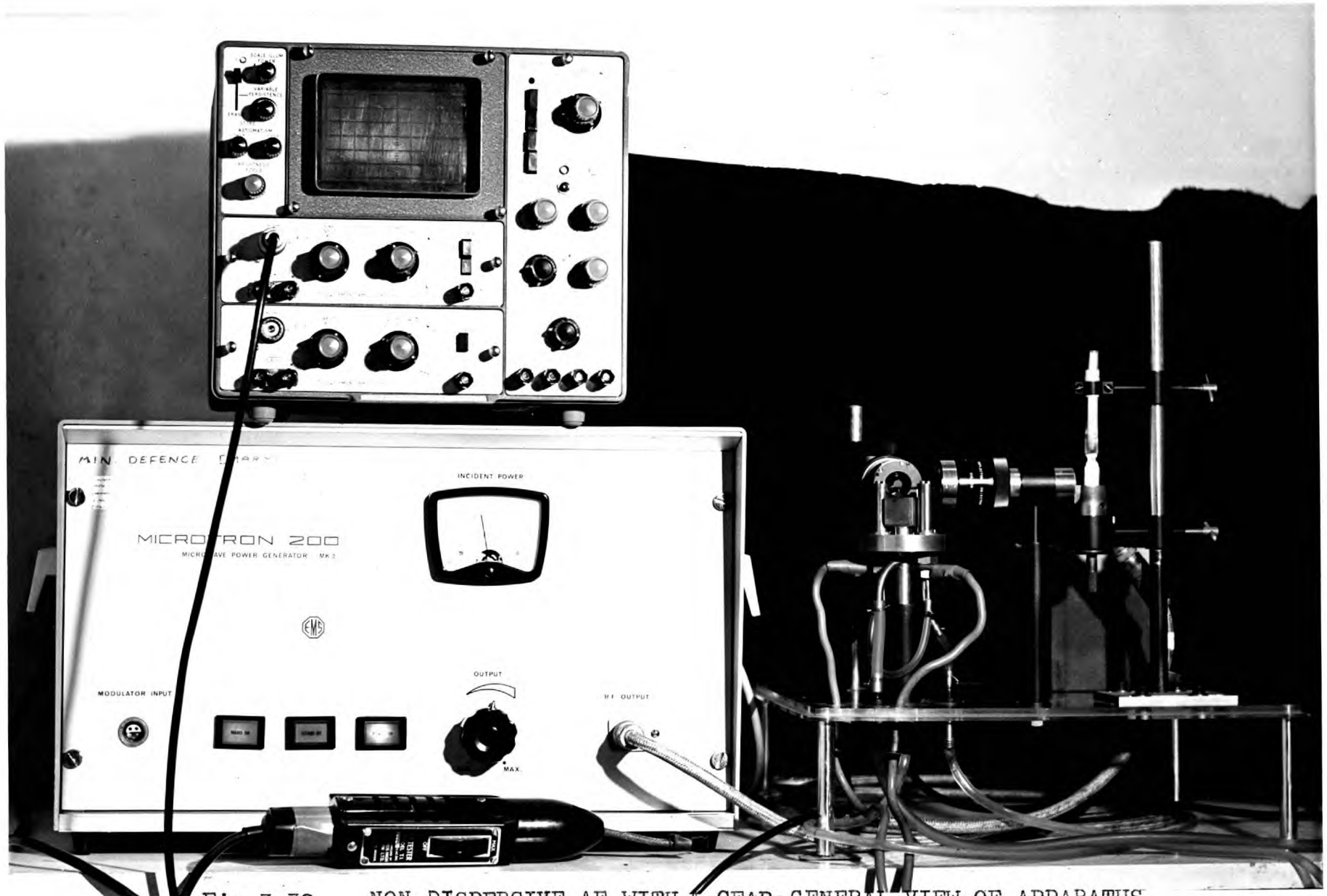


Fig 3.32 NON-DISPERSIVE AF WITH A CFAR: GENERAL VIEW OF APPARATUS

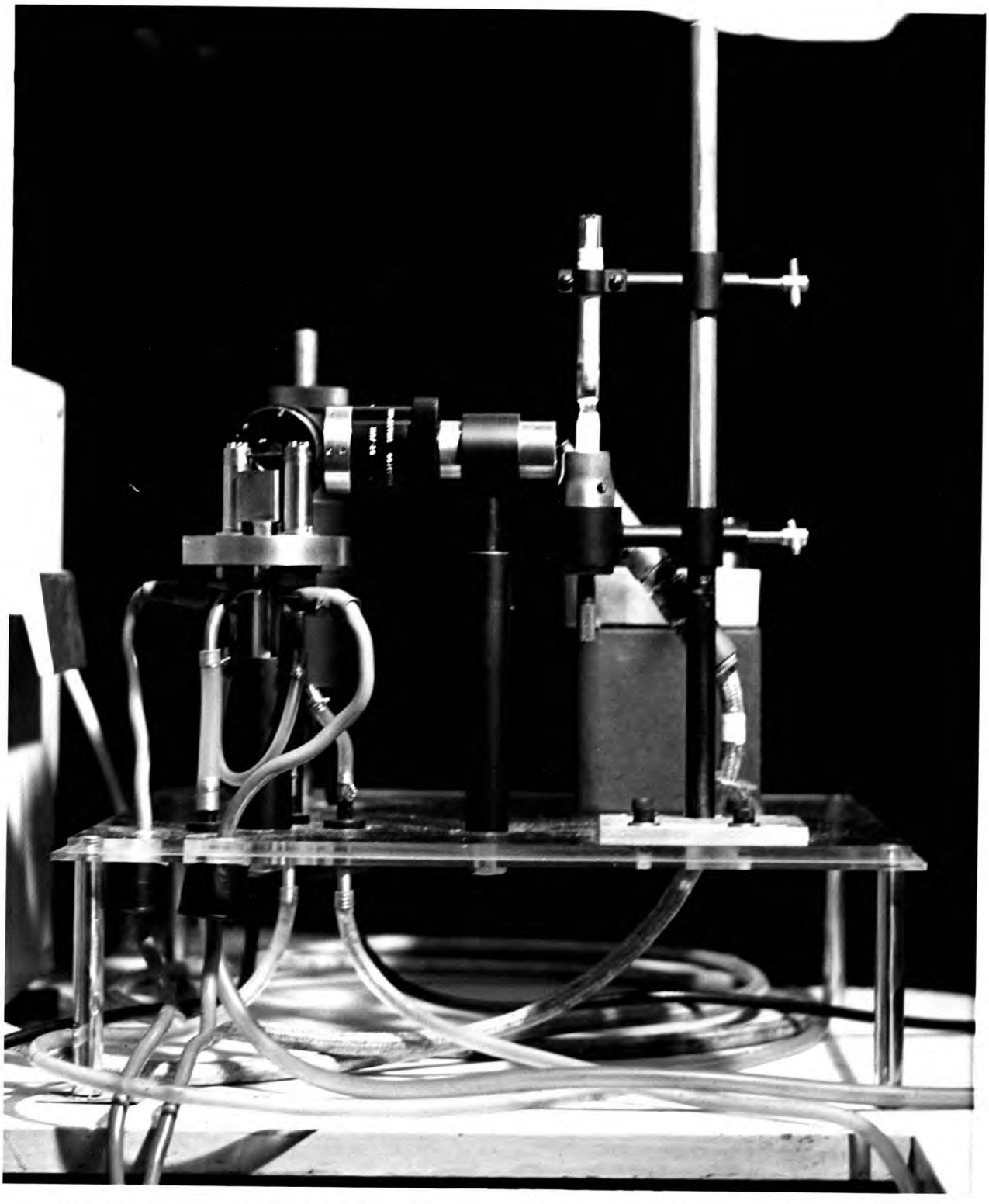


Fig 3.33 NON-DISPERSIVE AF WITH A CFAR: CLOSE-UP OF THE OPTICAL SYSTEM

Applications.

Approach.

Good atomisation and detection of cadmium on the CFAR had already been reported (40:III), and the 228.8 nm cadmium emission line is suited to the peak response of the solar-blind photomultiplier. Similarly, zinc and mercury AF at 213.9 nm and 253.7 nm were suitable for the initial testing of the non-dispersive AF system. After confirmation of AF signals in air for these elements, the system was tested more ambitiously, making measurements in argon for several elements to assess the scope and potential of the completed analytical system.

The AF emission signal comprised a partially resolved double peak or a narrower single peak, dependent on the element and its concentration, and preceding any emission from the carbon filament. They were checked against water and dry filament 'blank' signals. All signals were measured using a 1 sec/cm oscilloscope time-base. As tests proceeded, the most critical factors for successful detection became clear. Assuming adequate atomisation of a particular element by the carbon filament and the correct viewing position, the influential factors in order of priority were the intensity and quality of EDL, the operating wattage for the tuning-cavity, the Variac voltage for sample atomisation, the flow-rate of argon past the filament, and the EHT supply to the detection system.

Such conditions were found for the detection of several elements, and detection limits measured for the most promising. Some specialised aspects were also examined, including the influence of ambient atmosphere on detection, the chemical form

of elements, and the comparison of two different atomic line EDL sources for determinations where spectral overlap between contributing elemental emission lines occurs.

Cadmium, zinc and mercury.

Detection limits were measured for cadmium in argon and OFN, zinc in argon, and mercury in air and argon, to indicate the overall sensitivity of the system, confirm the photomultiplier range, and compare the contributions of specific emission lines.

Some aspects of cadmium fluorescence had been previously investigated with a CFAR. Resonance fluorescence at 228.8 nm occurred more strongly in argon than in nitrogen, but at 326.1 nm the associated stepwise fluorescence occurred more strongly in nitrogen than argon (40:III). However, on the non-dispersive AF system, any enhancement of AF at 326.1 nm due to use of OFN in place of argon was overwhelmed by the loss of sensitivity at 228.8 nm. Latter tests also demonstrated the low sensitivity of the solar-blind photomultiplier at the higher wavelength.

For mercury, however, a x 100 increase in sensitivity was obtained by using argon in place of an air atmosphere so that the strong vacuum uv 184.9 nm emission line could contribute significantly.

Element	Atomic lines nm	Sources
CADMIUM	228.8, 326.1	$3CdSO_4.8H_2O$
ZINC	213.9	$ZnSO_4.7H_2O$
MERCURY	184.9, 253.7	$HgCl_2$

Optimum working conditions.

	EDL	Power to EDL W	Variac V	EHT V	Argon flow-rate lt/min	Oscillo-scope y-scale V/cm
Cd	Cd	50	6.6	900	3.9	10
Zn	Zn	55	8.4	900	3.6	20
Hg	Hg	20	6.6	850	3.6	5

Results.

	Atmosphere	Contributing lines nm	Detection limits g 1 µl samples
Cd	Ar	228.8, 326.1	9×10^{-15}
Cd	OFN	228.8, 326.1	1×10^{-13}
Zn	Ar	213.9	1×10^{-15}
Hg	air	253.7	5×10^{-9}
Hg	Ar	184.9, 253.7	5×10^{-11}

Alternative elements.

The AF detection of several elements in argon was tested after consideration of the availability of EDLs, the possibility of CFAR atomisation, the number and range of AF lines, and the suitability of alternative detection techniques. The non-dispersive system measures emission at several lines simultaneously, but these tests demonstrated a very limited range of

sensitive response for the solar-blind photomultiplier. The most suitable elements for detection were those with several short-wave AF emission lines, 220.0 ± 20.0 nm being the best range. At 280.0 nm the photomultiplier was too insensitive for a useful response, but measurements at <200.0 nm can be worthwhile as sensitive alternatives are often unavailable at these wavelengths.

Element	Atomic lines nm (Relative AF intensities, 63)			N	L	Source
ARSENIC	235.0(10), 245.7(3), 197.2(3),	289.9(4), 286.0(3), 193.7(2),	249.3(4) 238.1(3) 189.0(2)	9	2	KH_2AsO_4
SELENIUM	204.0(10), 207.5(0.2)	196.0(7),	206.3(5)	4	3	$(NH_4)_2SeO_4$
IODINE	206.2, 184.4,	178.3, 178.9,	183.0 187.6	6	1	KI KIO_3
MANGANESE	279.5(10),	279.8(10),	280.1(10)	3	0	$KMnO_4$ $MnSO_4$
LEAD	283.3(10)			1	0	$PbNO_3$
BISMUTH	302.5(10), 269.7(0.6),	306.8(5), 289.8(0.5)	206.2(1)	5	1	Bi/HNO_3
TELLURIUM	238.3(10), 225.9(0.4)	238.6(10),	214.3(7)	4	4	K_2TeO_3
SULPHUR	180.7, 190.0,	182.0, 191.5	182.7	5	0	$3CdSO_4.8H_2O$ $CuSO_4.5H_2O$

KEY N number of atomic lines <310.0 nm

L number of atomic lines 220.0 ± 20 nm

Optimum working conditions.

	EDL	Power to EDL W	Variac V max	EHT V	Argon flow-rate lt/min	Oscillo-scope y-scale V/cm	Detection limits g 1 µl samples
As	As	75	7.2	900	1.4	2	4×10^{-7}
As	Cd	65	9.6	850	1.7	10	3.7×10^{-7}
Se	Se	50	9.6	850	1.4	5	1×10^{-7}
I	I	40	9.6	900	2.6	0.2	1×10^{-7}
I	Bi	60	9.6	850	2.6	10	4×10^{-8}
Mn	Mn	50	6.0 to 9.6	900	1.7 to 3.6	0.2	0
Pb	Pb	50	9.0	900	2.9	10	$>1 \times 10^{-6}$
Bi	Bi	60	8.4	850	2.9	10	1×10^{-9}
Te	Te	65	9.0	900	2.6	10	1×10^{-6}
S	S	50	7.2	900	1.7	5	$?1 \times 10^{-6}$
S	S	30	7.8	900	2.9	5	$?1 \times 10^{-6}$

It is particularly important to use intense atomic line sources. Therefore, a bismuth EDL was compared to an iodine EDL to demonstrate weak iodine AF at 206.2 nm. However, the very low AF sensitivity for iodine at 206.2 nm discouraged further development of this approach (64).

Similarly, a cadmium EDL was used to demonstrate arsenic AF at 228.8 nm. Detection limits were comparable to those obtained with several alternative arsenic EDLs, but are unlikely to exceed those attainable with an intense multi-line arsenic light source.

The possibility of relating the ease of reduction of compounds to the AF detection of some elements, was considered tentatively. Permanganate and a manganous salt gave

indistinguishable insensitive responses for manganese, while for iodine it appeared that iodide was marginally more easily reduced than iodate. It was hoped to extend the analogy to the evolution of sulphur from sulphide and sulphate, but the nature of atomic lines used for detection, and conditions of illumination and CF atomisation are of much greater importance.

Emission signals measured after the volatilisation of concentrated solutions of sodium sulphide and sulphate were probably mainly due to scattering of light by particles in the beam. Such signals were similar whether illuminating with a zinc or cadmium EDL or a sulphur source. Usually, for example for cadmium, emission signals were insignificant unless the illuminating source provided the correct atomic lines for excitation.

At high sulphur concentrations, the emission trace was a double peak. The first peak was attenuated in air compared to argon. The second was less reproducibly measurable in air, but of unchanged mean value. AF emission might contribute to the first peak, but this, not occurring with cadmium or copper sulphate solutions, could not be distinguished conclusively at the high concentrations, and was too weak to appear at low concentrations. It might be enhanced by using hydrogen to provide an inert, reducing atmosphere for atomisation.

Suggestions for development.

The potential of the CFAR system for non-dispersive AF has been assessed. The chosen working conditions and preliminary results will provide guidance during subsequent tests and development.

Four further elements, as yet unexamined, are theoretically suited to the system. Working conditions and detection limits should be investigated for cobalt, nickel, antimony and beryllium.

Element	Atomic lines nm (Relative AF intensities, 63)			N	L	Source
COBALT	240.7(10), 241.2(4), 252.9(1)	242.4(5), 243.2(2),	252.4(4) 241.5(2)	7	0	$CoSO_4.7H_2O$
NICKEL	232.0(10), 234.6(0.2),	231.0(0.5), 300.3(0.2)	229.0(0.2)	5	2	$NiCl_2.6H_2O$
ANTIMONY	231.2(10), 287.8(3),	206.8(5), 277.0(2)	259.8(5)	5	3	SbF_3
BERYLLIUM	234.8(10)			1	1	$BeSO_4.4H_2O$

KEY N number of atomic lines <310.0 nm

L number of atomic lines 220.0 ± 20 nm

It should then be possible to use the system for specific quantitative analyses, checking for interferences and idealising conditions. It is important to achieve a correct vertical and horizontal alignment of the filament with respect to the focal point of the mirror system in each case.

The following elements appear the most promising at this stage, so this is a recommended order for development.

1. Zinc, cadmium, mercury.
2. Cobalt, nickel, antimony, beryllium.
   (after preliminary tests.)
3. Bismuth, iodine.
4. Arsenic, selenium, tellurium.

Some general modifications will be necessary. Intense, reliable line sources are required for AF. Sometimes high intensity hollow-cathode lamps may compare favourably in intensity and stability to the best EDLs available.

An extended wavelength range and increased sensitivities might be provided by the use of an alternative photomultiplier. Response ranges and spectral sensitivity curves of those available should be compared, and a choice made.

It is proposed to use electronic integration for AA and AF signal measurement with conventional CFAR systems. This technique should also be applicable to the measurement of non-dispersive atomic fluorescence.

BIBLIOGRAPHY

1. Platt,P., Selected Ann.Revs.Anal.Sciences, AAS, (SAC), 1, 177 (1971), 372 refs.
2. Manual for the Jobin Yvon 'delta Modele Kuhlmann' AA flame spectrometer.
3. Atwill,W., Int.Electronics, 7, 18 (1964).
4. Snetsinger,K.G. and Keil,K., Am.Min., 52, 1842 (1967).
5. Brech,F. and Cross,L., Proc.Xth Coll.Spectrosc.Int. Spartan Books, Paper No.80, (1963).
6. Blackburn,W.H., Pelletier,Y.J.A. and Dennen,W.H. App.Spectrosc., 22, 4 (1968).
7. Rasberry,S.D., Scribner,B.F. and Margoshes,M., App.Optics, 6, 81 (1967).
8. Ibid., 6, 87 (1967).
9. Brech,F., Jarrell-Ash Company Reprint, No.2, (1969).
10. Sherman,D.B., Ruben,M.P., Goldman, H.M. and Brech, F. Ann.N.Y. Acad.Sci., 22, 767 (1965).
11. Targonski,S. and Wurlitzer,P., 53rd Gen.Motors Spectrosc. Conf., Jarrell-Ash Company Reprint, (1967).
12. Brech,F., Anal.Instr., 6, 215 (1969).
13. Moenke,H., Moenke-Blankenburg,L. and Quillfeldt,W., Anal.Abs., 18(4), 2196 (1970).
14. Georgieva,L. and Petrakiev,A., Bol.Geol.Minero, 80(5), 491 (1969).
15. McCormack,J.T., Metals Review, 6, 6 (1965).
16. Mosotti,V.G., Laqua,K. and Hagenah,W.D., Spectrochim. Acta, 23B, 197 (1967).

17. Karyakin,A.V. and Kaigorodov,V.A. Zh.Analit.Khim., 23(6), 930 (1968).

18. Maxwell,J.A., Chem.in Canada, April, 10 (1963).

19. Whitehead,A.B. and Heady,H.H., App.Spectrosc., (22(1), 7 (1968).

20. Cerrai,E. and Trucco,R., Energia Nucl.Milano, 15, 581 (1968).

21. Glick,D., Marich,K.W., Carr,P.W., Beatrice,E.S., and Edwin,E.S., Ann.N.Y.Acad.Sci., 168(3), 507 (1970).

22. Webb,M.S.W. and Cotterill,J.C., Anal.Chim.Acta, 43, 351 (1968).

23. Ryan,J.R., Clark,C.B. and Ruh,E., 67th Ann.Meeting Am. Ceramic Soc., Jarrell-Ash Company Reprint No.27, (1965).

24. Goldman,H.M., Ruben,M.P. and Sherman,D., Oral Surg., Oral Med., and Oral Path., 17(1), 102 (1964).

25. Mandelstam,S.L., Proc.XVth Coll.Spectrosc.Int., Hilger, 115 (1969).

26. Janosikova, Vladimira, Tomasova, Miluse, Chem.Abs. (Czech original), 75(8), 58294p (1971).

27. Scott,R.H. and Strasheim,A., Spectrochim.Acta 26B, 707 (1971).

28. Tretyl,W.J., Orenberg,J.B., Marich,K.W. and Glick,D., App.Spectrosc., 25(3), 376 (1971).

29. Felske,A., Hagenah,W.D. and Laqua,K., Spectrochim.Acta, 27(B), 1 (1972).

30. Ibid., Naturwiss., 57(9), 428 (1970).

31. Tretyl,W.J., Marich,K.W., Orenberg,J.B., Carr,P.W., Miller,D.C. and Glick,D., Anal.Chem., 43, 1452 (1971).

32. Piepmeir,A.H. and Osten,D.E., App.Spectrosc., 25(6), 642 (1971).

33. Bunshah,R.F., Modern Analytical Techniques for Metals and Alloys, III, Techniques of Metals Research, Wiley, (1970).

34. Fassel,V.A., Iron and Steel Institute, Special Report No.68, 103 (1960).

35. Harrison,G.R., MIT Wavelength Tables, Wiley, (1939).

36. Brand,M.J.D. and Fleet,B., Chem.in Britain, 5(12), (1969)

37. Sullivan,J.V. and Walsh,A., Spectrochim.Acta, 23B, 131 (1967).

38. Twelve steel samples from the Ministry of Defence Quality Assurance Directorate, Bragg Laboratory, Sheffield.

39. Candler,C., Atomic Spectra, 2nd Ed., Hilger, (1964).

40. West,T.S. et al, Atomic Absorption and Fluorescence Spectroscopy with a Carbon-Filament Atom Reservoir, Anal.Chim.Acta.

I. West,T.S. and Williams,X.K., 45, 27 (1969).

II. Anderson,R.G., Maines,I.S. and West,T.S., 51, 355 (1970).

III. Alder,J.F. and West,T.S., 51, 365 (1970).

IV. Aggett,J. and West,T.S., 56, 349 (1971).

V. Aggett,J. and West,T.S., 57, 15 (1971).

VI. Alger,D., Anderson,R.G., Maines,I.S and West,T.S., 57, 271 (1971).

VII. Anderson,R.G., Johnson,H.N. and West,T.S., 58, 281 (1972).

VIII. Ebdon,L., Kirkbright,G.F. and West,T.S., 58, 39 (1972).

IX. Alder,J.F. and West,T.S., 58, 331 (1972).

X. Jackson,K.W. and West,T.S., 59, 187 (1972).

41. West,T.S., Plenary Lecture: Graz International Symposium on Microtechniques, 47, Butterworths (IUPAC), (1971).

42. Cooke,D.O., Dagnall,R.M. and West,T.S., Anal.Chim.Acta, 54, 381 (1971).

43. Drummond Microcaps disposable 1 µl pipettes and teat syringes from the Shandon Scientific Company Ltd., Pound Lane, London, N.W.10.

44. Rubeška,I. and Moldan,B., Atomic Absorption Spectrophotometry, Iliffe, (1967).

45. L'vov,B.V., Atomic Absorption Spectrochemical Analysis: 253-60 Hilger (1970).

46. Smith,D., Ph.D. thesis (Sheffield), 15 and 72 (1970).

47. Dagnall,R.M., Thompson,K.C. and West,T.S., Analyst, 92, 506 (1967).

48. L'vov,B.V. and Khartsysov,A.D., Zh.Prikl.Spektrosk.(Russ.) 11 413 (1969).

49. Aldous,K.M., D.I.C./Ph.D. thesis (London Imperial College) 89 (1970).

50. Kirkbright,G.F., Sargent,M. and West,T.S. AA News.,8 34 (1969).

51. Clark,D., Dagnall,R.M. and West,T.S., Anal.Chim.Acta, 58, 339 (1972)

52. Slavin,W., Atomic Absorption Spectroscopy, 140, Wiley, (1968).

53. Manning,D.C. and Slavin,S., AA News., 8, 132 (1969)

54. Kerber, J.D., Barnett,W.B. and Kahn,H.L., AA News., 9, 39 (1970).

55. L'vov,B.V. and Khartsysov,A.D., Zh.Prikl.Spektrosk.(Russ.), 10, 383 (1969)

56. L'vov,B.V. and Khartsysov,A.D., Zh. Anal.Khim. (Russ.) 24, 799 (1969).

57. West,T.S., Chem.in Britain, 10, 378 (1971).

58. Vickers,T.J. and Vaught,R.M. Anal.Chem., 41, 1476 (1969)

59. Warr,P.D., Talanta, 17, 543 (1970).

60. Elser,R.C. and Winefordner,J.D., App.Spectrosc., 25, 345 (1971).

61. Vickers,T.J., Slavin,P.J., Muscat,V.I. and Farias,L.T., Anal.Chem., 44, 6 930 (1972).

62. Larkins,P.L., Lowe,R.M., Sullivan,J.V. and Walsh,A., Spectrochim.Acta, 24B, 187 (1969).

63. Parsons,M.L. and McElfresh,P.M., Flame Spectroscopy, Atlas of Spectral Lines, IFI/Plenum, (1970).

64. Thompson,C.K., Spec.Lett., 3, 59 (1970).